

**Physical Stability of Pharmaceutical Tablets:
From Mechanistic Understanding to Prediction of
Long-Term Stability**

Natalie Maclean

Strathclyde Institute of Pharmacy and Biomedical Sciences
University of Strathclyde
Glasgow, UK

A thesis submitted in fulfilment of the requirements for the degree of
Doctor of Philosophy

July 25, 2022

This thesis is the result of the author's original research. It has been composed by the author and has not been previously submitted for examination which has led to the award of a degree.

The copyright of this thesis belongs to the author under the terms of the United Kingdom Copyright Acts as qualified by University of Strathclyde Regulation 3.50. Due acknowledgement must always be made of the use of any material contained in, or derived from, this thesis.

Abstract

Stability studies play a crucial role in the development of drug products, with the data collected being used to optimise formulation and manufacturing settings; determine the required packaging for the product; assign the retest date or shelf life; and contributing towards regulatory submissions. In this thesis, we consider the physical stability of pharmaceutical tablets, which focuses on physical tablet properties such as tensile strength, disintegration and dissolution performance.

In the first instance, 16 different formulations of placebo tablets were characterised to determine the tensile strength, porosity, initial contact angle, and disintegration time. A simple workflow is proposed to classify the performance-controlling mechanism of tablets. These mechanisms include dissolution controlled, wettability controlled, and swelling controlled.

Each of the 16 placebo formulations were then stored under 5 different accelerated temperature and humidity conditions for 2 and 4 weeks to investigate the changes in physical tablet properties. The correlations in disintegration time with temperature and humidity for each formulation are discussed in relation to the performance-controlling mechanisms.

Finally, three of the formulations were selected (one for each performance-controlling mechanism) to manufacture tablets containing griseofulvin as a model drug. Tablets were manufactured with 30% wt. griseofulvin and the characterisation and stability studies were repeated, with the addition of dissolution studies. The change in dissolution performance of each formulation is discussed, and long-term stability predictions are made.

Contents

| | |
|--|-------------|
| Abstract | ii |
| List of Figures | xiii |
| List of Tables | xiv |
| Nomenclature | xvi |
| Acknowledgements | xvii |
| Research Outputs | xix |
| 1 Introduction | 1 |
| 1.1 From Drug Substance to Drug Product | 2 |
| 1.2 The Role of Stability Studies | 4 |
| 1.3 Stability Study Design | 6 |
| 1.3.1 Traditional Stability Studies | 7 |
| 1.3.2 Accelerated Predictive Stability Studies | 8 |
| 1.4 Tablet Performance – Disintegration and Dissolution | 9 |
| 1.4.1 Tablet Disintegration | 9 |
| 1.4.2 Tablet Dissolution | 11 |
| 1.4.3 The Influence of Formulation on Tablet Performance | 14 |
| 1.4.4 The Influence of Manufacturing Processes on Tablet Performance | 17 |
| 1.5 The Influence of Formulation on Physical Stability | 19 |
| 1.5.1 Solubility | 19 |

| | | |
|----------|---|-----------|
| 1.5.2 | Hygroscopicity | 20 |
| 1.6 | Physical Tablet Properties and the Effects of Storage | 20 |
| 1.6.1 | Tensile Strength | 21 |
| 1.6.2 | Disintegration & Dissolution | 23 |
| 1.7 | Modelling & Predictions | 25 |
| 1.8 | Conclusion | 27 |
| 2 | Aims and Objectives | 28 |
| 3 | Materials & Methods | 30 |
| 3.1 | Materials | 31 |
| 3.1.1 | Tablet Excipients | 31 |
| 3.1.2 | Active Pharmaceutical Ingredient | 31 |
| 3.1.3 | Saturated Salt Solutions | 32 |
| 3.1.4 | Surfactant | 32 |
| 3.1.5 | Storage of Materials | 33 |
| 3.2 | Methods | 33 |
| 3.2.1 | Raw Material Characterisation | 33 |
| 3.2.2 | Tablet Manufacture | 34 |
| 3.2.3 | Accelerated Stability Sample Storage | 35 |
| 3.2.4 | Tablet Characterisation | 36 |
| 4 | Exploring the Performance-Controlling Tablet Disintegration Mechanisms for Direct Compression Formulations | 41 |
| 4.1 | Introduction | 42 |
| 4.2 | Materials and Methods | 45 |
| 4.2.1 | Materials | 45 |
| 4.2.2 | Characterisation of Raw Materials | 45 |
| 4.2.3 | Tablet Manufacture | 46 |
| 4.2.4 | Characterisation of Tablets | 47 |
| 4.3 | Results | 49 |
| 4.3.1 | Characterisation of Raw Materials | 49 |

| | | |
|----------|--|-----------|
| 4.3.2 | Characterisation of Tablets | 51 |
| 4.3.3 | Investigating the Performance-Controlling Properties | 54 |
| 4.4 | Discussion | 57 |
| 4.4.1 | The Influence of Formulation on Disintegration | 57 |
| 4.4.2 | The Influence of Porosity on Disintegration | 61 |
| 4.4.3 | The Influence of Disintegrant Concentration on Disintegration | 62 |
| 4.5 | Conclusions | 63 |
| 5 | Investigating the Role of Excipients on the Physical Stability of Directly Compressed Tablets | 65 |
| 5.1 | Introduction | 66 |
| 5.2 | Materials and Methods | 69 |
| 5.2.1 | Materials | 69 |
| 5.2.2 | Dynamic Vapor Sorption (DVS) | 69 |
| 5.2.3 | Tablet Manufacture | 70 |
| 5.2.4 | Sample Storage | 70 |
| 5.2.5 | Characterisation of Tablets | 71 |
| 5.3 | Results | 72 |
| 5.3.1 | Moisture Sorption | 72 |
| 5.3.2 | Tensile strength | 72 |
| 5.3.3 | Porosity | 74 |
| 5.3.4 | Contact angle | 75 |
| 5.3.5 | Disintegration time | 76 |
| 5.3.6 | Effects of Storage Time | 76 |
| 5.3.7 | Correlation between temperature, humidity and physical tablet properties | 77 |
| 5.3.8 | Correlation between physical tablet properties and disintegration time | 80 |
| 5.4 | Discussion | 82 |
| 5.4.1 | MCC/lactose tablets | 82 |
| 5.4.2 | MCC/mannitol tablets | 82 |

| | | |
|----------|---|------------|
| 5.4.3 | DCPA-based tablets | 83 |
| 5.4.4 | Effect of Disintegrant Choice | 83 |
| 5.5 | Conclusions | 84 |
| 6 | Assessing the Dissolution Stability of Directly Compressed Tablet Formulations with Griseofulvin | 86 |
| 6.1 | Introduction | 87 |
| 6.2 | Materials and Methods | 89 |
| 6.2.1 | Materials | 89 |
| 6.2.2 | Raw Material Characterisation | 89 |
| 6.2.3 | Tablet Manufacture | 89 |
| 6.2.4 | Sample Storage | 90 |
| 6.2.5 | Tablet Characterisation | 91 |
| 6.2.6 | Predicting Dissolution after Long-Term Storage | 91 |
| 6.3 | Results | 93 |
| 6.3.1 | Weight and Dimensional Analysis | 93 |
| 6.3.2 | Tensile Strength | 94 |
| 6.3.3 | Porosity | 95 |
| 6.3.4 | Contact Angle | 96 |
| 6.3.5 | Disintegration Time | 96 |
| 6.3.6 | Dissolution | 97 |
| 6.4 | Discussion | 99 |
| 6.4.1 | Comparison of Placebo and Griseofulvin Tablets | 99 |
| 6.4.2 | The Effects of Temperature and Humidity | 101 |
| 6.4.3 | The Effects of Storage on Product Performance | 105 |
| 6.4.4 | Prediction of Long-Term Dissolution Changes | 106 |
| 6.5 | Conclusions | 108 |
| 7 | Conclusions & Future Outlook | 109 |
| 7.1 | General Conclusions | 109 |
| 7.2 | Future Work | 110 |

| | | |
|---------------------|--|------------|
| 7.2.1 | Further Development of the Workflow for Classifying the Performance-Controlling Disintegration Mechanisms | 110 |
| 7.2.2 | Advancing Current Accelerated Stability Approaches for Physical Stability | 111 |
| Appendices | | 114 |
| A | Selected Conference Abstracts | 115 |
| B | Study Design and COVID-19 Implications | 128 |
| C | Material Data Sheets | 130 |
| D | Additional Data for Chapter 4 | 158 |
| E | Additional Data for Chapter 5 | 161 |
| Bibliography | | 161 |

List of Figures

| | | |
|-----|--|----|
| 1.1 | Summary of the stages, duration, and success rate of the drug development process, modified from Compound Interest (2016). | 2 |
| 1.2 | Some of the main uses of stability testing in the pharmaceutical industry, modified from (Qiu, 2018b) | 5 |
| 1.3 | The USP II (paddle) apparatus (A) at the beginning of a dissolution test, (B) with dissolution in progress and the particles dispersed throughout the dissolution media as it stirs, and (C) with powder coning at the base of the vessel. | 14 |
| 3.1 | Experimental set-up for storage of stability samples | 35 |
| 3.2 | The solubility of griseofulvin in varying concentrations of SDS solution. | 39 |
| 4.1 | Moisture sorption isotherms of (A) fillers and (B) disintegrants | 48 |
| 4.2 | Example images from the measurement of the dissolution of individual particles of lactose and mannitol at 0, 10, 20, 30 and 40 seconds after hydration. | 50 |
| 4.3 | The tensile strength of each formulation ($n = 10$, mean \pm standard deviation) | 51 |
| 4.4 | The porosity of each formulation ($n = 10$, mean \pm standard deviation) | 52 |
| 4.5 | The disintegration time of each formulation ($n = 6$, mean \pm standard deviation) | 52 |
| 4.6 | Examples of the contact angle measurements for MCC/mannitol-based tablets containing (A) CCS, (B) XPVP, (C) L-HPC and (D) SSG | 53 |

| | | |
|------|---|----|
| 4.7 | Contact angle profiles of tablets containing (A) CCS, (B) XPVP, (C) L-HPC and (D) SSG ($n = 2$) | 54 |
| 4.8 | The initial contact angle of each formulation ($n = 2$) | 55 |
| 4.9 | The (A) porosity and (B) disintegration time of tablets compressed at 8 and 10 kN (MCC/lactose, MCC/mannitol and MCC/DCPA) or 12 and 16 kN (DCPA/lactose). $n =$ (A) 10 or (B) 6; mean \pm standard deviation; $*p < 0.05$; ns: not significant. | 55 |
| 4.10 | The (A) tensile strength and (B) porosity of tablets containing 5% and 8% w/w CCS, respectively. | 56 |
| 4.11 | Disintegration times of batches prepared with 5% and 8% w/w CCS ($n = 6$; mean \pm standard deviation; $*p < 0.05$) | 56 |
| 4.12 | The initial contact angle, $\theta_{c,0}$, of tablets containing 5 and 8% w/w CCS ($n = 2$ and $n = 4$, for 5 and 8% w/w CCS, respectively). | 57 |
| 4.13 | Summary of raw material and tablet properties for each filler combination with 5% w/w CCS. Raw material properties ($\rho_{t,mix}$, relative swelling and moisture uptake) expressed as the weighted arithmetic mean of each excipient. | 58 |
| 4.14 | Workflow for the classification of IR tablets based on the disintegration mechanism. | 59 |
| 5.1 | The theoretical moisture uptake for each formulation (%), based on the individual moisture sorption of each excipient. | 72 |
| 5.2 | The change in (A) tensile strength, (B) porosity, (C) $\theta_{c,0}$, and (D) disintegration time for all batches after storage under accelerated conditions. Grey data points represent points where no data is available. | 73 |
| 5.3 | Pearson correlation coefficient between (A) storage temperature and (B) storage humidity with physical tablet properties. Only significant correlations ($p < 0.05$) are shown. | 78 |
| 5.4 | Pearson correlation coefficient between the disintegration time and the tensile strength, porosity and initial contact angle of all tablet during storage. Only significant correlations ($p < 0.05$) are shown. | 81 |

| | | |
|-----|---|-----|
| 6.1 | A summary of the accelerated dissolution stability modelling approach proposed by Scrivens (2019). | 92 |
| 6.2 | The tensile strength of (A) MCC/lactose-, (B)MCC/mannitol-, and (C) MCC/DCPA-based tablets containing griseofulvin before and after storage under accelerated temperature and humidity conditions (mean \pm standard deviation, n = 4). | 94 |
| 6.3 | The porosity of (A) MCC/lactose-, (B) MCC/mannitol-, and (C) MCC/DCPA-based tablets containing griseofulvin before and after storage under accelerated temperature and humidity conditions (mean \pm standard deviation, n = 210 at 0 weeks, and n = 14 at subsequent timepoints). | 95 |
| 6.4 | The mean relative change in porosity for tablets containing griseofulvin after storage under accelerated temperature and humidity conditions. . . | 95 |
| 6.5 | The relative change in $\theta_{c,0}$ after 1, 2 and 4 weeks storage at accelerated temperature and humidity conditions (mean of n = 4). | 96 |
| 6.6 | The disintegration time of griseofulvin tablets containing (A) MCC/lactose-, (B) MCC/mannitol, and (C) MCC/DCPA after storage under accelerated conditions (mean \pm standard deviation, n = 3). | 97 |
| 6.7 | The dissolution profiles of griseofulvin from tablets composed of MCC/mannitol, MCC/lactose, and MCC/DCPA with paddle speeds of 50 and 75 rpm, shown as a percentage of the final release of griseofulvin after a 30 min infinity spin at 200 rpm. | 98 |
| 6.8 | Dissolution profiles of (A) MCC/lactose-, (B) MCC/mannitol-, and (C) MCC/DCPA-based tablets containing griseofulvin before and after 4 weeks of storage under accelerated temperature and humidity conditions (mean \pm standard deviation, n =3 with the exception of the 60°C/30%RH and 60°C/75%RH condition for MCC/DCPA for which n=6). | 99 |
| 6.9 | The acceleration factors of (A) MCC/lactose, (B) MCC/mannitol, and (C) MCC/DCPA, using experimental values (0, 1, 2, and 4 weeks) and values imputed by spline interpolation (0.5, 1.5, and 3 weeks), including the fit of a first-order exponential decay curve for each condition. | 100 |

| | | |
|------|--|-----|
| 6.10 | The predicted and experimental values for griseofulvin dissolution at 15, 20, and 30 min at each condition for (A) MCC/lactose, (B) MCC/mannitol and (C) MCC/DCPA tablets. | 101 |
| 6.11 | The predicted dissolution profiles for (A) MCC/lactose, (B) MCC/mannitol, and (C) MCC/DCPA tablets containing griseofulvin after storage under ICH long-term (25°C/60%RH), intermediate (30°C/65%RH), and accelerated (40°C/75%RH) storage conditions. | 101 |
| 6.12 | The (A) tensile strength, (B) porosity, (C) initial contact angle ($\theta_{c,0}$) and (D) disintegration time of placebo tablets (see Chapter 4) and griseofulvin tablets prior to storage (mean \pm standard deviation, except for (C) where $n = 2$ for placebo tablets and so no standard deviation is shown). | 102 |
| 6.13 | Pearson correlation coefficients between (A) temperature and (B) humidity with the change in physical tablet properties during storage. Only significant correlations ($p < 0.05$) are shown. | 103 |
| 6.14 | A summary of the potential mechanisms of physical change during the storage of tablets under accelerated conditions, including the expected effects on the physical tablet properties. | 105 |
| 6.15 | Pearson correlation coefficients between the Weibull dissolution parameters, (A) k_s and (B) b , with the change in physical tablet properties during storage. Only significant correlations ($p < 0.05$) are shown. | 106 |
| A.1 | Disintegration time (s) of each filler and disintegrant combination (showing mean and standard deviation). | 123 |
| A.2 | Loading values from the PLS analysis of MCC/mannitol, MCC/lactose and MCC/DCPA formulations with each disintegrant. $\theta_{c,0}$ is the initial contact angle. | 124 |
| B.1 | The original study design (top) and the actual study design (bottom), including the justification for changes to the testing plan. | 129 |
| D.1 | Settling plots from the dynamic vapour sorption measurements of each filler and disintegrant. | 159 |

| | | |
|-----|--|-----|
| D.2 | Settling plot from the dynamic vapour sorption measurement of magnesium stearate. | 160 |
| E.1 | The change in tensile strength for MCC/lactose-based tablets with (A) CCS, (B) XPVP, (C) L-HPC and (D) SSG after storage under accelerated storage conditions for 2 and 4 weeks. Mean \pm standard deviation, n = 10. | 162 |
| E.2 | The change in tensile strength for MCC/mannitol-based tablets with (A) CCS, (B) XPVP, (C) L-HPC and (D) SSG after storage under accelerated storage conditions for 2 and 4 weeks. Mean \pm standard deviation, n = 10. | 163 |
| E.3 | The change in tensile strength for MCC/DCPA-based tablets with (A) CCS, (B) XPVP, (C) L-HPC and (D) SSG after storage under accelerated storage conditions for 2 and 4 weeks. Mean \pm standard deviation, n = 10. | 164 |
| E.4 | The change in tensile strength for DCPA/lactose-based tablets with (A) CCS, (B) XPVP, (C) L-HPC and (D) SSG after storage under accelerated storage conditions for 2 and 4 weeks. Mean \pm standard deviation, n = 10. | 165 |
| E.5 | The change in porosity for MCC/lactose-based tablets with (A) CCS, (B) XPVP, (C) L-HPC and (D) SSG after storage under accelerated storage conditions for 2 and 4 weeks. Mean \pm standard deviation, n = 100 (0 weeks) and n = 10 (2 and 4 weeks). | 166 |
| E.6 | The change in porosity for MCC/mannitol-based tablets with (A) CCS, (B) XPVP, (C) L-HPC and (D) SSG after storage under accelerated storage conditions for 2 and 4 weeks. Mean \pm standard deviation, n = 100 (0 weeks) and n = 10 (2 and 4 weeks). | 167 |
| E.7 | The change in porosity for MCC/DCPA-based tablets with (A) CCS, (B) XPVP, (C) L-HPC and (D) SSG after storage under accelerated storage conditions for 2 and 4 weeks. Mean \pm standard deviation, n = 100 (0 weeks) and n = 10 (2 and 4 weeks). | 168 |
| E.8 | The change in porosity for DCPA/lactose-based tablets with (A) CCS, (B) XPVP, (C) L-HPC and (D) SSG after storage under accelerated storage conditions for 2 and 4 weeks. Mean \pm standard deviation, n = 100 (0 weeks) and n = 10 (2 and 4 weeks). | 169 |

| | | |
|------|---|-----|
| E.9 | The change in initial contact angle ($\theta_{c,0}$) for MCC/lactose-based tablets with (A) CCS, (B) XPVP, (C) L-HPC and (D) SSG after storage under accelerated storage conditions for 2 and 4 weeks. Mean, $n = 2$ | 170 |
| E.10 | The change in initial contact angle ($\theta_{c,0}$) for MCC/mannitol-based tablets with (A) CCS, (B) XPVP, (C) L-HPC and (D) SSG after storage under accelerated storage conditions for 2 and 4 weeks. Mean, $n = 2$ | 171 |
| E.11 | The change in initial contact angle ($\theta_{c,0}$) for MCC/DCPA-based tablets with (A) CCS, (B) XPVP, (C) L-HPC and (D) SSG after storage under accelerated storage conditions for 2 and 4 weeks. Mean, $n = 2$ | 172 |
| E.12 | The change in initial contact angle ($\theta_{c,0}$) for DCPA/lactose-based tablets with (A) CCS, (B) XPVP, (C) L-HPC and (D) SSG after storage under accelerated storage conditions for 2 and 4 weeks. Mean, $n = 2$ | 173 |
| E.13 | The change in disintegration time for MCC/lactose-based tablets with (A) CCS, (B) XPVP, (C) L-HPC and (D) SSG after storage under accelerated storage conditions for 2 and 4 weeks. Mean \pm standard deviation, $n = 6$ | 174 |
| E.14 | The change in disintegration time for MCC/mannitol-based tablets with (A) CCS, (B) XPVP, (C) L-HPC and (D) SSG after storage under accelerated storage conditions for 2 and 4 weeks. Mean \pm standard deviation, $n = 6$ | 175 |
| E.15 | The change in disintegration time for MCC/DCPA-based tablets with (A) CCS, (B) XPVP, (C) L-HPC and (D) SSG after storage under accelerated storage conditions for 2 and 4 weeks. Mean \pm standard deviation, $n = 6$ | 176 |
| E.16 | The change in disintegration time for DCPA/lactose-based tablets with (A) CCS, (B) XPVP, (C) L-HPC and (D) SSG after storage under accelerated storage conditions for 2 and 4 weeks. Mean \pm standard deviation, $n = 6$ | 177 |

List of Tables

| | | |
|-----|---|----|
| 1.1 | The ICH Q1 stability safety guidelines | 7 |
| 1.2 | General storage conditions recommended for traditional stability studies for products to be stored at room temperature, as described in ICH Q1A (R2). | 7 |
| 3.1 | HPLC conditions used for the analysis of griseofulvin-based dissolution samples | 40 |
| 4.1 | Direct compression tablet formulations | 47 |
| 4.2 | True density, particle size and sphericity of each excipient | 49 |
| 5.1 | Accelerated stability storage conditions | 70 |
| 6.1 | Accelerated stability study design for griseofulvin-containing tablets. . . | 90 |
| 6.2 | Sampling plan for the accelerated stability study of griseofulvin-containing tablets, including the number of tablets tested at initial (n_{initial}) and at each stability timepoint (n_t). | 91 |
| 6.3 | The initial weight and dimensions of each batch, showing mean and relative standard deviation (%). All tablets were measured prior to storage, $n = 330$ per batch. | 94 |

Nomenclature

| | |
|----------------|-------------------------------------|
| ϵ | Porosity |
| σ_t | Tensile strength of a tablet |
| $\theta_{c,0}$ | Initial contact angle |
| $\theta_c(t)$ | Contact angle at time, t |
| $\rho_{t,i}$ | True density (of a raw material) |
| $\rho_{t,mix}$ | True density (of formulation) |
| ρ_t | True density |
| b | Weibull shape parameter |
| c_i | Weight fraction (of a raw material) |
| d | Tablet diameter |
| D_{50} | Particle size |
| F | Tablet hardness |
| k_s | Rate of change of AF |
| k_d | Weibull dissolution rate constant |
| L | Tablet thickness |
| m | Tablet mass |

| | |
|------------|--|
| S_{50} | Particle sphericity |
| t_s | Storage time |
| AF | Acceleration factor |
| AF_{inf} | Acceleration factor at infinite time |
| API | Active pharmaceutical ingredient |
| APS | Accelerated Predictive Stability |
| ASAP | Accelerated Stability Assessment Program |
| CCS | Croscarmellose sodium |
| DCP | Dibasic calcium phosphate |
| DCPA | Dibasic calcium phosphate anhydrous |
| DCPD | Dibasic calcium phosphate dihydrate |
| DVS | Dynamic vapor sorption |
| ICH | International Council for Harmonisation |
| IR | Immediate-release |
| L-HPC | Low-substituted hydroxypropylcellulose |
| MCC | Microcrystalline cellulose |
| MgSt | Magnesium stearate |
| RH | Relative humidity |
| SDS | Sodium dodecyl sulfate |
| SSG | Sodium starch glycolate |
| XPVP | Crospovidone |

Acknowledgements

First and foremost, I would like to thank my supervisor, Dr Daniel Markl. This PhD has been the most challenging experience of my life, and I cannot adequately express how grateful I am to have undertaken this challenge with such a supportive and encouraging mentor. Your insight and guidance has shaped not only this project, but also who I am as a researcher.

I would like to thank Dr Ibrahim Khadra for his support throughout this project. I would also like to express my sincere gratitude to my industrial supervisors, Dr James Mann, Ms Helen Williams, Mr Alexander Abbott, and Ms Heather Mead at AstraZeneca, for all of the time they invested in this project, as well as the expertise and support offered over the past 4 years.

Thank you to Erin, my PhD partner. There are no words to express my gratitude for the friendship we've formed during these past few years – from writing sessions at iCafe, to growing virtual focus trees in the middle of a global pandemic, to interview prep in the Ark. It's rare to meet someone and instinctively know they will be a lifelong friend, but I feel confident that I've found that in you. It was a relief to do this PhD side by side with you and to know that no matter what had gone wrong in the lab (and out of it!) that you were right there every step of the way.

John, Scott, Ivan, Eleanor, and Alice, thank you for helping me find my feet in SIPBS and for all the laughs together. Siobhan, you are the best friend I could have ever asked for, and without your friendship and support, I wouldn't be the person I am today. I'd like to give a special mention to my feline familiar, Gus, for always keeping my heart (and lap) warm.

Finally, to my brother Stephen – they say "you can't choose your family", but even if I could, I'd still choose you to be my brother (and best friend) every time. Thanks for always looking out for me and keeping me right when we were little kids, and thanks for continuing to do that now that we're big kids.

"You can trust us to stick to you through thick and thin – to the bitter end. And you can trust us to keep any secret of yours – closer than you yourself keep it. But you cannot trust us to let you face trouble alone, and go off without a word. We are your friends."

Funding Acknowledgement

This work was funded by the UK Engineering and Physical Sciences Research Council (EPSRC) with AstraZeneca sponsorship.

Research Outputs

Publications

1. M. Al-Sharabi, D. Markl, V. Vivacqua, P. Bawuah, **N. Maclean**, M. Bentley, A. P. E. York, M. Marigo, K. Huang and J. A. Zeitler. Terahertz Pulsed Imaging as a New Method for Investigating the Liquid Transport Kinetics of α -Alumina Powder Compacts. *Chemical Engineering Research and Design*. **165**, 386 - 397 (2020).
2. **N. Maclean**, E. Walsh, I. Khadra, J. Mann, H. Williams and D. Markl. Exploring the Performance-Controlling Tablet Disintegration Mechanisms. *International Journal of Pharmaceutics*, **599**, 120221 (2021).
3. D. Markl, **N. Maclean**, J. Mann, H. Williams, A. Abbott, H. Mead and I. Khadra. Tablet Disintegration Performance: Effect of Compression Pressure and Storage Conditions on Surface Liquid Absorption and Swelling Kinetics. *International Journal of Pharmaceutics*, **601**, 120382 (2021).
4. **N. Maclean**, I. Khadra, J. Mann, H. Williams, A. Abbott, H. Mead and D. Markl. Investigating the Role of Excipients on the Physical Stability of Directly Compressed Tablets. *International Journal of Pharmaceutics: X*, **4**, 100106 (2022).

Conference Contributions

Selected abstracts for conference contributions are included in Appendix A.

1. **N. Maclean**, I. Khadra, G. Halbert, D. Markl, J. Mann and H. Williams. The Effect of Accelerated Temperature and Humidity Conditions on the Physical Stability of Direct Compression Formulations. Compaction Simulation Forum, 2018. Cambridge, UK.

Poster Presentation.

2. **N. Maclean**, I. Khadra, D. Markl, H. Williams and J. Mann. The Effect of Accelerated Storage Conditions on the Physical Properties of Tablets. AstraZeneca PhD Research Day, 2019. Macclesfield, UK.

Poster Presentation.

3. **N. Maclean**, I. Khadra, H. Williams, J. Mann and D. Markl. Exploring the Stability-Controlling Tablet Disintegration Mechanisms. PSSRC 14th Annual Meeting, 2020. Online.

Oral Presentation.

4. **N. Maclean**, E. Walsh, M. Soundaranathan, I. Khadra, A. Abbott, H. Mead, H. Williams, J. Mann and D. Markl. Exploring the Performance- and Stability-Controlling Tablet Disintegration Mechanisms. PBP 12th World Meeting, 2021. Online.

Poster Presentation.

5. **N. Maclean**, I. Khadra, A. Abbott, H. Williams, H. Mead, J. Mann and D. Markl. The Role of Disintegration Mechanism in Physical Tablet Stability. PSSRC 15th Annual Meeting, 2021. Online.

Oral Presentation.

6. **N. Maclean**. The Role of Disintegration Mechanism on the Physical Stability of Directly Compressed Tablets. AstraZeneca In Vitro Product Performance Day, 2021. Online.

Flash Presentation.

7. **N. Maclean**, I. Khadra, A. Abbott, H. Williams, H. Mead, J. Mann and D. Markl.
The Role of Disintegration Mechanism in Physical Tablet Stability. AstraZeneca
CASE Symposium, 2021. Online.

Oral Presentation.

Chapter 1

Introduction

Chapter Summary

This chapter provides an introduction to the physical stability of pharmaceutical products. The physical tablet properties which can be affected by storage are discussed, as well as the influence of formulation selection and manufacturing settings on the stability of a drug product.

1.1 From Drug Substance to Drug Product

To bring a new drug to market, it typically takes over 10 years from the point that a new drug substance is identified to the point of approval for a final drug product (PhRMA, 2015). In terms of cost, Wouters *et al.* (2020) estimated that the average cost of developing a new drug products was around \$1.3 billion, based on a study of pharmaceutical products approved in the US between 2009 and 2018. Ultimately, this combination of high cost and lengthy development times result in long delays for the patients who would benefit from these pharmaceutical products reaching the market.

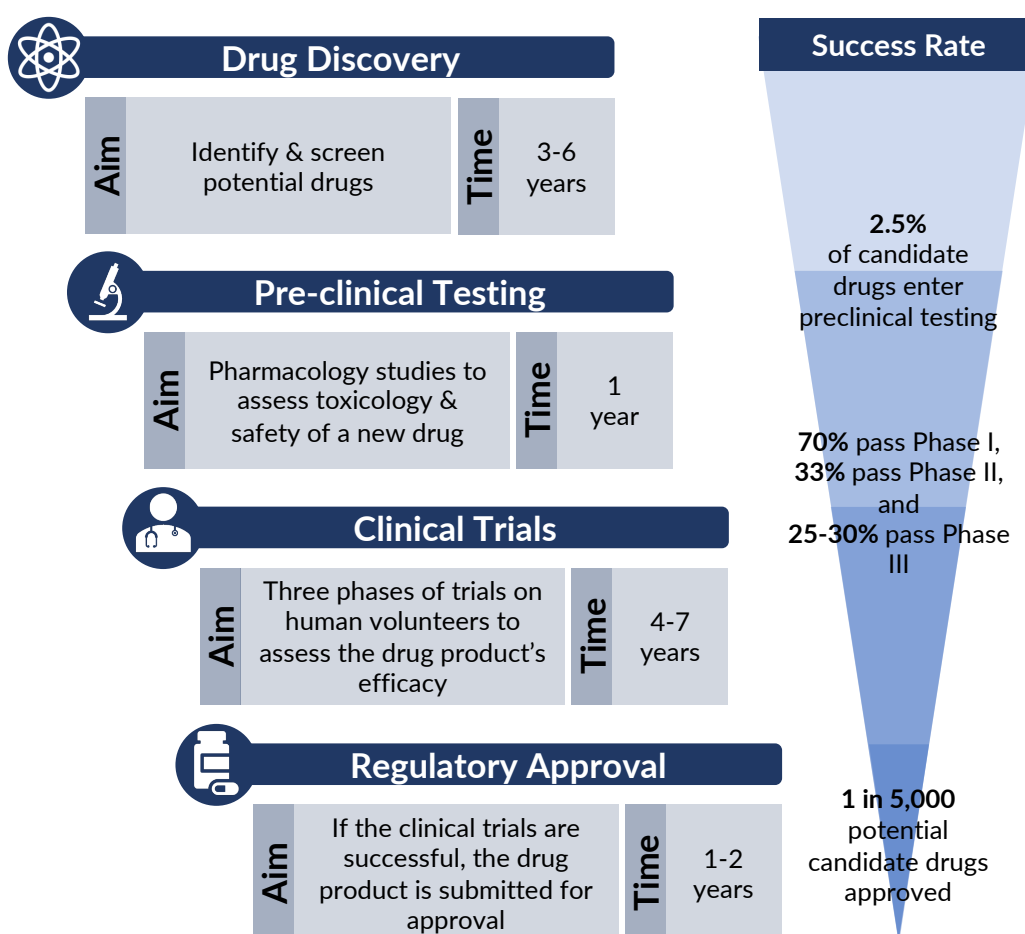


Figure 1.1: Summary of the stages, duration, and success rate of the drug development process, modified from Compound Interest (2016).

A brief outline of the steps involved in bringing a new drug to market is shown in Fig 1.1. During the drug discovery phase, high-throughput screening identifies candidate drugs which may be therapeutically active against a certain disease. Pre-clinical testing focuses on defining the exposure limits and identifying safe doses, whilst also identifying potential side effects. During the pre-clinical phase, formulation selection and manufacturing will also begin in order to develop the optimal product to enter clinical trials. The drug product must prove to be safe and effective in three successive phases of clinical trials. Phase I focuses mainly on the safety of the product in 10 to 100 healthy human volunteers. There are some exceptions to this, such as therapy areas like oncology, where Phase I studies may not use healthy volunteers and would instead focus on the extent to which therapeutic effects outweigh any side effects. If the product proves to be safe, Phase II studies the efficacy and safety of the product in 50 to 500 volunteer patients with the specific disease that the drug targets. Studies in Phase II also focus on identifying the dose strength which will be brought forward for the Phase III studies. Phase III studies can include up to a few hundred thousand patients, or far less depending on the drug product and the condition that it treats. These studies also allow the identification of interactions between the new drug product and other medications (PhRMA, 2015). Finally, products which complete the clinical trial phases and prove to be both safe and effective can request approval from the regulatory authorities to allow the product to reach the market. Throughout these stages, many potential products do not meet the rigorous standards of safety and efficacy which are required, and therefore many products do not complete this process. Approximately 1 in every 5,000 drug candidates identified in the discovery phase will be released to the market (Torjesen, 2015).

The price of developing a new medicine is high, in part due to the time, materials, and labour required to do so. For the many products which fail to reach approval, there is a financial loss for the pharmaceutical companies. By developing new approaches and technologies capable of predicting the safety or performance of drug products based on material attributes, this would enable early identification of products which are unlikely to meet the quality or safety standard required for approval. As well as identifying

failures earlier in the development process, these tools could also be used to drive the optimisation of the formulation and manufacturing processes for new products. Ultimately, this would reduce the financial risk of developing a new product, allowing patients to receive high-quality new medicines in a reduced time frame and at a lower cost.

1.2 The Role of Stability Studies

Stability studies are employed throughout the drug product development process, as demonstrated in Fig 1.2 (Qiu, 2018b). During early development, stability studies will help to identify the most suitable dosage form (e.g. tablet or capsule, suspension, etc) as well as the formulation selection. Stability studies are required to determine the shelf life of the product, as well as the storage conditions and packaging requirements (Bajaj *et al.*, 2012). For example, products which are adversely affected during storage at high relative humidity (RH) may be packaged with a desiccant to mitigate the effects of moisture. Stability studies will also ensure that the product is not compromised while it is ‘in-use’, i.e. after the primary packaging is opened. Even after the product received regulatory approval, stability studies will continue to confirm the quality of batches released to the market. In the case of any post-approval changes to the formulation or manufacturing process, stability studies are employed to confirm that the product quality is not impacted (Qiu, 2018b). Stability data is a key component of all regulatory submissions - from investigational new drug (IND) applications to allow clinical trials to begin, through to registration dossiers to allow the product to reach the market (Colgan *et al.*, 2018).

The stability of a drug product encompasses both the chemical stability and the physical stability of the product. Chemical stability relates to the rate and extent of chemical degradation of the drug substance to form degradation products (degradants) during storage. As well as the formation of potentially harmful degradants, this process also results in a loss of potency of the active pharmaceutical ingredient (API) as it degrades. Studies of chemical degradation primarily ensure that the drug product is safe for patients. The physical stability of a product describes any changes in the



Figure 1.2: Some of the main uses of stability testing in the pharmaceutical industry, modified from (Qiu, 2018b)

physical properties of the tablet, including the tensile strength of tablets, the porosity, and the disintegration and dissolution performance. Assessment of the physical stability is essential to ensure that the performance of the product is not compromised during storage.

1.3 Stability Study Design

The design of a stability study will vary depending on its intended purpose (Bajaj *et al.*, 2012). During early product development, stress testing may be used in order to rapidly identify potential degradants which may form during the product's shelf life. Additionally, this data may be used to investigate the pathways and mechanisms of formation of these degradants, and then toxicology studies can be performed to assess the safe dosing limits for each degradant.

On the other hand, stability studies intended to allow for the determination of shelf life and retest periods are more likely to include long-term stability under standardised ambient storage conditions, as well as some accelerated stability testing under higher temperatures and humidities.

The International Council for Harmonisation (ICH), formerly the International Conference on Harmonisation, were formed with the aim of bringing together regulatory authorities from around the world in order to harmonise the regulatory guidance on the development and approval of drug products. This regulatory harmonisation allows new medicines to reach the international market faster and at a lower cost by reducing the strain on pharmaceutical companies to repeat clinical trials or studies in order to satisfy slightly different criteria from different regulatory bodies.

Since their conception in 1990, the ICH have published a series of technical guidelines outlining the regulatory requirements in terms of the quality, safety and efficacy of drug products. The quality guidelines Q1-Q14 outline aspects such as stability studies, impurities testing and the manufacturing process. The safety guidelines S1-S12 describe the requirements for assessing toxicity, carcinogenicity, and all other health risks. The efficacy guidelines E1-E16 outline the design and performance of clinical trials. Finally, a fourth category is reserved for multidisciplinary guidance which cannot be clearly

Table 1.1: The ICH Q1 stability safety guidelines

| Guideline Title | |
|-----------------|--|
| Q1A | Stability Testing of New Drug Substances and Products |
| Q1B | Stability Testing: Photostability Testing of New Drug Substances and Products |
| Q1C | Stability Testing for New Dosage Forms |
| Q1D | Bracketing and Matrixing Designs for Stability Testing of New Drug Substances and Products |
| Q1E | Evaluation of Stability Data |
| Q1F | Stability Data Package for Registrations Applications in Climatic Zones III and IV |

assigned to one of the aforementioned categories.

The guidelines which direct the design and implementation of stability studies are the ICH Q1A-F guidelines. Additional guidelines are also provided for biotechnological/biological products in Q5C. A brief outline of the ICH Q1 guidelines is given in Table 1.1.

1.3.1 Traditional Stability Studies

The ICH Q1A(R2) guidelines outline the stability requirements for the registration of new drug substances and products (ICH, 2003). The storage conditions specified in the guidelines for products targeted for storage at room temperature are shown in Table 1.2, however the ICH state that these conditions can be adapted provided sufficient justification is given.

Table 1.2: General storage conditions recommended for traditional stability studies for products to be stored at room temperature, as described in ICH Q1A (R2).

| | Storage condition | Minimum study duration for submission |
|---------------------|-------------------|---------------------------------------|
| Long term (Zone II) | 25°C/60%RH | 12 months |
| Long term (Zone IV) | 30°C/75%RH | 12 months |
| Intermediate | 30°C/60%RH | 6 months |
| Accelerated | 40°C/75%RH | 6 months |

The ICH recommends testing at regular intervals, and for the long term condition they recommend testing every 3 months during the first year, then every 6 months during the second year, and annually thereafter (ICH, 2003).

Within the ICH guidelines, it is stated that alternative approaches may be employed provided that sufficient scientific justification is given (ICH, 2003). Whilst this opens

the floor to alternative science-based stability approaches, it provides no guidance for the industry or the regulatory authorities as to how these studies should be performed, interpreted and assessed (McMahon *et al.*, 2021). In lieu of this guidance, implementing these alternative approaches carries a high risk, in terms of both time and cost, if regulators request further data to satisfy their criteria.

1.3.2 Accelerated Predictive Stability Studies

Industrial interest and use of accelerated predictive stability (APS) approaches has increased in recent years (Qiu, 2018a; McMahon *et al.*, 2021; Williams *et al.*, 2017). These types of techniques are also sometimes referred to as science and risk-based stability studies (S&RB) or risk-based predictive stability studies (RBPS). These approaches offer research and development scientists a tool to rapidly screen formulations and also to assess packaging selection and identify potential stability issues prior to performing real-time studies. These benefits reduce both the time and resources required compared to traditional stability testing, allowing for medicines to be reach the end consumer faster and at a lower cost.

APS studies replace the traditional storage conditions of 25°C/60%RH and 40°C/75%RH with a number of temperature and humidity conditions which span a wider range of temperatures and humidities, for example, 50 to 80°C and 11 to 75%RH (Qiu, 2018b; Williams *et al.*, 2019). The more storage conditions which are assessed, generally, the more reliable a predictive stability model may be, provided that the temperature and relative humidity are independently varied to an adequate degree to create a robust modelling design space. Relative humidity describes the amount of moisture in the air, relative to the maximum volume of water which could be held in the air at a given temperature. With increasing temperature, the maximum amount of moisture which can be held increases, meaning that more moisture is required to maintain the same relative humidity. At 25°C, the saturation point of moisture in the air (i.e. 100%RH) is when the air holds 20 g/m³ of moisture.

During APS studies, it is assumed that there is no change in the physical state of the API, and so the use of techniques such as powder X-ray diffraction may be required

to confirm the state of the API after storage under accelerated conditions (Williams *et al.*, 2019).

During a traditional stability study, sampling timepoints are typically quite long. For example, testing may occur after 3 months of storage, 6 months of storage, 12 months of storage (ICH, 2003). In an APS study, the sampling timepoints will be very short, for example, a matter of days or weeks (Waterman, 2011; Waterman *et al.*, 2007). This is beneficial as it drastically reduces the time required for stability studies, allowing for rapid screening of formulations or studies to assess potential packaging selections.

1.4 Tablet Performance – Disintegration and Dissolution

Stability studies are essential for assessing both the safety and quality of a product. The performance of a tablet is often measured by its dissolution rate, as the *in vivo* dissolution of the API is pivotal to inducing a therapeutic effect. Any change in the dissolution and disintegration performance of a tablet during storage could indicate a change in the bioavailability of the formulation, and therefore the disintegration and dissolution are important properties to consider from a stability standpoint.

1.4.1 Tablet Disintegration

The disintegration of a tablet describes the process of the interparticle bonds within a tablet breaking upon contact with liquid, leading to the tablet breaking apart into smaller particles. This process begins when the tablet comes into contact with a liquid (the disintegration medium), at which point several mechanisms may begin to occur at different rates and to different extents depending on the tablet formulation and properties.

Firstly, the disintegration medium will begin to wet the tablet surfaces and penetrate the tablet via pores in the microstructure (Nogami *et al.*, 1967). This can trigger the dissolution of soluble particles within the matrix, which may be either the API or soluble excipients such as lactose or mannitol. As particles dissolve, the pore space expands which allows further liquid penetration of the disintegration medium, as well

as weakening the microstructure.

Another process which may occur is the expansion of particles of certain materials, known as tablet disintegrants. Disintegrants are a class of excipient which are used in formulations to promote rapid disintegration. The most common disintegrants can be classified as either swelling (e.g. croscarmellose sodium (CCS) and sodium starch glycolate (SSG)), or shape recovery (e.g. crospovidone (XPVP)). Swelling disintegrants have the capacity to absorb vast quantities of liquid upon contact with a disintegration mechanism, resulting in the omni-directional swelling of disintegrant particles (Desai *et al.*, 2016; Markl *et al.*, 2017; Quodbach & Kleinebudde, 2016). In the case of shape recovery disintegrants, contact with liquid results in the uni-directional expansion of disintegrant particles against the direction of compression. For shape recovery disintegrants, expansion is a result of the release of energy stored during compaction (Markl *et al.*, 2017). Regardless of the mechanism, this particle expansion will fill the surrounding pore space, and subsequently result in a force being exerted against the surrounding matrix as the particle continues to expand against the pore walls. When this swelling force exceeds the interparticle bonds within the tablet, the bonds between particles will break (Desai *et al.*, 2016; Patel & Hopponen, 1966).

Each of these processes ultimately contributes towards the overall weakening of interparticle bonds, allowing the disintegration of the tablet into smaller and smaller particles. The increased surface area that results from this process then contributes towards faster dissolution.

Recent publications have provided extensive reviews on the disintegration process (Quodbach & Kleinebudde, 2016); tablet disintegrants (Desai *et al.*, 2016); disintegration measurement techniques (Markl & Zeitler, 2017); and an update on recent studies with respect to disintegration (Berardi *et al.*, 2021).

1.4.1.1 Disintegration Testing

The pharmacopoeial disintegration test is based on a simple apparatus consisting of basket-rack assembly with 6 vertical tubes with an open top and a wire-mesh base. The basket rack is attached to a mechanical arm in the tester and suspended over a beaker

of disintegration medium in a water bath (USP, 2020a). When the medium reaches the target temperature of the test (often 37°C to mimic body temperature), a tablet is placed in each tube and the basket is then lowered and raised into and out of the disintegration medium at a fixed dip speed (29 to 32 cycles per min, as per USP (2020a)) and stroke height (53 to 57 mm, as per USP (2020a)). The basket is raised and lowered for the duration of the test, and at the end tablets are assessed to ensure disintegration has taken place - i.e. the tablet has broken apart sufficiently to pass through the wire base of the tube (USP, 2020a). Plastic discs are placed on top of the product in the tube, for example, to prevent the product from floating and ensure complete wetting (USP, 2020a).

During drug product development, disintegration testing is routinely performed using the pharmacopeial apparatus described above. However, this apparatus and testing procedure does not provide any mechanistic information on the disintegration process. This gap in the knowledge has been addressed by several research groups, who have applied novel approaches to assess the disintegration process in more detail. For example, several studies in the literature employ magnetic resonance imaging (MRI) (Dvořák *et al.*, 2020; Quodbach *et al.*, 2014a,b), broadband acoustic resonance spectroscopy (BARDS) (O'Mahoney *et al.*, 2020), and terahertz spectroscopy (Al-Sharabi *et al.*, 2020; Markl *et al.*, 2017; Yassin *et al.*, 2015) to develop a deeper understanding of the of disintegration process.

1.4.2 Tablet Dissolution

Dissolution of the API is an essential pre-requisite for the drug to reach systemic circulation where it facilitates a therapeutic effect. The dissolution performance of a product must be studied, and changes in the dissolution rate during storage must be investigated due to the implication that these changes may have on the bioavailability of the drug.

Dosage forms may be classified as immediate- or controlled-release. Immediate-release tablets are those which are designed for rapid disintegration and dissolution, such that the therapeutic effect of the API happens soon after administration of the product, for example, rapid onset of pain relief for head aches or stomach pains. For

these products, specific formulation and manufacturing tactics may be employed to ensure the disintegration and dissolution of the tablet occurs quickly. For example, the API may be micronised to increase the surface area, leading to faster dissolution, and disintegrants may be added to the formulation to ensure rapid disintegration. In the case of controlled-release, tablets may be designed to release the drug slowly in order to maintain a concentration within the therapeutic window over a prolonged period of time, for example, pain medication for those with chronic illness, or products such as the contraceptive implant.

1.4.2.1 Dissolution Testing

In vitro dissolution testing is used across industry as a quality control (QC) test. Development of a suitable dissolution test method requires careful selection of the apparatus, dissolution medium, sampling timepoints, and paddle speed in order to develop a method which is both robust and suitably discriminatory to detect changes in performance.

Apparatus. The USP describes seven different types of apparatus for use in dissolution testing (USP, 2020b). The rotating basket (USP Apparatus I) and the paddle method (USP Apparatus II) are the most commonly used, however other apparatus may be needed depending on the intended use. The reciprocating cylinder (USP Apparatus III) allows testing to be performed across several medium within a single test, allowing a range of pH to be used in order to mimic the change in physiological conditions through the gastrointestinal (GI) tract (Dressman & Kramer, 2005). In terms of the paddle apparatus, this is a simple set-up which allows testing to be performed with large volumes of medium, typically up to 1000 mL. The apparatus comprises of round-bottom cylindrical glass vessels, which are filled with the dissolution medium. A metal paddle spins axially in the centre of the vessel to provide gentle mixing of the media, and the tablet is simply dropped into the vessel to begin the test (USP, 2020b). This apparatus is robust and well-suited to automation through the addition of an autosampler, which could carry small volumes samples directly from the vessels,

through a filter, and towards a UV detector or into vials for further analysis by liquid chromatography (LC).

Dissolution medium. The selection of dissolution medium for a test will vary depending on the physicochemical properties of the API, as well as some formulation factors. Typically, it is preferable to use aqueous media, and the dissolution test is usually performed at 37°C to simulate body temperature (FDA Centre for Drug Evaluation and Research, 1997). The pH of the media is often within the physiological range, and the choice of pH will depend on both the area of the GI tract in which the dose will dissolve, as well as the pK_a of the API (Krishna & Yu, 2008). The volume of dissolution media, as well as the optional addition of surfactant, will depend on the solubility of the API. Ideally, dissolution testing is performed under sink conditions, whereby the volume of test media is sufficient to dissolve multiple times (often triple) the nominal dose. For poorly soluble drugs, it may be necessary to add a surfactant such as sodium dodecyl sulfate (SDS) or polysorbate to the dissolution medium in order to achieve sink conditions (Krishna & Yu, 2008). Dissolution testing may also be performed using biorelevant medium, which is designed to better mimic *in vivo* dissolution under physiological conditions. Simulated gastric fluid (SGF) and simulated intestinal fluid (SIF) are both compendial media which are prepared to pH 1.2 and 6.8, respectively. More recently, these media have been further developed to simulate 'fasted' and 'fed' conditions (FaSSIF and FeSSIF) by including varying levels of bile salts and phospholipids at varying pH. These media were originally developed by Galia *et al.* (1998), but several variations to the composition have been proposed over the years to try to achieve a media as close as possible to realistic conditions (Fuchs *et al.*, 2015; Jantratid *et al.*, 2008; Kossena *et al.*, 2004; Psachoulis *et al.*, 2012).

Hydrodynamics. In terms of the paddle apparatus, hydrodynamics within the vessel are controlled by determining the paddle speed. Typically, paddle speeds of 50 rpm or 75 rpm are used (Dressman & Kramer, 2005), however in some cases higher speeds are required to obtain sufficient agitation. Due to the vessel shape and hydrodynamics of the paddle spinning, in some cases coning may occur, whereby powder from a tablet

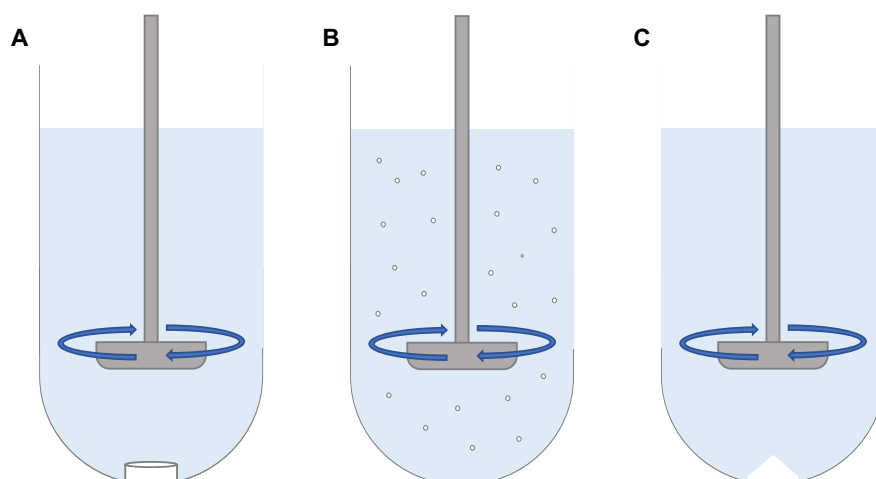


Figure 1.3: The USP II (paddle) apparatus (A) at the beginning of a dissolution test, (B) with dissolution in progress and the particles dispersed throughout the dissolution media as it stirs, and (C) with powder coning at the base of the vessel.

settles in a small mound at the base of the vessel and is not exposed to adequate shear forces to fully wet the material. This is generally caused by high density excipients, such as dibasic calcium phosphate anhydrous (DCPA). In these cases, low rates and extents of dissolution may be observed due to inefficient agitation within the vessel (Dressman & Kramer, 2005; Krishna & Yu, 2008). An increased paddle speed may be required to prevent this hydrodynamic artefact. To combat the effects of coning without increasing the paddle speed, a modified vessel has been proposed as an alternative to the standard round-bottom vessel. The Apex vessel has a peak in the centre of the base of the vessel, directly under the paddle, thus minimising the build-up and settling of powder in this zone (Collins & Nair, 1998). In recent years, efforts have been made to standardise the use of apex vessels in an industrial setting to prevent coning issues and improve the robustness of dissolution methods (Mann *et al.*, 2021).

1.4.3 The Influence of Formulation on Tablet Performance

The first edition of the Handbook of Pharmaceutical Excipients (published in 1986) contained monographs for 145 excipients. Now on the ninth edition, this handbook now

contains detailed entries for 420 different excipients for use in pharmaceutical preparations (Shesky *et al.*, 2020). Given the wide range of excipients available, developing an in-depth understanding of the impact of each excipient on the performance of a formulation is not possible. However, many studies have assessed specific physicochemical properties, for example, solubility and hygroscopicity, to develop a general understanding of the relationship between the physicochemical properties of the excipients and the performance of the drug product.

1.4.3.1 Solubility

Solubility describes the maximum amount of a material which can dissolve in a specified medium (often water) and at a specific temperature (20°C or 25°C are typically used as examples). Solubility should be measured after a period of time to ensure that the equilibrium solubility is reported.

It has been demonstrated that the use of insoluble tablet fillers results in faster disintegration compared to soluble fillers. (Berardi *et al.*, 2018; Johnson *et al.*, 1991; Rubinstein & Birch, 1977). In the case of insoluble fillers, the force resulting from the expansion and swelling of disintegrant particles is fully exerted against the surrounding matrix, resulting in effective disintegrant action. If a tablet is composed mainly of soluble materials, liquid penetration and wetting will result in the dissolution of filler particles, thus hindering the effectiveness of disintegrant swelling.

Some studies suggested that the use of soluble fillers may hinder liquid penetration by increasing the viscosity of the dissolution medium in the tablet pores (Rubinstein & Birch, 1977), however, it is generally believed that this increase in medium viscosity would be negligible relative to the overall disintegration and dissolution of the tablet.

More recently, Ekmekciyan *et al.* (2018) attributed the effects of solubility on disintegration performance to the tablet components (disintegrants and fillers) competing for the available water. It was demonstrated that soluble fillers required more water to dissolve compared to insoluble fillers which required only a small amount of water for full wetting, therefore leaving more water available for the hygroscopic disintegrants.

1.4.3.2 Hygroscopicity

The hygroscopicity of a material describes the ability of the material to absorb or adsorb moisture from the environment. The effect of composite hygroscopicity on disintegrant and dissolution has been assessed by Gordon & Chowhan (1987); Johnson *et al.* (1991); López-Solís & Villafuerte-Robles (2001). It has generally been found that lower hygroscopicity formulations promote faster disintegration and dissolution, which further supports the competition-for-water theory proposed by Ekmekciyan *et al.* (2018).

1.4.3.3 Disintegrant Selection

The effectiveness of disintegrants has been evaluated using different techniques in the literature. For example, a study by Zhao & Augsburger (2005a) found that for a range of disintegrant concentrations, croscarmellose sodium (CCS) performed better than crospovidone (XPVP) and sodium starch glycolate (SSG) in terms of rapid disintegration and dissolution. Through video imaging, it was observed that CCS promoted disintegration into finer, more uniform particles compared to SSG and XPVP, which created coarser particles after disintegration (Zhao & Augsburger, 2005a).

Aside from the choice of disintegrant, the excipient grade can also impact the performance of a tablet. For example, Mishra & Sauer (2022) compared 6 grades of low-substituted hydroxypropyl cellulose (L-HPC) and found that slower disintegration was observed for L-HPC grades with higher hydroxypropyl content and smaller particle sizes.

1.4.3.4 Disintegrant Concentration

The effect of varying disintegrant concentration has been evaluated in several studies. Zhao & Augsburger (2005a) found that for tablets composed of either DCPD or aspirin, differences could be observed in both the disintegration and dissolution when 1 and 2% wt. (DCPD tablets) or 1, 2, and 5% disintegrant (aspirin tablets) of CCS, XPVP and SSG were used. This study demonstrated that for both tablet bases, the performance was improved for tablets containing 2 or 5% disintegrant, compared to those with 1%. For aspirin tablets, the dissolution rate of tablets with XPVP and SSG was significantly increased with higher disintegrant concentrations. For example, at 1% wt. XPVP, only

15% of the aspirin was dissolved after 45 min. When the XPVP concentration was increased to 5% wt., dissolution reached 100% within 45 min.

1.4.4 The Influence of Manufacturing Processes on Tablet Performance

Following formulation selection, the excipients and API must be processed together to produce the final dosage form. There are a number of options for pharmaceutical manufacturing, with the preferred option being direct compression. Direct compression is the process by which powder excipients and APIs are blended together and then compressed to produce a tablet with no additional processing steps. This is usually the first choice of manufacturing process as it is the most time and cost effective process, with no additional operations or materials required. Direct compression is well-suited to APIs which are heat- or moisture-sensitive, as neither are required in the manufacturing process. This manufacturing process also lends itself to continuous manufacturing, which offers many benefits with regards to scale-up of manufacturing.

Depending on the material properties of the API and blend, it may be the case that direct compression is not an appropriate manufacturing technique. To produce a batch of directly compressed tablets, it is important that the powder blend has adequate flowability and compaction properties (Leane *et al.*, 2015). In many cases, the API may exhibit poor flowability or compaction properties. Whilst it is sometimes possible to tailor the excipient choice and concentrations to mitigate these effects, tablets with high drug loading or very poor material properties may not be possible to manufacture by direct compression.

In cases where direct compression is not a viable option, a granulation step is introduced. Granulation processes fall into two categories – dry granulation, or wet granulation. Dry granulation involves the pre-compression of powder blends to form either a ribbon or a large compact, which is then crushed using a sieve to produce granules. In the case of wet granulation, the powder blend is mixed with a binder solution before being roughly sieved to break apart large clumps of material. This sieved mixture is then dried, before being sieved to the desired granule size. Following granulation, more

excipients may be blended with the granules, for example disintegrants or lubricants, and then the mixture is compacted to produce tablets (Leane *et al.*, 2015; Suresh *et al.*, 2017).

With each additional step in the manufacturing process, additional factors are presented which may influence the final performance of the product. Some of these factors which have been discussed in the literature are addressed below.

1.4.4.1 Compression Force

For directly compressed tablets, the porosity of a tablet is the combination of both the intraparticle porosity of the tablet components and the interparticle porosity resulting from the compaction process. The porosity of a tablet will directly influence the rate of liquid penetration, as larger pores allow for faster liquid penetration, whilst lower porosity can impede liquid penetration through the tablet. As discussed previously, liquid penetration is the necessary pre-requisite for disintegration or dissolution, and the wetting of the tablet may then trigger the other disintegration mechanisms, such as swelling or dissolution. As such, the compression force and porosity are likely to play a critical role in the disintegration and dissolution of many formulations. It is generally expected that increased porosity results in faster disintegration, partly due to the increased potential for liquid penetration, and also due to the weaker mechanical strength of the tablet (Sun, 2017; Sunada & Bi, 2002).

1.4.4.2 Granule moisture content

Gordon *et al.* (1993) investigated the effect of granule moisture content on the dissolution rate of tablets composed of either lactose, naproxen, or DCP. The results showed that whilst moisture content did impact dissolution performance, the effects were specific to each formulation tested and so cannot be generalised (Gordon *et al.*, 1993).

1.4.4.3 Mode of disintegrant addition

If tablets are manufactured by wet or dry granulation, the disintegrant may be added either intra-granularly (prior to granulation), extra-granularly (after the granulation

step), or may be distributed between both phases.

The effectiveness of intra- or extra-granular disintegrant incorporation has been assessed by several different researchers, however conflicting results have been found. This likely indicates that the optimal mode of disintegrant addition is dependent on a number of different formulation-based factors, for example, the solubility, hygroscopicity, porosity or moisture content of the tablet.

Gordon *et al.* (1990) compared the dissolution and friability of naproxen tablets manufactured with CCS added either intra- or extra-granularly. The results indicated that the fastest dissolution could be achieved through intra-granular incorporation of CCS (Gordon *et al.*, 1990). In 1993, another study by Gordon *et al.* (1993) assessed intra- and extra-granular addition of CCS, XPVP, and SSG, using dissolution as a measure of the effectiveness of each mode of incorporation. In most cases (26 out of 27 formulations tested), it was found that a combination of intra- and extra-granular disintegrant provided the fastest dissolution. This result was also supported by Khattab *et al.* (1993), based on a study of CCS, XPVP, and SSG which found combined incorporation at the intra- and extra-granular level to deliver the most rapid dissolution.

1.5 The Influence of Formulation on Physical Stability

The effects of formulation properties such as solubility and hygroscopicity on the disintegration and dissolution performance of a product were discussed in Section 1.4.3. Given the influence that these properties have on the performance of a product prior to storage, it follows that these properties may also affect the performance when exposed to accelerated temperature or humidity conditions.

1.5.1 Solubility

The role of filler solubility on the stability of tablets was assessed by Gordon & Chowhan (1990); Molokhia *et al.* (1982). In both cases, tablets composed of soluble fillers displayed increases in hardness after storage at high humidity. This was attributed to the partial dissolution and recrystallisation of soluble particles upon expose to high humid-

ity conditions. In addition to adversely affecting the mechanical strength of tablets, (Gordon & Chowhan, 1990) also demonstrated that reduced dissolution rates were observed for tablets composed of soluble materials post-storage.

1.5.2 Hygroscopicity

In the same study, Gordon & Chowhan (1990) also compared the effects of filler hygroscopicity on the physical stability. It was observed that tablets containing hygroscopic materials showed decreases in dissolution rate after storage, compared to those containing non-hygroscopic fillers. This is likely due to the absorption of moisture by hygroscopic materials, such as disintegrants, during storage at high humidity. Several studies have demonstrated decreased efficiency of disintegrants after storage at high humidity (Gordon & Chowhan, 1990; Hersen-Delesalle *et al.*, 2007; Hiew *et al.*, 2016; Li *et al.*, 2004; Quodbach & Kleinebudde, 2015). Generally, decreases in disintegration efficiency, increases in disintegration time, or decreases in dissolution rate are observed after exposure to high relative humidity. This is attributed to the premature swelling of disintegrants, either due to the absorption of moisture from the high humidity environment directly (Hersen-Delesalle *et al.*, 2007), or due to the plasticisation of moisture enabling the partial release of shape recovery energy from XPVP (Hiew *et al.*, 2016; Quodbach & Kleinebudde, 2015).

1.6 Physical Tablet Properties and the Effects of Storage

Predicting the effects of storage on physical tablet properties offers several unique challenges. As physical properties are not necessarily controlled by chemical reactions, a more mechanistic approach is often required to understand the underlying driving force of change. Additionally, many physical properties share complex interrelationships which can be challenging to unravel. For example, changes in porosity are likely to occur simultaneously with changes in tensile strength, as a higher porosity suggests fewer contact points between particles, and therefore weaker interparticle bonds. A softer tablet might be expected to dissolve faster as the barrier to overcome inter-

particle bonds is lower, however, the increase in porosity may result in less efficient disintegrant performance, which could actually slow the disintegration process. These mechanisms and stability changes are often also dependent on the formulation, and given the wide range of pharmaceutical excipients, active pharmaceutical ingredients and manufacturing process/process settings, there are many aspects to consider when comparing separate studies from the literature.

1.6.1 Tensile Strength

The tensile strength of a tablet (also called the breaking force) is a measure of the mechanical strength of the tablet. A tablet must have sufficient tensile strength, or else there is a risk that it could be damaged or deformed during handling or shipping. Equally, if the tensile strength is too high then this risks hindering the disintegration process as the interparticle bonds will be stronger and therefore more difficult to disrupt.

In the literature, many different groups have investigated the effect of storage at accelerated temperature and/or humidity conditions on the mechanical properties of the tablet. In particular, many studies include measurements of the tablet hardness as it may be expected to affect the disintegration rate of tablets. Previous studies have reported both increases and decreases in the hardness of tablets after storage, depending on the formulation design (including disintegrant choice), the manufacturing process parameters and the storage conditions.

Ahlneck & Alderborn (1989) investigated the impact of storage for 30 days at high humidity on pure DCP tablets. The authors found no change in hardness, except for tablets stored at 100%RH. For these tablets, it was further found that subsequent transfer of the tablets to lower humidity conditions (33 or 68%RH) led to recovery of the original hardness value.

Tablet hardness studies were also performed on tablets composed of pure disintegrant for both CCS and XPVP (Bauhuber *et al.*, 2021). In this study it was found that storage at 40°C/75%RH for just 1 day led to a decrease in hardness of around 70% for tablets composed of CCS (after which point the hardness remained fairly constant for the remainder of the study), whilst XPVP tablets softened below the minimum threshold

for measurement. Decreases were also observed for both disintegrant tablet batches after storage at ambient conditions 21°C/50%RH, however the softening of tablets was markedly less for the lower temperature and humidity conditions.

Several studies have demonstrated decreases in tablet hardness for DCP-based tablets containing 2.5% disintegrant stored at high humidity conditions (Horhota *et al.*, 1976; Lausier *et al.*, 1977). These studies also show that the decrease in hardness occurs within the first 7 (Lausier *et al.*, 1977) and 10 (Horhota *et al.*, 1976) days of storage, after which point the hardness remains relatively constant. Lausier *et al.* (1977) found that the decrease in tablet hardness correlated with a decrease in tablet weight, suggesting that the change in tensile strength could be a result of the loss of waters of hydration during storage. A study by Chowhan (1980a) found that tablets composed of DCPD with 10% starch disintegrant decreased in hardness after storage at 23°C/93%RH, whilst tablets stored at 23°C/44%RH increased slightly within the first day of storage before remaining constant for the remainder of the study. For the tablets stored at 93%RH, post-storage equilibration at a lower humidity of 44%RH after resulted in a slight recovery of tablet hardness.

It has been suggested that increases in tablet tensile strength for tablets composed of mainly soluble materials are a result of the partial dissolution and subsequent recrystallisation of soluble particles, leading to increased bonding and the formation of solid bridges (Chowhan, 1980b; Molokhia *et al.*, 1982). Molokhia *et al.* (1982) stored tablets with a range of different fillers for up to 8 weeks at 50°C/50%RH and 40°C/90%RH and found varying results. Tablets composed of mannitol and lactose both showed increases in tensile strength after storage at high humidity, which the authors attributed to the partial dissolution and recrystallisation of these soluble fillers. However, in the same study, tablets composed of sorbitol showed decreases in tensile strength. Tablets containing tricalcium phosphate and cellulose both showed little change in hardness after storage (Molokhia *et al.*, 1982). These results suggest that we cannot make a conclusive statement about the effect of matrix solubility on the tablet hardness during storage, as both increases and decreases are observed from soluble components such as sorbitol, mannitol and lactose.

The effect of both filler selection, disintegrant selection, and disintegrant concentration have also been the subject of investigation by various research groups (Hersen-Delesalle *et al.*, 2007; Marais *et al.*, 2003; Sacchetti *et al.*, 2017; Uhumwangho & Okor, 2005). Marais *et al.* (2003) found that the decrease in tensile strength of microcrystalline cellulose (MCC)-based tablets after storage at high humidity was greater with increasing concentrations (0.625 to 10% wt.) of CCS. In terms of disintegrant choice, Uhumwangho & Okor (2005) found that paracetamol tablets showed no effect of storage on hardness for tablets containing maize starch as a disintegrant, whereas tablets formulated with α -cellulose as the disintegrant showed decreases in hardness during storage at 100%RH. Hersen-Delesalle *et al.* (2007) compared the change in hardness for tablets with XPVP, CCS and SSG and found that XPVP resulted in the largest decrease in tensile strength. In fact, visible cracks and defects were found when the tablet surface was examined with a microscope, with larger cracks being found on XPVP-containing tablets than for the other disintegrants. The formation of these defects was attributed to the premature swelling of disintegrant particles upon exposure to high humidity, resulting in the disruption of interparticle bonds and consequently decreasing the tablet hardness (Hersen-Delesalle *et al.*, 2007). Sacchetti *et al.* (2017) performed a systematic study of tablets formulated with 3 different API, each with different fillers and disintegrants. The tablets were stored at 40°C/75%RH and the results showed that large amounts of sorbed water exerted force on the surrounding matrix, leading to weakening of the interparticle bonds. The authors found that the weakening of interparticle bonds is greater for tablets containing brittle rather than plastically-deforming fillers (Sacchetti *et al.*, 2017).

1.6.2 Disintegration & Dissolution

The disintegration and dissolution performance of a drug product are key attributes which must not change significantly during the shelf-life of a product. Ensuring that product performance is not significantly affected by temperature or humidity is important when considering potential conditions during the shipment of tablets, or for products marketed in different climatic zones. The current literature on the effects of

ageing on disintegration and dissolution performance demonstrate that a wide range of factors may influence the product stability.

In most cases, a general trend of increasing disintegration time and decreasing dissolution rates is reported in the literature (Bauhuber *et al.*, 2021; Chang *et al.*, 2008; Chowhan, 1980a; Horhota *et al.*, 1976; Lausier *et al.*, 1977; Li *et al.*, 2004; Marais *et al.*, 2003; Molokhia *et al.*, 1982; Quodbach & Kleinebudde, 2015; Rohrs *et al.*, 1999; Sacchetti *et al.*, 2017; Uhumwangho & Okor, 2005), however, drawing direct comparisons between these studies is challenging due to the wide range of formulations, manufacturing processes/settings, storage conditions, and storage times used in different studies.

Horhota *et al.* (1976) found a decrease in dissolution rate for DCPD-based tablets stored at 65°C/40%RH after storage for 20 and 30 days, but a much smaller change in tablets stored at 23°C/75%RH and 45°C/75%RH for the same duration. A decrease in dissolution rate was also observed for DCPD-based tablets by Lausier *et al.* (1977), who found that storage at 25°C/50%RH caused an increase in disintegration time from 2.5 to 5 mins over 16 weeks of storage. In contrast, the tablets stored at 45°C/75%RH showed no significant change in dissolution rate during the first 8 weeks of storage, after which point there was a sharp decrease in dissolution rate for the remainder of the storage time. The disintegration time of these samples was found to decrease within the first week, after which point it remained constant – similarly to the change in tensile strength of these tablets (Lausier *et al.*, 1977).

DCPD-based tablets were also used by Chowhan (1980a), who found that the disintegration time of tablets drastically increased after storage at 93%RH, but could be somewhat recovered by storing the samples at 44%RH for 1 day before testing. This study also reported a decrease in dissolution rate, with high variability between the dissolution profiles after 14 weeks of storage. This variability was attributed to variability between the surface area during the dissolution test, caused by the slow disintegration of the tablets.

The change in dissolution of tablets containing different fillers was investigated by Molokhia *et al.* (1982), and it was found that storage for 8 weeks at 40°C/90%RH and 50°C/50%RH resulted in slower disintegration and dissolution of tablets composed of

sorbitol, mannitol, and lactose. However, tablets composed of tricalcium phosphate and cellulose both showed no effect of storage. In the case of mannitol- and lactose-based tablets, storage also resulted in increased tensile strength of tablets, which may reduce the dissolution rate due to the stronger interparticle bonds. On the other hand, the decrease in dissolution rate of sorbitol-based tablets was accompanied by a decrease in tensile strength, which was attributed to moisture absorption during storage.

Changes in dissolution rate may also occur as a result of chemical changes during storage, for example, Rohrs *et al.* (1999) used solid state NMR and infrared spectroscopy to confirm the conversion of delavirdine mesylate from the salt to the free base form upon exposure to high humidity. As a result, the authors attributed the associated decrease in dissolution rate to two mechanisms – firstly, the decreased solubility of the free base compared to the salt; and secondly, the protonation of CCS by methanesulfonic acid released from the salt form, which could affect the disintegrant efficiency (Rohrs *et al.*, 1999).

A study by Chang *et al.* (2008) demonstrated decreased dissolution rates of capsules containing lactose-based granules after storage at 40°C/75%RH, as well as the formation of pellicles on the granules. In the case of mannitol-based granules, neither a slowdown in dissolution nor pellicle formation were observed. This decrease in dissolution rate was attributed to the cross-linking of the gelatin capsule shell with molecules of lactose during storage.

1.7 Modelling & Predictions

In recent years, the advances in risk-based predictive stability (RBPS) and lean stability approaches has led to the publication of several papers on the application of these techniques, or novel approaches, to modelling and predicting changes in dissolution behaviour during storage.

The Accelerated Stability Assessment Program (ASAP) and the associated software (ASAP*prime*®) was originally proposed and developed by Waterman *et al.* (2007) as a novel approach to carry out accelerated stability studies for chemical degradation. This approach focuses on the concept of the isoconversion time, which is the time taken

for the product to reach the specification limit (i.e. the ‘time to failure’) for a given temperature and humidity condition (Waterman, 2011). This data is then considered with respect to a moisture-corrected Arrhenius equation in order to predict the ‘time to failure’ under long-term storage conditions, e.g. 25°C/60%RH. This approach is well suited to chemical degradation, which can be expected to follow Arrhenius behaviour, however the physical stability of tablets may not always follow Arrhenius behaviour. More recently, this approach has been applied to dissolution studies, with the obtained predictions being accurate to the data from long-term stability studies (Li *et al.*, 2016).

Another approach for predicting long-term dissolution profiles was proposed by Scrivens (2019), which assumes that during storage, the shape of dissolution profiles remains constant and can therefore be overlapped with the adjustment of the x-axis (time). In this approach, dissolution profiles are fit to a Weibull curve, which defines a rate parameter (k_d) and a shape parameter (b) for each profile. Based on the assumption that the profile shape does not change, b is fixed for a given formulation or batch. An ‘acceleration factor’ (AF) is then calculated as the ratio of the rate constants before and after storage (Scrivens, 2019). Using profiles of the acceleration factor as a function of time, a first-order exponential decay curve is used to model the rate of change in AF (k_s) and the plateau which AF approaches (AF_{inf}). Using the k_s and AF_{inf} values for a range of temperatures and conditions, multiple linear regression (MLR) can then be applied to determine temperature and humidity coefficients for a given batch, allowing for the prediction of dissolution profiles after long-term storage (Scrivens, 2019).

More recently, Tsunematsu *et al.* (2020) used analysis of the available surface area to predict changes in the dissolution performance on stability. This approach aimed to bridge the gap between empirical and mechanistic predictions of dissolution stability by basing long-term dissolution stability predictions on the change in available surface area of the API. In this approach, the dissolution profiles are modelled to obtain rate and shape parameters, which are then used to determine new parameters ($T_{22.1}$ and $T_{63.2}$), which describe the time taken to generate 22.1% and 63.2%, respectively, of the total available surface area for dissolution (S_t) (Tsunematsu *et al.*, 2020). Profiles of S_t can be used to visualise the release of API from the dosage form, as the surface area will show

a rapid increase during disintegration, then subsequently decrease as the API dissolves. If the disintegration step is not present, and drug release is based on erosion, this initial increase in the profile of S_t will not be present (Tsunematsu *et al.*, 2020). To determine a predictive model based on changes in S_t , Tsunematsu *et al.* (2020) compared both linear and non-linear regression in order to find the most appropriate model to describe changes in $T_{22.1}$ and $T_{63.2}$ using data from four different temperature conditions. This approach allowed for the accurate prediction of the dissolution profile after storage for 6 months at 40°C/75%RH.

1.8 Conclusion

Stability studies are crucial to the drug product development process, with the data being used to optimise the formulation and manufacturing settings; determine the packaging requirements; assign the retest date or shelf life; and contribute towards regulatory submissions. Recently, industrial interest in the application of APS approaches has increased. These techniques allow for the accurate prediction of the rate and extent of chemical degradation in a matter of weeks. However, equivalent approaches for the prediction of physical stability are not yet available as changes in the physical properties of tablets may not follow the Arrhenius behaviour which underlies most APS models. Currently, the underlying mechanisms of change in physical tablet properties are not well defined in the literature. A systematic approach is required to distinguish the effects of different API and excipient properties on the physical stability of pharmaceutical tablets, and to elucidate the underlying mechanisms of change. With an improved understanding of these mechanisms, mechanistic models could be developed to better predict the physical stability of tablets.

Chapter 2

Aims and Objectives

With the increasing industrial interest in the development and application of accelerated predictive stability techniques for the prediction of chemical degradation, the demand for equivalent tools to predict physical stability is growing. Currently, most APS techniques are based on a moisture-corrected Arrhenius equation. In the case of physical stability, storage effects are not always based on chemical changes, and therefore we cannot assume Arrhenius behaviour and we must investigate alternative approaches which are adaptable to study the physical stability of pharmaceuticals.

The aim of this project is to investigate the application of accelerated stability techniques for the assessment of physical tablet stability, whilst also developing a mechanistic understanding of the relationship between the different physical tablet properties which may impact product performance during storage. This aim can be divided into several discrete objectives, outlined below.

1. To explore the performance-controlling disintegration mechanisms of directly compressed placebo tablets. Placebo tablets were manufactured to assess the mechanism of disintegration of tablets. This includes the characterisation of the raw materials, and the measurement of a range of physical tablet properties such as tensile strength, porosity, disintegration time, and contact angle. The proposed mechanisms were then probed by assessing additional tablets with varying porosity or disintegrant concentration. By generating a comprehensive understanding of the disintegration

mechanism and the critical formulation and processing properties which influence it, we can then predict the key properties which might influence performance during storage.

2. To examine the role of excipient properties and disintegration mechanism in the physical stability of placebo tablets. Using the placebo tablets characterised above, accelerated stability studies were performed using five temperature and humidity conditions (from 37°C to 70°C and 30% to 75% RH) for 2 and 4 weeks. After each timepoint, tablets were removed from storage and characterised to measure changes in the physical properties of tablets. Using this data, and considering the initial disintegration mechanisms, correlations between different properties were used to identify the key mechanisms of change during storage for each formulation.

3. To assess and predict the physical stability of drug loaded formulations, in particular, the disintegration and dissolution performance. Stability studies were repeated using selected formulations from the placebo study, with the addition of griseofulvin as a model API to enable dissolution studies to be performed. Correlations between the dissolution rate and the other physical properties after storage then provide a mechanistic insight into the dissolution shift. Finally, long-term dissolution stability was predicted using data collected during these accelerated studies.

An outline of the original and final study design, including details of the impact of COVID-19, is included in Appendix B.

Chapter 3

Materials & Methods

Chapter Summary

This chapter describes the materials and methods used throughout this thesis. The general methods included in this chapter are: raw material characterisation, tablet manufacture, sample storage under accelerated conditions, and analysis of the tablets. Where appropriate, further chapter-specific methods have been described in the individual experimental chapters.

3.1 Materials

Certificates of analysis and material data sheets for the excipients, as provided by the suppliers, are provided in Appendix C.

3.1.1 Tablet Excipients

Microcrystalline cellulose (MCC) (Avicel[®] PH-102, FMC International), mannitol (Pearlitol[®] 200 SD, Roquette), lactose (FastFlo[®] 316, Foremost Farms USA) and dibasic calcium phosphate anhydrous (DCPA) (Anhydrous Emcompress[®], JRS Pharma) were used as fillers for the tablet formulations.

The disintegrants used in these studies were croscarmellose sodium (CCS) (FMC International), crospovidone (XPVP) (Kollidon[®] CL, BASF), low-substituted hydroxypropyl cellulose (L-HPC) (LH-21, Shin-Etsu Chemical Co.) and sodium starch glycolate (SSG) (Primojel[®], DFE Pharma).

Magnesium stearate (Mallinckrodt) was used as a lubricant.

All of the excipients used in this study were chosen due to their widespread use in direct compression formulations. The fillers used in this study represent a broad range of physicochemical properties. MCC is a hygroscopic, insoluble filler which swells when in contact with liquid. DCPA is an insoluble filler which is non-hygroscopic. Lactose and mannitol are both soluble fillers. The disintegrants CCS, L-HPC and SSG are swelling disintegrants, whilst XPVP acts by shape recovery.

3.1.2 Active Pharmaceutical Ingredient

For the second phase of this project, tablets were manufactured with an active pharmaceutical ingredient (API) in order to compare the mechanisms observed for the placebo tablets with those containing a drug. For these purposes, a target API was selected based on a few criteria. Firstly, the selected API should not have any known chemical stability issues (including polymorphic transformations) within the limits of the study design (i.e. between 25 to 60°C and 30 to 75% RH) as these could result in changes to the physical properties of the tablet which are based on chemical stability issues, rather

than physical stability. This also included chemical interactions with other excipients, for example, any API containing primary amines in the structure would be unsuitable for this study as the Maillard reaction could occur between the API and lactose during storage at high temperatures. Secondly, the API should contain a chromophore such that it is easy to detect by HPLC with a UV-vis detector. Finally, the target API would ideally have moderate to low solubility. If an API with particularly high solubility was selected, it may be challenging to develop a dissolution method with suitable discriminating power to detect changes caused by the storage of these samples.

The API selected for this study was griseofulvin, a poorly soluble drug typically used in the treatment of fungal infections. Griseofulvin was obtained from VWR International Ltd. (Lutterworth, Leicestershire, UK).

3.1.3 Saturated Salt Solutions

Saturated salt solutions were prepared using sodium chloride, magnesium chloride and sodium bromide, all sourced from Merck Life Science UK Limited (Gillingham, Dorset, UK). To make the saturated salt solutions, the required salt was added in excess to bottles of purified water. Bottles were stirred with gentle heating (approx 40°C), and more salt was gradually added until no more salt could be dissolved. At this point, additional salt was added to ensure an excess amount of solid salt was present in the solution. To further ensure that the solution remained saturated during storage at high temperatures, additional solid salt was added to each vial of the saturated solution (see Fig 3.1), with the amount of salt filling approximately one third of each vial of salt solution. Upon removal from storage, each vial was checked to ensure that there was still solid salt in the base of the vial, to indicate that each solution was still saturated.

3.1.4 Surfactant

In Chapter 6, sodium dodecyl sulfate (SDS) was added to the dissolution medium (0.4% w/v SDS in water) to enhance the solubility of griseofulvin during dissolution testing. SDS was obtained from Fisher Scientific UK (SDS Micro Pellets (>99%), Fisher Scientific UK Ltd, Loughborough, Leicestershire, UK).

3.1.5 Storage of Materials

The tableting excipients were stored in sealed drums, as supplied. After opening and during use, materials were kept in the original drums under ambient temperature and humidity conditions (uncontrolled, due to the facilities within the formulation suite). Griseofulvin was stored in plastic bottles, as supplied, and only opened immediately prior to tableting.

3.2 Methods

3.2.1 Raw Material Characterisation

Each of the raw materials used in the tablet formulations were characterised to ascertain properties such as the moisture uptake and the true density. In addition, particle size and shape data was available for the excipients used in this study.

3.2.1.1 Dynamic Vapour Sorption

Moisture sorption isotherms were collected by dynamic vapour sorption (DVS) at 25°C for each excipient. Samples of approximately 10 mg were analysed using the DVS Advantage (Surface Measurement Systems, London, UK). Prior to analysis, samples were conditioned at 0% RH. After conditioning, the sample mass was recorded as the reference mass. The humidity was then increased in increments of 10% RH until 90% RH. At each stage, the change in mass was recorded once the balance reading had stabilised to less than 0.002% change in mass per minute.

To calculate the moisture sorption under specific storage conditions, additional DVS data was collected for each excipient at 37°C, 50°C and 60°C. Due to temperature limitations on the DVS instrument, moisture sorption data could not be collected at 70°C, and so 60°C was used instead.

The same DVS method described above for 25°C was used to screen several candidate drugs during the API selection phase, including griseofulvin, to assess the hygroscopicity of these API.

3.2.1.2 Particle Size & Shape

The shape and size of particles of each excipient was measured using a QICPIC instrument (Sympatec GmbH, Clausthal-Zellerfeld, Germany).

For each sample, the primary container was thoroughly mixed by rolling and inverting by hand, as well as using a spatula to stir. Sample sizes of approximately 2 g were gently agitated to evenly disperse the particles and reduce loss of material in the vials. Analysis was performed using the M7 lens. Each sample was measured in triplicate.

Particle size measurements were performed by Mithushan Soundaranathan for the manuscript ‘Exploring the Performance-Controlling Mechanisms of Tablet Disintegration’ (see page xvii), and the results are included in Chapter 4 for completeness.

3.2.1.3 True Density

The true density of each excipient and the API was measured using a gas pycnometer with nitrogen (MicroUltrapyc 1200e, Quantachrome instrument, Graz, Austria). Measurements were taken in triplicate for each sample.

3.2.2 Tablet Manufacture

All batches used in these studies were manufactured by direct compression. For each formulation, all excipients (and API, where included) were blended for 15 minutes in a Pharmatech AB-015 bin blender, with a speed of 20 rpm, and an agitator speed of 200 rpm. After 15 minutes, the blender was stopped and the magnesium stearate was added to the mixture. The blend was then mixed for a further 5 minutes under the same settings, before being transferred to be compressed into tablets.

Tablets were manufactured using a single-punch automated tablet press (FlexiTab, Bosch Packaging Technology Ltd). The tablet press was fitted with 9 mm flat round punches. The compression force and fill depth were adjusted based on the formulation to target a tablet weight of approximately 300 mg across each batch. Full details of the manufacturing settings for each batch are given in the experimental chapters.

3.2.3 Accelerated Stability Sample Storage

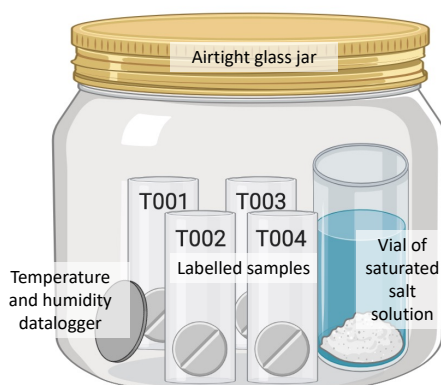


Figure 3.1: Experimental set-up for storage of stability samples

In order to perform stability testing, tablets were stored for set periods of time under accelerated temperature and humidity conditions. Tablets were stored in clear airtight glass jars, each containing an open vial of saturated salt solution to provide humidity control. Each tablet stored in the jar was placed in a labelled sample holder so that tablets could be traced throughout the stability study to calculate precise changes in weight and porosity for each tablet. Jars were sealed and stored in temperature controlled rooms (37°C and 50°C) or ovens (60°C and 70°C) for the required storage time, as described for each experimental chapter.

For placebo tablets, nominal conditions for humidity were assumed based on the saturated salt solution, as shown in the table below. For studies with the griseofulvin-containing tablets (Chapter 6), iButton data loggers were used to monitor both temperature and humidity during storage. For each batch and storage condition, one jar contained a DS1923 Hygrochron iButton Temperature/Humidity logger (Measurement Systems Ltd, Berkshire, UK). The dataloggers recorded the temperature and humidity ($\pm 0.5^{\circ}\text{C}$, 5%RH) every 600 seconds for the duration of storage. The use of data loggers ensures that the temperature and humidity is maintained throughout the duration of the stability study.

It should be noted that the glass jars used in this study were clear and therefore did

not protect the samples from light, however it is assumed that light exposure (which could drive photolytic degradation) is minimal during storage in the temperature-controlled rooms and the sample ovens.

3.2.4 Tablet Characterisation

3.2.4.1 Weight, Dimensions & Tensile Strength

Tablet weight was measured to the nearest 0.1 mg using an analytical balance. The diameter and thickness of each tablet were measured using a set of digital callipers and reported to the nearest 0.01 mm.

Tablet hardness was measured using a hardness tester (Copley TBF 1000, Copley Scientific Ltd, Nottingham, UK). The tensile strength, σ_t , of tablets was calculated using the tablet hardness, F , diameter, d , and thickness, L (Fell & Newton, 1970):

$$\sigma_t = \frac{2 \cdot F}{\pi \cdot d \cdot L}. \quad (3.1)$$

Tensile strength was measured as a rapid measure of the tablets mechanical strength. This measurement was used as a rapid alternative to measuring tablet friability, with the assumption that tablets with sufficient tensile strength (for example, ~ 2 MPa) are unlikely to display friability issues.

3.2.4.2 Porosity

The porosity, ε , of tablets was calculated using the measured weight, m , dimensions and the true density, $\rho_{t,\text{mix}}$, of the formulation. $\rho_{t,\text{mix}}$ was calculated as the weighted harmonic mean considering the true density, $\rho_{t,i}$, and the weight fraction, c_i , of each tablet component (Sun *et al.*, 2018):

$$\rho_{t,\text{mix}} = \left(\sum_i^N \frac{c_i}{\rho_{t,i}} \right)^{-1} \quad (3.2)$$

with $N = 4$ as the number of different excipients in the placebo formulations and

$N = 5$ as the number of tablet components in the griseofulvin-containing formulations. The porosity can then be calculated using:

$$\varepsilon = 1 - \frac{\frac{m}{\pi \cdot (d/2)^2 \cdot t}}{\rho_{t,\text{mix}}} \quad (3.3)$$

3.2.4.3 Dynamic Contact Angle

Dynamic contact angle measurements were taken using a drop shape analyser (Krüss DSA30, Krüss GmbH, Hamburg, Germany). Video recordings were taken at a rate of 30 frames per second as a single droplet of MilliQ[®] Ultra-pure water was dispensed on to the surface of the tablet. The video files were analysed using MATLAB (R2019a, MathWorks, Massachusetts, USA) to determine the contact angle between the droplet and the tablet surface at each frame in the recording.

Using the data collected within the first minute of contact with the liquid droplet for each pair of replicates, a two-phase exponential decay model (Eq. 3.4) was fitted to the data using GraphPad Prism 8 (version 8.3.1, GraphPad Software LLC, San Diego).

$$\begin{aligned} \theta_c(t) &= \theta_{c,p} + s_f e^{-k_f \cdot t} + s_s e^{-k_s \cdot t} \\ s_f &= \theta_{c,0} \cdot x_{fs} \\ s_s &= \theta_{c,0} (1 - x_{fs}) \end{aligned} \quad (3.4)$$

$\theta_{c,0}$ and $\theta_{c,p}$ are the contact angles at initial and infinite time, respectively. k_f and k_s are the rate constants for the fast and slow phases, respectively. The fraction of time dominated by the fast phase of the reaction is described as x_{fs} .

3.2.4.4 Disintegration Time

For placebo tablet studies in Chapters 4 and 5, the disintegration time of tablets was measured using a Copley DTG 2000 Disintegration Tester (Copley Scientific Ltd, Nottingham, UK) with the vessel discs. Tablets were disintegrated in 800 mL of distilled water at 37°C. Disintegration time was measured in seconds for 6 tablets per formula-

tion. The mean and standard deviation of these 6 tablets is reported.

For the griseofulvin-containing batches tested in Chapter 6, tablet disintegration testing was performed as above using an Erweka ZT 122 (Total Laboratory Services Ltd, Dorset, UK). For the griseofulvin batches, 3 tablets were tested per formulation. The mean and standard deviation of these 3 tablets is reported.

3.2.4.5 Dissolution

Dissolution testing was performed using USP II (paddle) apparatus (Copley DIS 6000 Dissolution Tester, Copley Scientific Ltd, Nottingham, UK). The dissolution testing was performed using 0.4% SDS in water at 37°C, with a paddle speed of 75 rpm.

The dissolution medium was selected based on the method described in the United States Pharmacopeia (USP) monograph for griseofulvin tablets, which suggests dissolution studies are performed in water with SDS as a surfactant to enhance the solubility of this poorly soluble API. Due to the lower concentration of griseofulvin used in the model formulations (90 mg instead of 1 g), the concentration of SDS must be reduced to prevent the dissolution rate from being too fast to allow adequate discrimination between dissolution profiles. A solubility study was performed whereby the solubility of griseofulvin was measured in SDS solutions containing 0.3, 0.7, 1.0, 2.0, and 4.0% w/v SDS in water. To prepare the samples, an excess of griseofulvin was added to 4 mL of each SDS solution in a centrifuge tube. The samples were mixed for 24 hours using an orbital shaker at 240 rpm in a 37°C temperature room. Samples were centrifuged at 13,000 rpm for 5 min and the supernatant was separated for UV analysis. For samples prepared in 1, 2, 3, and 4% SDS, the sample was further diluted to allow UV analysis. These samples were diluted by making a 1 mL sample to a volume of 4 mL with water. Samples were analysed by UV using λ_{max} of 291 nm. The results of the solubility study are presented in Fig 3.2.

The results of the solubility study showed that there is a strong linear correlation between the SDS concentration and the solubility of griseofulvin. Based on this correlation, an SDS concentration of 0.4% SDS was selected for the dissolution studies. This concentration of SDS provides sink conditions for testing the griseofulvin tablets

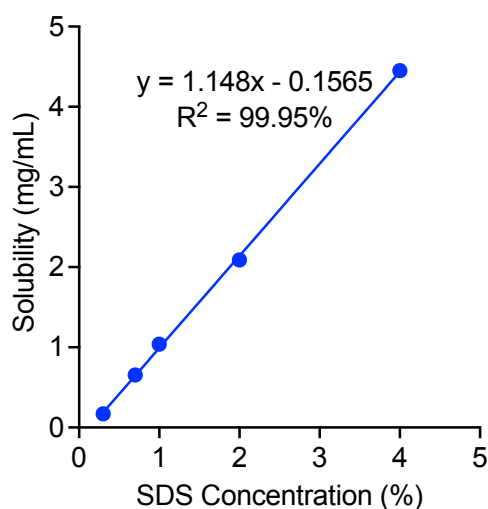


Figure 3.2: The solubility of griseofulvin in varying concentrations of SDS solution.

manufactured in Chapter 6, which contained a nominal dose of 90 mg. For a 0.4% SDS medium, the solubility of griseofulvin is calculated as 0.303 mg/mL, allowing 3 times the nominal dose of griseofulvin to dissolve in 900 mL of test media.

Paddle speeds of 50 and 75 rpm were compared to assess whether or not the dissolution profiles of each batch were affected by coning. Coning during dissolution testing describes the settling of powder in a mound at the base of the dissolution vessel, where the hydrodynamic effect of the paddle rotation does not sufficiently stir the settled powder. The profiles obtained for each formulation when tested at 50 and 75 rpm are shown in Chapter 6 (see Figure 6.7). A comparison of the profiles indicated that tablets composed of MCC/DCPA were significantly impacted by coning, with only around 50% of the total dose dissolving after 60 min at 50 rpm. To mitigate the effects of coning, a paddle speed of 75 rpm was selected for the dissolution studies.

Samples of 10 mL were manually drawn and filtered through a 0.2 μm PTFE filter. The first 5 mL drawn through each syringe was discarded to allow sufficient saturation of the filter. The remaining volume was sampled into HPLC vials for analysis. Samples were drawn at 3, 7, 10, 15, 20, 25, 30, 45 and 60 minutes. At the 60 minute sampling timepoint, the paddle speed was increased from 75 rpm to 200 rpm for a 30 minute infinity spin. Samples from each sampling timepoint were then analysed by HPLC (see

Table 3.1).

Table 3.1: HPLC conditions used for the analysis of griseofulvin-based dissolution samples

| Method Details | |
|-----------------------------|--|
| HPLC system | Shimadzu Prominence-i LC-2030 |
| Chromatographic data system | Shimadzu LabSolutions Chromatography Software |
| Dissolution media | 0.4% w/v SDS in water |
| Mobile phase A | 10 mM ammonium formate adjusted to pH 3 with formic acid |
| Mobile phase B | 10 mM ammonium formate in acetonitrile:water (9:1) |
| Standards | Standard solutions of concentrations 0.05, 0.08, 0.10, and 0.25 mg/mL griseofulvin prepared in 1% w/v SDS in water |
| Column | Waters XBridge [®] C18 5 μ m (2.1 \times 50 mm) at 37°C |
| Injection volume | 20 μ L |
| Flow rate | 1 mL/min |
| Gradient Details | |
| 0 min | 30% mobile phase A, 70% mobile phase B |
| 3 min | 0% mobile phase A, 100% mobile phase B |
| 4 min | 0% mobile phase A, 100% mobile phase B |
| 4.5 min | 30% mobile phase A, 70% mobile phase B |
| 6.5 min | 30% mobile phase A, 70% mobile phase B |
| Detection | UV-vis detection at 291 nm |

Chapter 4

Exploring the Performance-Controlling Tablet Disintegration Mechanisms for Direct Compression Formulations

Chapter Summary

This chapter describes the manufacture and characterisation of directly compressed placebo tablets composed of commonly used fillers and disintegrants. Each batch was classified based on the performance-controlling disintegration mechanism, and a simple workflow for determining the mechanism of disintegration is presented. The contents of this chapter have been published in the International Journal of Pharmaceutics (see page xix), however some sections have been adapted to expand on some of the key concepts.

4.1 Introduction

The disintegration and dissolution performance of immediate-release (IR) tablets plays a central role in the therapeutic efficacy of a product. Before the active pharmaceutical ingredient (API) can have a therapeutic effect, it must first dissolve and then be absorbed into the systemic circulation. For most IR formulations, rapid disintegration is essential for dissolution. As the tablet breaks into smaller particles, the surface area available for dissolution increases, resulting in faster drug release.

For a tablet to disintegrate, the repulsive forces within the tablet must exceed the interparticle bonding forces. The first stage in tablet disintegration is liquid penetration. When in contact with liquid, the disintegration medium will penetrate the tablet through pores in the microstructure. Although liquid penetration is not directly responsible for disintegration, it is a prerequisite for all other disintegration mechanisms (Nogami *et al.*, 1967). The most common cause of disintegration is the expansion of particles within the tablet. As the particles swell, the void space in the pores is soon filled and a force is exerted on the surrounding matrix. When this force exceeds the cohesive forces between particles in the matrix, disintegration will occur (Caramella *et al.*, 1990). Depending on the material, particle expansion can be omni-directional or uni-directional. The omni-directional expansion of particles is a result of moisture uptake and is typically referred to as swelling. On the other hand, some materials will only expand uni-directionally as a result of its deformation during compaction. For these materials, contact with liquid causes the particles to regain their original shape prior to compaction, and therefore expansion occurs only axially against the direction of compression (Desai *et al.*, 2012; Quodbach *et al.*, 2014a). In this thesis, this mechanism will be termed shape recovery, however it is also known as strain recovery or deformation recovery. Aside from swelling and shape recovery, disintegration can also be a result of the dissolution of particles from the matrix. Each of these mechanisms are influenced either by the raw material properties, manufacturing conditions or both (Markl & Zeitler, 2017).

For tablets manufactured by direct compression, the pore structure of the tablet is

formed during compaction and this can impact the disintegration performance. Higher compression forces result in tablets with lower porosity. The tablet porosity influences the rate of liquid penetration into the tablet, and therefore the rate of disintegration (Marais *et al.*, 2003; Patel & Hopponen, 1966). In addition to compression force, the disintegration performance of tablets manufactured by wet or dry granulation may also be influenced by granule density or moisture content or the mode of disintegrant addition (i.e. intra- or extra-granular) (Gordon *et al.*, 1993).

The effect of formulation on tablet disintegration has been widely studied. In addition to the swelling and shape recovery mechanisms of disintegrants, other excipients in the formulation will also influence the disintegration process. Microcrystalline cellulose (MCC) is a popular filler used in direct compression, which swells when it comes in contact with liquid (Markl *et al.*, 2017). It has been shown that the use of soluble fillers hinders disintegration compared to insoluble fillers (Berardi *et al.*, 2018; Johnson *et al.*, 1991; Rubinstein & Birch, 1977). As the soluble filler will begin to dissolve as liquid penetrates the tablet, the efficiency of swelling and shape recovery materials is reduced. With soluble or hygroscopic materials, there may be competition for water with the disintegrants (Berardi *et al.*, 2018; Johnson *et al.*, 1991). For insoluble matrices, the expansion of the disintegrant results in the disintegrating force being fully exerted on the surrounding particles. It has also been suggested that dissolution of the filler will increase the viscosity of the medium and result in slower liquid penetration (Rubinstein & Birch, 1977), however, these effects are likely to be small relative to the effect on disintegration time. Ekmekciyan *et al.* (2018) demonstrated that solubility effects can be explained by tablet components competing for the available water. Soluble binders and fillers were found to require more water molecules to dissolve, compared to insoluble fillers which can be fully wetted by a small amount of medium. As a result, the use of insoluble fillers leaves more water available for the disintegrants. These results supported previous studies which have shown that increased hygroscopicity of the tablet components could also result in decreased disintegration efficiency (Gordon & Chowhan, 1987; Johnson *et al.*, 1991; López-Solís & Villafuerte-Robles, 2001).

Disintegration testing is routinely performed throughout drug product develop-

ment. However, the standard disintegration test gives very little mechanistic information about the disintegration of the tablet. As a result, several groups have applied novel approaches such as magnetic resonance imaging (Dvořák *et al.*, 2020; Quodbach *et al.*, 2014a,b), broadband acoustic resonance dissolution spectroscopy (BARDS) (O'Mahoney *et al.*, 2020), image analysis (Berardi *et al.*, 2018) and stress relaxation measurements (Tomas *et al.*, 2018) which can be used to study the underlying processes occurring during disintegration and dissolution. Similarly, terahertz pulsed imaging (TPI) has been used to study liquid penetration in and swelling of powder compacts (Al-Sharabi *et al.*, 2020; Markl *et al.*, 2017; Yassin *et al.*, 2015). The test conditions have also been shown to influence the disintegration and dissolution rates. Bisharat *et al.* (2019) investigated the role of ethanol on disintegrant efficiency, whilst Zhao & Augsburger (2005b) explored the role of pH of the disintegrating medium. The disintegration process is also affected by the choice of dissolution medium (e.g. biorelevant medium) (Anwar *et al.*, 2005) and its temperature (Basaleh *et al.*, 2020). Several recent reviews have evaluated the current literature on the disintegration process, the measurement techniques available, and the mechanisms of action of tablet disintegrants (Desai *et al.*, 2016; Markl & Zeitler, 2017; Quodbach & Kleinebudde, 2016).

The objective of this study was to propose a workflow which could allow identification of the performance-controlling disintegration mechanism. In this study, a performance-controlling mechanism is referred to as a rate process that directly impacts the overall disintegration time. In other words, a minor alteration of one or multiple material and/or product attributes strongly affects the rate of the identified mechanism which in turn causes a change in the disintegration performance. This workflow is demonstrated for 16 different placebo formulations, each composed of commonly used excipients. Both raw material (e.g. moisture sorption, intrinsic dissolution rate) and tablet properties (e.g. porosity) were considered within the workflow. This study applies simple and routine analytical tests to gain a greater understanding of the formulation properties which affect disintegration. By applying these principles to understand the mechanism of a given formulation, it is possible to optimise formulation design in terms of the disintegration performance.

4.2 Materials and Methods

4.2.1 Materials

All materials used in this study are described in Chapter 3.

4.2.2 Characterisation of Raw Materials

4.2.2.1 Dynamic Vapor Sorption

Moisture sorption isotherms for each excipient were collected as described in Section 3.2.1.1.

4.2.2.2 Particle Size and Shape

The shape and size of particles of each excipient was measured following the method described in Section 3.2.1.2.

4.2.2.3 True Density

The true density of each excipient was measured by the method described in Section 3.2.1.3.

4.2.2.4 Single Particle Dissolution

The dissolution of individual particles of lactose and mannitol was studied using a custom-built flow cell, as described by Soundaranathan *et al.* (2020). Briefly, particles are placed in a small spherical sample holder in the centre of the flow cell. A peristaltic pump was used to pump deionised water at 20°C through the flow cell at a rate of 1.73 mL/min. This process is recorded using an optical microscope (Leica DM6000, Leica Microsystems CMS GmbH, Germany) at 10x magnification. A full description and diagrams of the flow cell apparatus are given by (Soundaranathan *et al.*, 2020). For each material, the dissolution of 12 particles was measured.

4.2.2.5 Relative Swelling

The relative swelling (Δs) for each formulation was calculated using the average particle size (D_{50}) and the maximum swelling capacity (Δr_{max}). The measurement of Δr_{max} is described by Soundaranathan *et al.* (2020). The relative swelling was then calculated as the average increase in particle size after wetting, based on the weight fraction of each excipient (c_i).

$$\Delta s = \sum_i^N \left(\frac{\Delta r_{max}}{D_{50}/2} \right) c_i \quad (4.1)$$

4.2.3 Tablet Manufacture

4.2.3.1 Investigating Formulation Effects

The formulations manufactured are listed in Table 4.1. For each formulation, 300 g of blend was prepared as described in Section 3.2.2. Each formulation contained 47% w/w each of two different fillers, 5% w/w disintegrant and 1% w/w magnesium stearate.

Tablets were compacted with a 9 mm flat round die using a single punch automated tablet press (FlexiTab, Bosch Packaging Technology Ltd, Merseyside, UK). For each formulation, the filling depth and compression force were adjusted to obtain tablets with a target weight of approximately 350 mg and target tensile strength of >2.5 MPa. For MCC/mannitol, MCC/lactose and MCC/DCPA, tablets were compressed at 10 kN. For DCPA/lactose formulations, 16 kN was used.

4.2.3.2 Investigating Porosity and Disintegrant Concentration Effects

Additional tablets were manufactured for each filler combination with CCS. These tablets were manufactured with either higher porosity or higher disintegrant concentration.

To investigate the effect of porosity, the compression force was set to 8 kN for MCC/mannitol, MCC/lactose and MCC/DCPA formulation. The DCPA/lactose formulation was compressed 12 kN. This decrease in compression force resulted in tablets with higher porosity than the original batches (see Section 4.2.3.1).

Table 4.1: Direct compression tablet formulations

| Filler 1 | Filler 2 | Disintegrant |
|----------|----------|--------------|
| MCC | Mannitol | CCS |
| MCC | Mannitol | XPVP |
| MCC | Mannitol | L-HPC |
| MCC | Mannitol | SSG |
| MCC | Lactose | CCS |
| MCC | Lactose | XPVP |
| MCC | Lactose | L-HPC |
| MCC | Lactose | SSG |
| MCC | DCPA | CCS |
| MCC | DCPA | XPVP |
| MCC | DCPA | L-HPC |
| MCC | DCPA | SSG |
| DCPA | Lactose | CCS |
| DCPA | Lactose | XPVP |
| DCPA | Lactose | L-HPC |
| DCPA | Lactose | SSG |

To investigate the effect of disintegrant concentration, additional tablets of these formulations were also prepared with 8% w/w of CCS at 10 kN (MCC/mannitol, MCC/lactose and MCC/DCPA) and 16 kN (DCPA/lactose). For tablets containing 8% w/w CCS, the concentration of magnesium stearate was kept at 1% w/w and the quantity of each filler was adjusted to 45.5% w/w for each formulation.

4.2.4 Characterisation of Tablets

4.2.4.1 Weight, Dimensions and Tensile Strength

The weight, dimensions and tensile strength were measured as described in Section 3.2.4.1. For each batch, 10 tablets were measured.

4.2.4.2 Porosity

The porosity was calculated for 10 tablets per batch using the method outlined in Section 3.2.4.2.

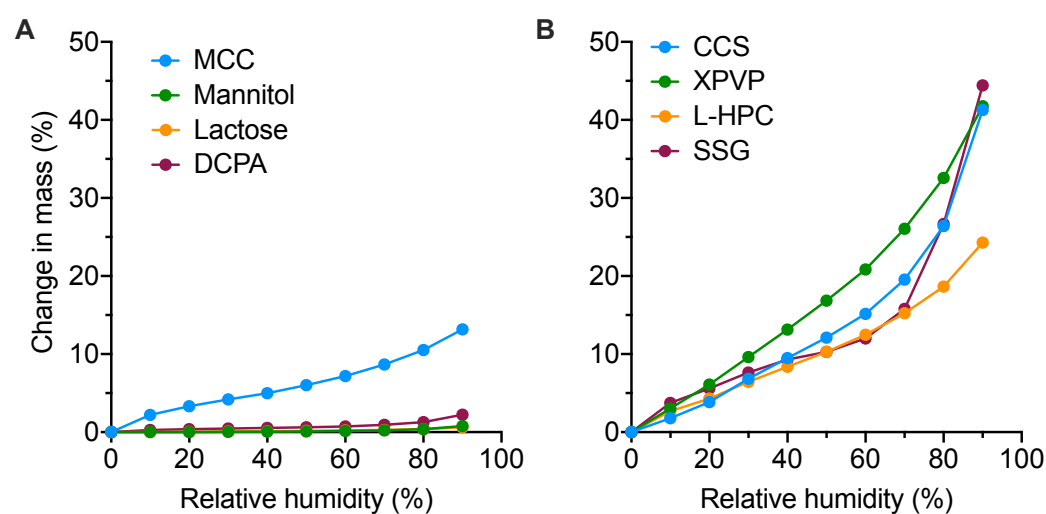


Figure 4.1: Moisture sorption isotherms of (A) fillers and (B) disintegrants

4.2.4.3 Disintegration time

The disintegration time of each batch was measured for 6 tablets using water at 37°C as the disintegration medium, following the method described in Section 3.2.4.4.

4.2.4.4 Dynamic Contact Angle

The dynamic contact angle was measured for 2 tablets per batch using the method described in Section 3.2.4.3.

4.2.4.5 Statistical Analysis

To compare the effects of porosity and increased CCS concentration, individual t-tests were performed using GraphPad Prism 8 (version 8.3.1, GraphPad Software LLC, San Diego). Differences were considered statistically significant for $p < 0.05$.

4.3 Results

4.3.1 Characterisation of Raw Materials

4.3.1.1 Dynamic Vapour Sorption

Moisture sorption isotherms of the fillers (Fig 4.1A) show that lactose, mannitol and DCPA are non-hygroscopic and do not absorb moisture, even at high relative humidity conditions. MCC is hygroscopic and absorbs a substantial amount of moisture.

For the disintegrants (Fig 4.1B), the moisture sorption isotherms show high hygroscopicity. For L-HPC, the moisture sorption at 80 and 90% RH is lower than for the other excipients. For CCS, XPVP and SSG, each disintegrant absorbs approximately 42% moisture at 90% RH.

Settling plots from the DVS measurement of each excipient are given in Appendix D.

4.3.1.2 True Density, Particle Size and Sphericity

The results of particle size, sphericity and true density measurements for each excipient are given in Table 4.2. For all excipients the sphericity of the particles was >0.6 . The smallest particle sizes were observed for SSG and CCS, whilst DCPA had the largest particle size.

Table 4.2: True density, particle size and sphericity of each excipient

| Excipient | $\rho_t(g/cm^3)$ | $D_{50}(\mu m)$ | S_{50} |
|-----------|------------------|-----------------|----------|
| MCC | 1.56 | 111.14 | 0.75 |
| Mannitol | 1.49 | 177.30 | 0.85 |
| Lactose | 1.55 | 130.76 | 0.85 |
| DCPA | 2.98 | 190.52 | 0.79 |
| CCS | 1.60 | 54.32 | 0.66 |
| XPVP | 1.25 | 105.07 | 0.80 |
| L-HPC | 1.48 | 79.03 | 0.63 |
| SSG | 1.55 | 53.59 | 0.87 |

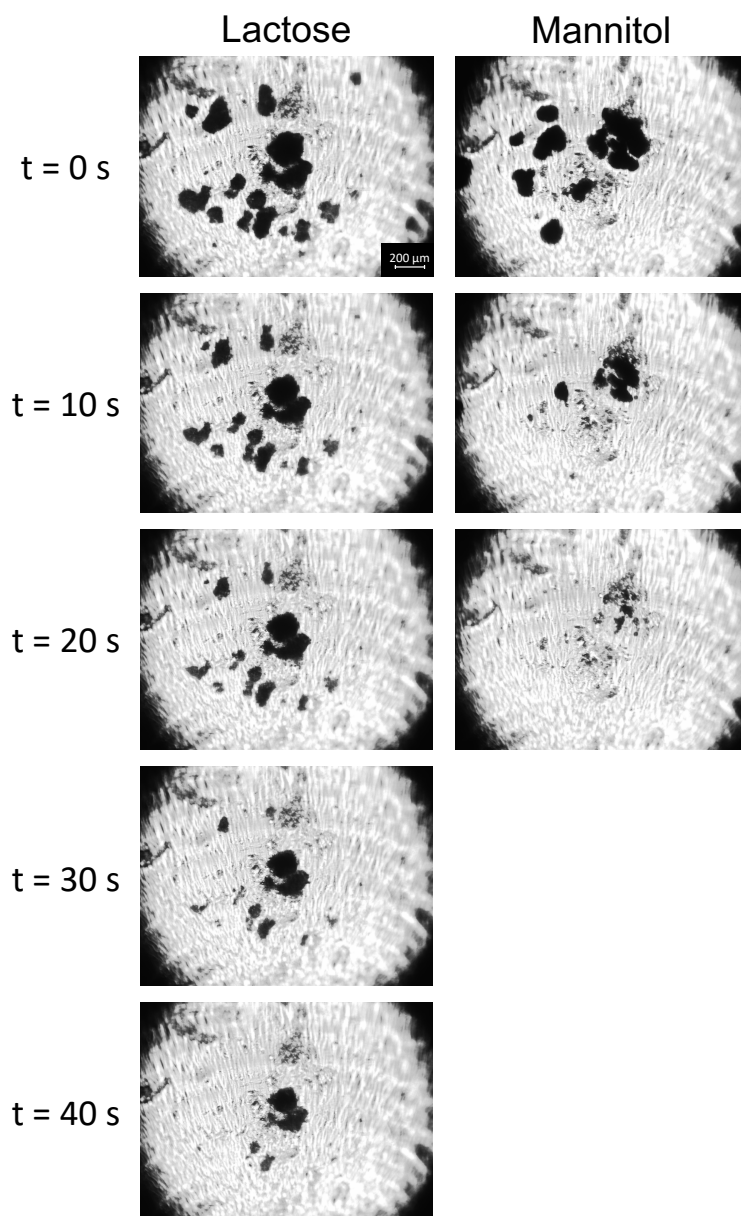


Figure 4.2: Example images from the measurement of the dissolution of individual particles of lactose and mannitol at 0, 10, 20, 30 and 40 seconds after hydration.

4.3.1.3 Single Particle Dissolution

The measurement of single particle dissolution showed that mannitol particles dissolve in 12.5 ± 7.2 s, and lactose particles dissolve in 42.7 ± 13.6 s. Example images from the analysis are shown in Fig 4.2.

4.3.2 Characterisation of Tablets

4.3.2.1 Tensile Strength and Porosity

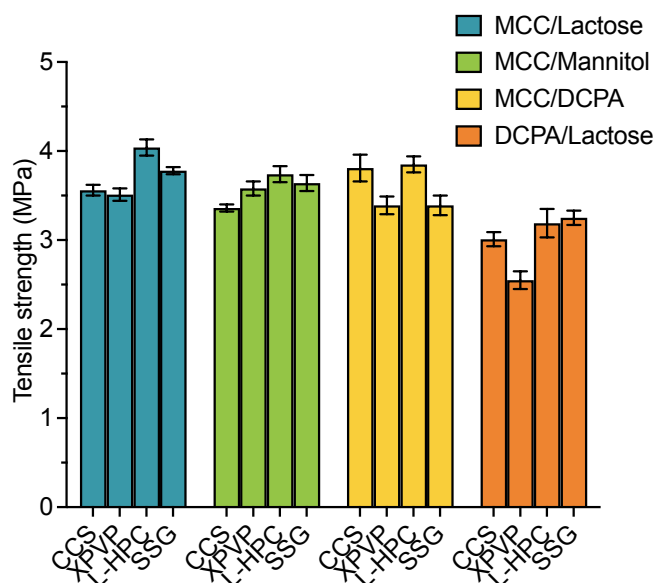


Figure 4.3: The tensile strength of each formulation ($n = 10$, mean \pm standard deviation)

The tensile strength of all formulations is shown in Fig 4.3. For all batches, tensile strength was between 2.5 and 4.1 MPa. The porosity of tablets containing MCC/mannitol and MCC/lactose was approximately 13%, whilst the porosity of MCC/DCPA and DCPA/lactose tablets were around 23% and 19%, respectively (as shown in Fig 4.4).

4.3.2.2 Disintegration Time

The disintegration times of each formulation is shown in Fig 4.5. Disintegration times were lowest for MCC/DCPA formulations. For MCC/mannitol, MCC/DCPA and

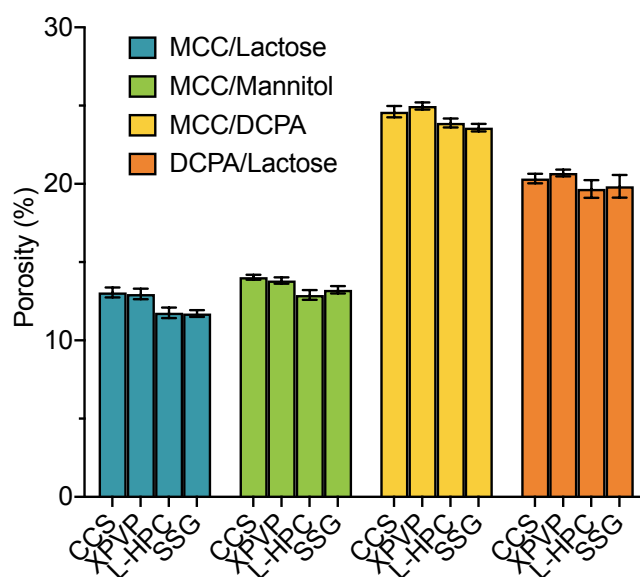


Figure 4.4: The porosity of each formulation ($n = 10$, mean \pm standard deviation)

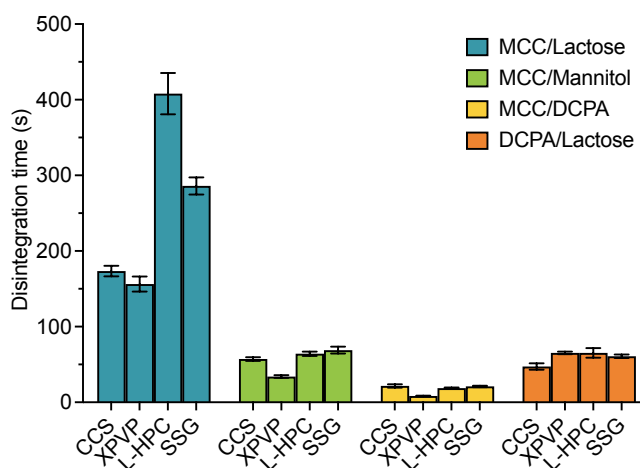


Figure 4.5: The disintegration time of each formulation ($n = 6$, mean \pm standard deviation)

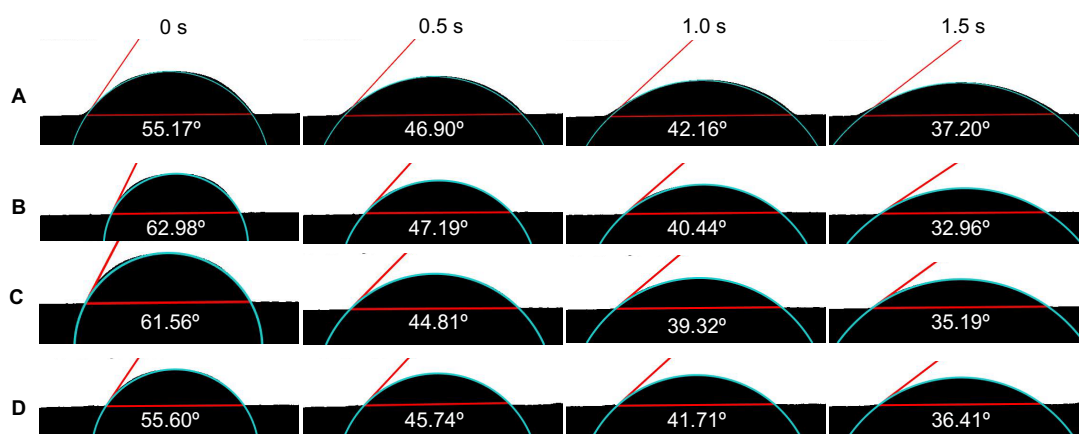


Figure 4.6: Examples of the contact angle measurements for MCC/mannitol-based tablets containing (A) CCS, (B) XPVP, (C) L-HPC and (D) SSG

DCPA/lactose, disintegration times were under 2 minutes for all disintegrants, whereas disintegration took significantly longer and large differences between the different disintegrants could be observed for MCC/lactose.

For MCC/lactose, MCC/mannitol and MCC/DCPA, the batches containing XPVP resulted in the fastest disintegration. For DCPA/lactose, the batch containing CCS disintegrated slightly faster.

4.3.2.3 Dynamic Contact Angle

The initial contact angle $\theta_{c,0}$ was extracted from the dynamic contact angle measurements of the tablets. Examples of the images obtained by contact angle measurements are shown in Fig 4.6 for tablets containing MCC/mannitol.

Using the contact angle extracted from each frame, contact angle profiles can be prepared to show the change in contact angle after the droplet first makes contact with the tablet surface. These profiles are shown in Fig 4.7 for each filler with (A) CCS, (B) XPVP, (C) L-HPC, and (D) SSG.

The initial contact angle for each batch is shown in Fig 4.8. The difference between tablets with each disintegrant are small for MCC/DCPA, whereas they are more distinct for MCC/lactose and MCC/mannitol formulations. For DCPA/lactose, the contact

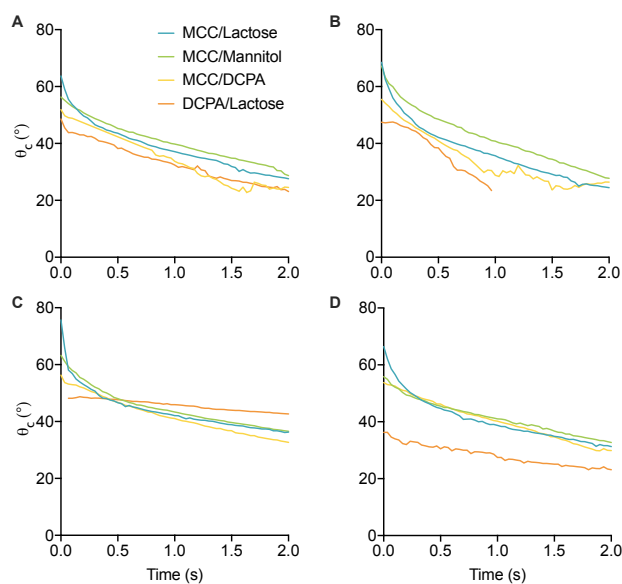


Figure 4.7: Contact angle profiles of tablets containing (A) CCS, (B) XPVP, (C) L-HPC and (D) SSG ($n = 2$)

angle is similar for CCS, XPVP and L-HPC, however $\theta_{c,0}$ is much lower for tablets containing SSG.

4.3.3 Investigating the Performance-Controlling Properties

4.3.3.1 Changing Tablet Porosity

Additional tablets were manufactured for each filler-combination with CCS to investigate the effect of changing the tablet porosity. The porosity and disintegration time of the new tablets are shown against the original tablets in Fig 4.9. When the porosity was increased, the disintegration time of MCC/lactose decreased significantly. This suggests that the disintegration time was limited by liquid penetration. On the other hand, the disintegration of tablets containing MCC/mannitol was much slower when the porosity was increased. For MCC/DCPA and DCPA/lactose, increasing the porosity did not significantly change the disintegration times.

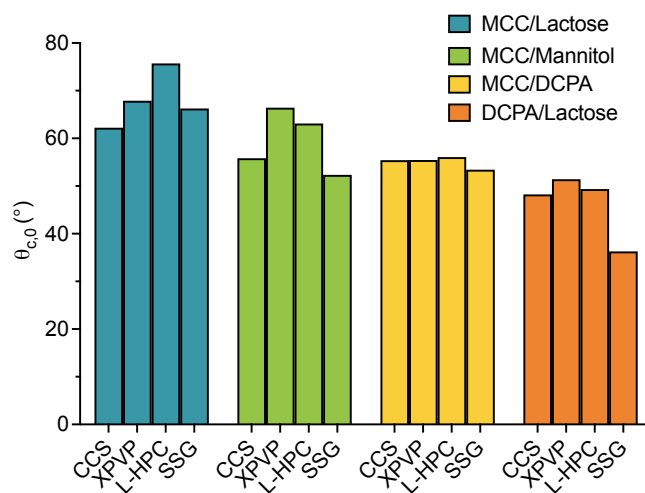


Figure 4.8: The initial contact angle of each formulation ($n = 2$)

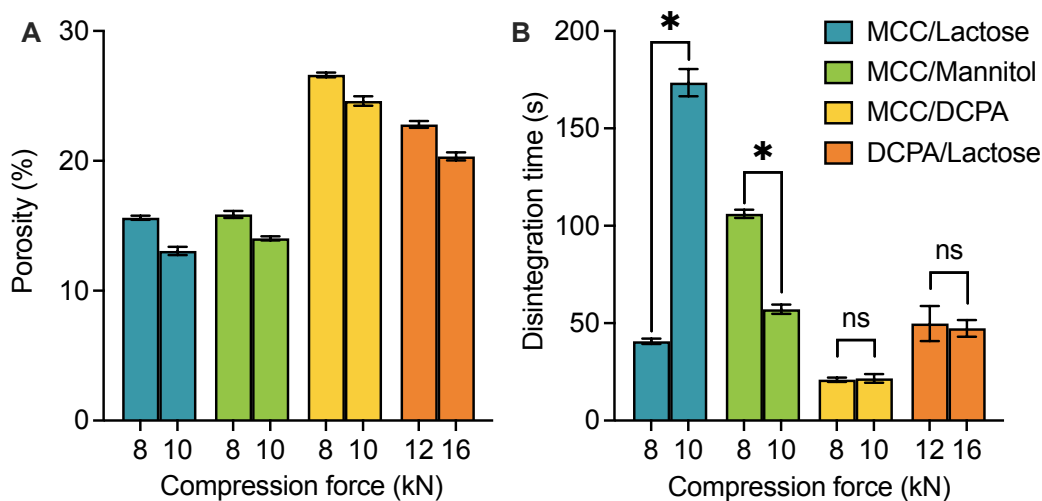


Figure 4.9: The (A) porosity and (B) disintegration time of tablets compressed at 8 and 10 kN (MCC/lactose, MCC/mannitol and MCC/DCPA) or 12 and 16 kN (DCPA/lactose). $n =$ (A) 10 or (B) 6; mean \pm standard deviation; * $p < 0.05$; ns: not significant.

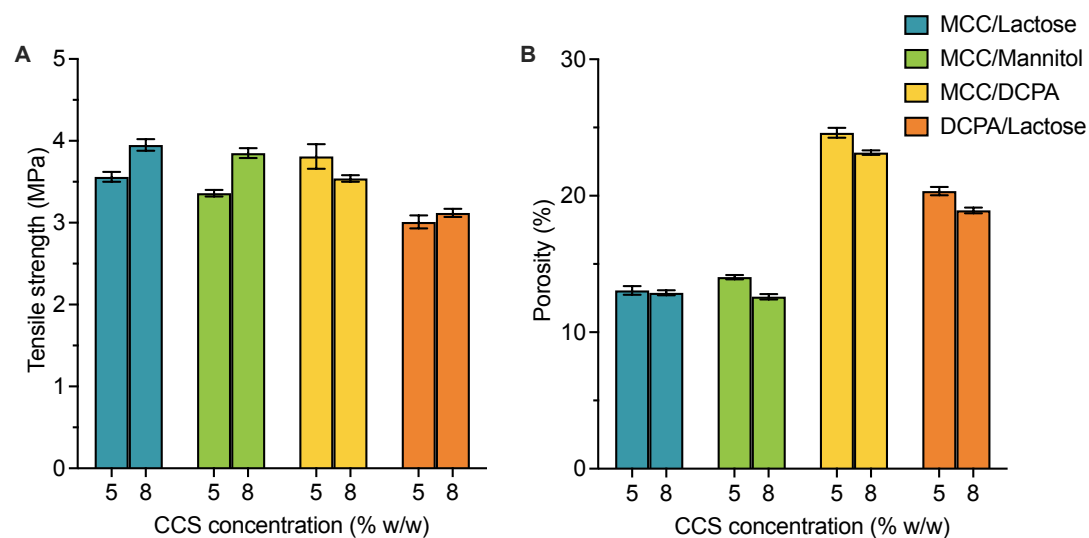


Figure 4.10: The (A) tensile strength and (B) porosity of tablets containing 5% and 8% w/w CCS, respectively.

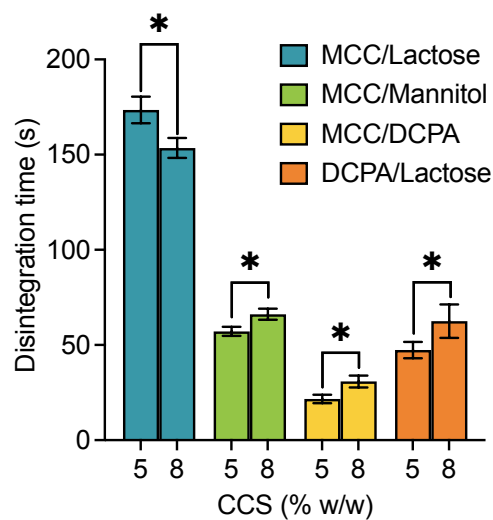


Figure 4.11: Disintegration times of batches prepared with 5% and 8% w/w CCS ($n = 6$; mean \pm standard deviation; $*p < 0.05$)

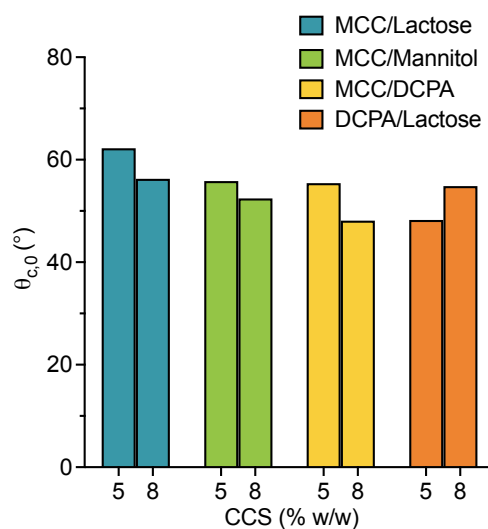


Figure 4.12: The initial contact angle, $\theta_{c,0}$, of tablets containing 5 and 8% w/w CCS ($n = 2$ and $n = 4$, for 5 and 8% w/w CCS, respectively).

4.3.3.2 Changing Disintegrant Concentration

The disintegration times of batches with 5% and 8% w/w CCS are shown in Fig 4.11. When the disintegrant concentration was increased, the disintegration times of all tablets changed. For MCC/lactose, an increase in CCS concentration resulted in a faster tablet disintegration. There was a slight increase in disintegration time observed for MCC/mannitol and DCPA-based formulations.

The initial contact angle of tablets containing 5% and 8% w/w CCS are shown in Fig 4.12. For tablets containing MCC/lactose, MCC/mannitol and MCC/DCPA, there was a decrease in initial contact angle for tablets containing 8% w/w CCS. For tablets containing DCPA/lactose, the initial contact angle increased with higher disintegrant concentration.

4.4 Discussion

4.4.1 The Influence of Formulation on Disintegration

The performance of IR tablets is controlled by different disintegration mechanisms. These mechanisms can be impacted by both raw material properties and the manufac-

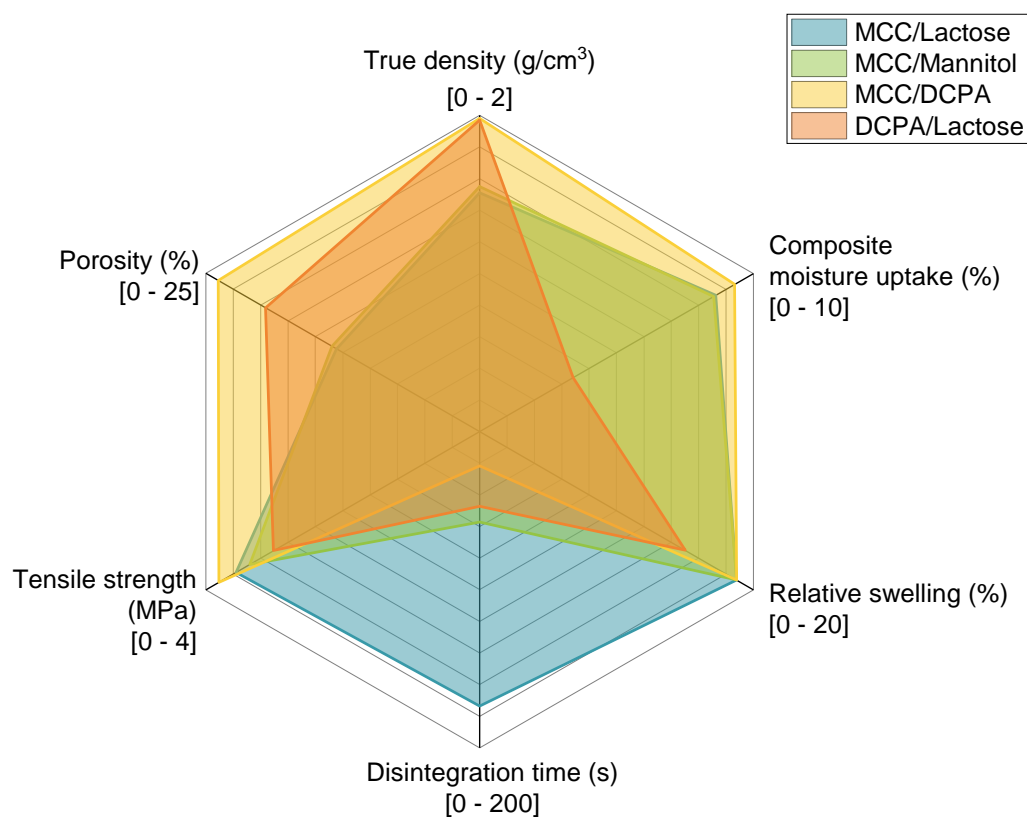


Figure 4.13: Summary of raw material and tablet properties for each filler combination with 5% w/w CCS. Raw material properties ($\rho_{t,mix}$, relative swelling and moisture uptake) expressed as the weighted arithmetic mean of each excipient.

turing conditions. The key differences between the raw material and tablet properties of tablets containing different filler combinations with 5% w/w CCS are shown in Fig 4.13 and the workflow used to classify these formulations is shown in Fig 4.14.

For all tablets, liquid penetration is the necessary pre-requisite for disintegration and dissolution. As such, ensuring rapid liquid penetration will always be a key consideration during the development of directly compressed tablets. In this study, each batch has been further classified based on the disintegration-controlling mechanisms. This allows the formulator to identify the properties which can be adjusted slightly in order to optimise the disintegration performance. For example, the DCPA-based tablets tested in Section 4.3.3.1 show that increasing the porosity of these tablets (as a result, increasing the rate of liquid penetration) did not result in faster disintegration (Fig 4.9). However,

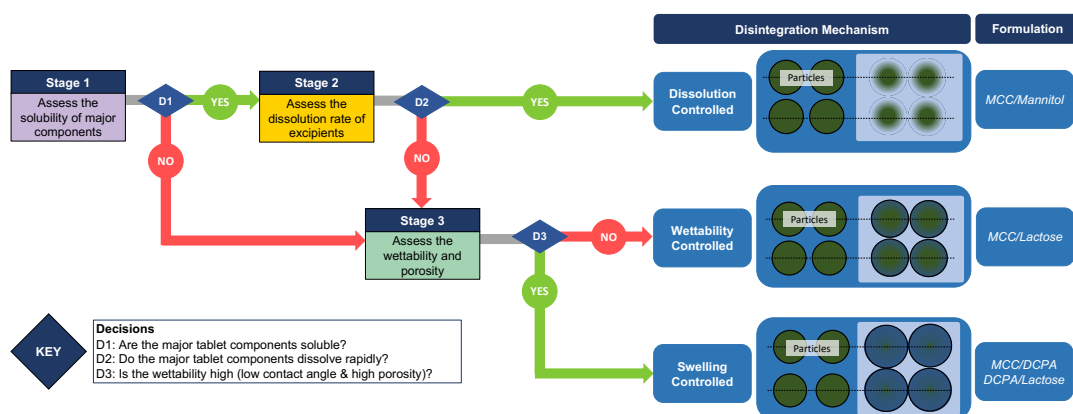


Figure 4.14: Workflow for the classification of IR tablets based on the disintegration mechanism.

changing the disintegrant concentration had a significant effect on disintegration time (Fig 4.11). This indicates that for the swelling-controlled DCPA-batches, disintegration can be optimised by careful selection of the disintegrant and concentration.

The first stage in the workflow is to assess the solubility of the major tablet components. Several studies in the literature have demonstrated that disintegration is faster for tablets composed of insoluble excipients compared to those with soluble excipients (Johnson *et al.*, 1991; Rubinstein & Birch, 1977). The disintegration times of these batches (shown in Fig 4.5) support these findings, as tablets containing MCC and DCPA disintegrate faster than those containing mannitol or lactose. If the tablet matrix is mostly composed of a soluble material, then liquid penetration will lead to the dissolution of filler particles. For tablets composed of an insoluble filler, only a small amount of water will be used to wet the filler particles, thus leaving more water available for the disintegrant (Ekmekciyan *et al.*, 2018). The solubility of most pharmaceutical materials is well-defined in the literature.

In addition to the solubility of the tablet components, it is also important to consider the intrinsic dissolution rate of the excipients in order to distinguish between components which will dissolve rapidly when in contact with liquid and those which will dissolve more slowly. For example, lactose and mannitol have very similar absolute solubility values (1 g in 5.24 mL and 1 g in 5.5 mL, respectively, for water at 20°C (Rowe

et al., 2009)), however, the rates at which these excipients dissolve are different. This was previously shown through determining the intrinsic dissolution rates by Wewers *et al.* (2020), and further supported by the single particle dissolution analysis performed for lactose and mannitol (Section 4.3.1). The difference in filler dissolution rate is evident when comparing the disintegration time of tablets containing MCC/mannitol and MCC/lactose (Fig 4.5). When mannitol is used as a filler, these particles will dissolve rapidly from the matrix, resulting in an increase in the apparent pore space and improved liquid penetration. On the other hand, lactose particles will take longer to dissolve, meaning that the porosity remains low during the initial stages of disintegration. If both the solubility and intrinsic dissolution rate are high for the major tablet components, then disintegration is driven by the dissolution of particles from the matrix which consequently leads to improved liquid penetration. The disintegration mechanism of MCC/mannitol is thus dissolution controlled.

The third stage in the workflow is to assess the wettability and porosity of the tablets. The porosity of the tablets strongly influences the performance as it relates directly to the rate of liquid penetration. The total porosity of the tablet includes both intraparticle and interparticle porosity. DCPA has a high intraparticle porosity, meaning that tablets composed of MCC/DCPA and DCPA/lactose have much higher total porosity than those containing MCC/lactose and MCC/mannitol (as shown in Fig 4.4). This high porosity promotes liquid penetration through the pores in the tablets, which then allows other processes such as swelling or dissolution to begin. Due to the rapid liquid penetration and wetting, disintegration is limited by the rate of swelling of the disintegrant particles. On the other hand, tablets containing MCC/lactose have much lower porosity (as shown in Fig 4.4) than those containing DCPA. Unlike the tablets containing mannitol (in which mannitol particles dissolve rapidly upon contact with liquid), the single particle dissolution analysis has shown that the wetting and dissolution of lactose particles is much slower. As a result, the porosity of this batch will remain low during the beginning of disintegration, leading to slow liquid penetration and delayed swelling compared to the DCPA-based batches. We have therefore classified the MCC/lactose batch as wettability-controlled.

The swelling ability of a formulation is determined by the swelling capacity of the raw materials (MCC, CCS, L-HPC, SSG) as well as shape recovery effects (XPVP). For the MCC-based formulations, both the disintegrant and MCC contribute to the swelling (both omni- and uni-directional, for swelling and shape recovery excipients respectively) within a tablet. The swelling of the DCPA/lactose formulation is only driven by the disintegrant used. MCC/DCPA and DCPA/lactose are both swelling-controlled, whereas the MCC/DCPA formulations disintegrate faster due to its higher swelling ability as exemplified by the relative swelling, Δs , in Fig 4.13.

Each filler combination was manufactured with four different disintegrants: CCS, XPVP, L-HPC and SSG. The difference in disintegration times between the disintegrants were relatively small for tablets composed of MCC/mannitol, MCC/DCPA and DCPA/lactose. On the other hand, disintegrant choice played a crucial role in determining the rate of disintegration of tablets containing MCC/lactose. For these batches, XPVP resulted in the fastest disintegration, followed by CCS, SSG and L-HPC. These findings are in agreement with previous studies which have ranked the effectiveness of different disintegrants based on moisture uptake and force development measurements. Specifically, Quodbach *et al.* (2014a) studied the development of fractal dimensions for dibasic calcium phosphate (DCP) based tablets containing different disintegrants. The results of this study showed that XPVP was the most effective disintegrant, followed by CCS and SSG (Quodbach *et al.*, 2014a).

The workflow shown in Fig 4.14 describes a classification system to determine the performance-controlling disintegration mechanism of a tablet. This workflow was developed based on the formulations used in this study. In order to fully explore the design space and establish criteria for the decision points in this workflow, further research is required to assess the influence of changing the composition or excipients, as well as the effects of API.

4.4.2 The Influence of Porosity on Disintegration

Additional batches were manufactured for each filler combination with CCS in order to investigate the effect of porosity on the disintegration mechanisms. Tablets containing

MCC/DCPA and DCPA/lactose showed no significant difference in disintegration time when manufactured at low and high porosity (as shown in Fig 4.9). This supports the conclusion that swelling, rather than liquid penetration, is the limiting step in the disintegration of these tablets.

The disintegration of MCC/mannitol tablets was slower for the batch of tablets with high porosity. For tablet disintegration to occur, disintegrants must exert a sufficient swelling force against the surrounding matrix. Liquid penetration of these tablets results in the rapid dissolution of mannitol. As mannitol dissolves, the apparent pore space in the tablet increases. If the empty pore space between the disintegrant and MCC particles is too large, then particles will swell into this space instead of exerting a force against the surrounding particles. This could cause an increase in disintegration time, as the swelling mechanism of the disintegrant and MCC is less efficient.

The disintegration time of MCC/lactose tablets was significantly faster for tablets manufactured at the lower compression force (i.e. higher porosity tablets). This confirms the conclusion that these tablets are wettability-controlled, as increased porosity accelerated the liquid uptake and, consequently, reduced the disintegration time.

4.4.3 The Influence of Disintegrant Concentration on Disintegration

The effect of disintegrant concentration was also investigated for each filler combination. Tablets were manufactured with 8% w/w CCS to allow comparison with the original batches containing 5% CCS.

When the disintegrant concentration was increased, the disintegration time of MCC/DCPA and DCPA/lactose tablets increased (Fig 4.11). Similar results were also found by Bernardi *et al.* (2018), with DCPA-based tablets showing slower disintegration with higher concentrations of CCS or SSG. The authors attributed these results to the formation of a hydrated gel matrix, which held the tablet together despite increased liquid uptake and swelling. It is possible that at 8% CCS a gel is formed that results in a barrier preventing further liquid penetration.

Tablets containing MCC/mannitol also showed a slight increase in disintegration time when the concentration of CCS was increased. Despite the higher wettability (as

shown by a lower initial contact angle in Fig 4.12), these tablets also showed lower porosity and higher tensile strength compared to those containing 5% w/w CCS. If disintegration of these tablets is controlled by dissolution of mannitol particles, then the lower porosity could impede liquid penetration and result in delayed dissolution of the mannitol. On the other hand, tablets composed of MCC/lactose show faster disintegration when 8% w/w CCS is used instead of 5% w/w. As shown in Fig 4.12, a decrease in initial contact angle for this batch suggests increased wettability. Unlike tablets containing MCC/mannitol, there is no effect on porosity (as shown in Fig 4.10). As a result, the increase in wettability accelerates liquid uptake and hence decreases the disintegration time.

4.5 Conclusions

The performance of tablets containing different formulations, porosities and compositions were investigated. This work provides a comprehensive explanation of the mechanisms which control disintegration time for tablets with different raw material and compact properties. The processes which may control disintegration are wettability (i.e. liquid penetration), swelling or dissolution. The mechanism of disintegration for a formulation may be determined by considering the properties of the raw materials. For fillers which contain a high proportion of rapidly-dissolving material, disintegration will likely be dissolution controlled. If the excipient wettability is low and the tablets have low porosity, disintegration will be controlled by the liquid penetration. For tablets which are insoluble or partially insoluble, swelling may be the controlling factor. These mechanisms were further supported by investigating the effect of increasing the tablet porosity. A 2% change in porosity for the wettability-controlled tablets (MCC/lactose) caused a 77% reduction in the disintegration time, whereas for swelling controlled tablets (MCC/DCPA and DCPA/lactose) a change in porosity of 2% (MCC/DCPA) and 7% (DCPA/lactose) did not significantly change the disintegration process (3% and 5% change in disintegration time, respectively). The use of the simple workflow presented in this study could allow formulators to identify the key formulation or manufacturing

parameters which could be adjusted to optimise disintegration.

In this study, placebo tablets were used to investigate the effects of different excipients, but the effect of API must also be assessed when considering the performance-controlling mechanism of a formulation. Moreover, the composition of the tablets is likely to have a strong influence on the disintegration controlling mechanism, and so changes to the ratio of fillers or disintegrant must be taken into account. In addition to the formulation, the choice of dissolution medium (e.g. biorelevant medium) and its temperature can affect the disintegration and dissolution. Generating a full picture of the relationship between given raw materials, manufacturing conditions and controlling disintegration mechanism will require the consideration of biorelevant dissolution media.

Chapter 5

Investigating the Role of Excipients on the Physical Stability of Directly Compressed Tablets

Chapter Summary

This chapter outlines the design, execution and results of the accelerated stability studies performed on the tablets manufactured in Chapter 3. Each batch of placebo tablets were stored under 5 different storage conditions and tested at 2 timepoints. The changes in physical tablet properties were then related to the raw material properties, as well as the performance-controlling disintegration mechanisms described previously. The contents of this chapter have been published in the *International Journal of Pharmaceutics: X* (see page xix), however some sections have been adapted to expand on some of the key concepts.

5.1 Introduction

Stability testing is a crucial step in the development of any drug product. A main focus of stability testing is on assessing the chemical degradation to ensure that the product remains safe throughout the duration of its shelf life. Accelerated stability studies are routinely used to study chemical degradation, and this data is often used to extrapolate for long-term storage. In recent years, industrial interest in accelerated predictive techniques has grown rapidly (Qiu, 2018a; Williams *et al.*, 2017). In addition to chemical stability, the physical stability of pharmaceutical products must also be evaluated to ensure that the product performance is not affected by storage. The modelling and prediction of physical stability presents unique challenges, as physical changes do not always follow the Arrhenius behaviour which is used to predict chemical reactions. A recent survey by Williams *et al.* (2017) documented the properties currently being studied with risk-based predictive stability techniques in industry. Responses from 16 companies using these approaches, the most common applications were for studying chemical impurities and assays (13 and 11 companies, respectively), with only 3 companies using these tools for dissolution testing and only 1 respondent each applying these tools to study hardness or disintegration. By developing an improved understanding of the underlying mechanisms of physical change during storage, more appropriate predictive tools could be developed which better fit the needs of physical stability testing.

Many studies in the literature have discussed the physical stability of different drug products, however the wide variety of formulations (including the choice of both active pharmaceutical ingredient(s) and excipients), manufacturing processes, and study designs make it challenging to compare different studies.

Tablet excipients often account for a large portion of the total tablet mass, and so the excipients will typically influence the physical properties of the tablet. Several studies have investigated the effect of different excipients on the physical stability of tablets, including the impact of filler solubility (Gordon *et al.*, 1993; Molokhia *et al.*, 1982), formulation hygroscopicity (Gordon & Chowhan, 1990), and disintegrant efficacy (Quodbach & Kleinebudde, 2015).

The effect of filler solubility was investigated by Molokhia *et al.* (1982) and Gordon *et al.* (1993), who both attributed increases in tablet hardness after storage to the partial dissolution and recrystallisation of soluble fillers. The exception to this would be sorbitol-based tablets, which showed a decrease in hardness after storage (Molokhia *et al.*, 1982). These changes were not found in tablet composed of mainly insoluble fillers. In addition to the change in hardness, Gordon *et al.* (1993) also found that tablets containing soluble fillers experienced a decrease in dissolution rate after storage under accelerated conditions. Filler hygroscopicity was also investigated to determine its effect on physical stability. Gordon & Chowhan (1990) found that tablets with a higher composite hygroscopicity show greater decreases in dissolution rate after storage at elevated humidity compared to those with non-hygroscopic excipients. In addition to factors like solubility and hygroscopicity, it has also been shown that the mode of deformation of a material can influence the physical stability, with differences in behaviour observed for brittle fracture fillers like DCPD and lactose monohydrate, compared to the plastically-deforming MCC (Sacchetti *et al.*, 2017).

Several studies have also investigated the effects of storage on disintegrants (Gordon *et al.*, 1993; Hersen-Delesalle *et al.*, 2007; Hiew *et al.*, 2016; Quodbach & Kleinebudde, 2015). Gordon *et al.* (1993) assessed changes in the physical properties of tablets containing CCS, XPVP, and L-HPC as disintegrants. This study found that the behaviour on stability changed depending on the disintegrant used, for example, tablets containing CCS were more strongly affected by storage at 37°C/80% RH despite still having a faster disintegration time than those containing XPVP or L-HPC. Hersen-Delesalle *et al.* (2007) found that a decrease in tensile strength with increased relative humidity was associated with the formation of cracks on the surface and internal structure of the tablets, likely due to premature activation of disintegrants as they absorb moisture from the air. Quodbach & Kleinebudde (2015) studied the effect of storage conditions on the water uptake and force development for tablets containing different disintegrants, finding that disintegration time increased after storage at high humidity for tablets containing two different grades of SSG. These changes are attributed to a plasticising effect on the polymer structure, resulting in the premature release of some of the shape re-

covery energy stored from compression. Hiew *et al.* (2016); Li *et al.* (2004) investigated the effect of relative humidity on dibasic calcium phosphate-based tablets with XPVP. After storage at 75% RH, the high moisture sorption of XPVP made the tablets become immeasurably soft and deformed. It was also shown by Sacchetti *et al.* (2017) that the moisture sorption properties of disintegrants cause volume expansion during storage, which in turn results in stress relaxation and prolonged disintegration times, particularly for tablets containing XPVP. This was further confirmed by Bauhuber *et al.* (2021), who showed that tablets containing XPVP showed the biggest change in disintegration time after storage at 40°C/75% RH compared to those containing CCS or SSG.

For chemical stability, predictions are typically based on the reaction rates of chemical degradation pathways, for example using the Arrhenius equation as a base, with the addition of terms to account for the humidity or other relevant factors. When considering physical stability changes, these often do not involve chemical changes, and so predicting the rate and extent of change can be challenging. In the literature, several studies have applied chemical stability techniques such as the Accelerated Stability Assessment Program (ASAP) or GSK's accelerated stability modelling (ASM) approach to study disintegration and dissolution changes on stability (Clancy *et al.*, 2018; Li *et al.*, 2004; Waterman, 2011). A study by Li *et al.* (2004), investigated the decrease in dissolution rate of benazepril hydrochloride tablets containing XPVP after storage at 40°C/75% RH. In this study, the change in behaviour was attributed to disintegrant pre-activation, and a simple model was proposed to predict dissolution slowdown based on the moisture uptake of the tablets. A technique was also proposed by Scrivens (2019), which calculated an "acceleration factor" (AF) which was used to correct the timescale of a dissolution profile of samples after storage to match it to the initial profile. The AF was found to decrease exponentially over time for each condition, and the calculation of the fitting parameters for this exponential allowed accurate predictions of the change in dissolution rate.

Previously, the formulations included in this study were classified as either dissolution controlled, wettability controlled or swelling controlled (see Chapter 4). To do

this, a workflow was developed which focused on the raw material and tablet properties, specifically the solubility and dissolution rate of the particles, as well as the porosity and wettability of the tablet. This classification process helped to identify the critical properties which influences the disintegration behaviour of the tablets. Following these classifications, the surface liquid-absorption and swelling processes were quantified using dynamic contact angle measurements for these formulations (Markl *et al.*, 2021). The liquid-absorption and swelling results supported the proposed mechanisms of disintegration for each formulation, with the disintegration of MCC/mannitol and MCC/lactose tablets primarily being influenced by the liquid absorption, whilst disintegration of MCC/DCPA tablets were generally swelling-controlled, and tablets composed of DCPA/lactose tablets showed some influence from both the liquid-absorption and swelling behaviour.

The objective of this study is to assess the relationship between physical tablet properties including tensile strength, porosity, initial contact angle, and disintegration time with storage temperature and humidity during stability studies. This study compares the effect of storage temperature and humidity on 16 different directly compressed placebo formulations with four different filler-combinations and four commonly used disintegrants. The effect of exposure to accelerated stability conditions are also compared against the performance-controlling disintegration mechanism for each formulation prior to storage.

5.2 Materials and Methods

5.2.1 Materials

Details of all materials used in sample preparation, storage, and testing are given in Section 3.1.

5.2.2 Dynamic Vapor Sorption (DVS)

Moisture sorption isotherms were collected as described previously in Section 3.2.1.1. To calculate the theoretical liquid sorption at the specific storage conditions used for

each formulation (v_{mix}), a weighted average was calculated based on the weight fraction of each excipient (c_i) and the individual moisture uptake values (v_i) using

$$v_{\text{mix}} = \sum_{i=1}^N c_i \cdot v_i \quad (5.1)$$

with $N = 3$ as the number of excipients (excluding magnesium stearate) in the formulation used.

5.2.3 Tablet Manufacture

Full details of the tablet manufacture are given in Chapter 4. In this study, all formulations described in Table 4.1 were used for the stability studies.

5.2.4 Sample Storage

For the stability studies, tablets were stored at five different temperature and humidity conditions as described in Section 3.2.3. The target storage conditions are shown in Table 5.1. Samples were removed from the oven for testing after 2 and 4 weeks. At each timepoint, jars were opened and allowed to equilibrate to ambient temperature and humidity of approximately 20-23°C and 50-60% RH for a minimum of 3 days prior to testing.

Table 5.1: Accelerated stability storage conditions

| Temperature (°C) | Humidity (% RH) | Timepoints (weeks) |
|------------------|-----------------|--------------------|
| 37 | 30 | 0, 2, 4 |
| 37 | 75 | 0, 2, 4 |
| 50 | 75 | 0, 2, 4 |
| 70 | 30 | 0, 2, 4 |
| 70 | 75 | 0, 2, 4 |

5.2.5 Characterisation of Tablets

5.2.5.1 Weight, Dimensions and Tensile Strength

The weight, dimensions and tensile strength are reported as the mean of 10 tablets per timepoint and condition for each formulation, as described in Section 3.2.4.1.

5.2.5.2 Porosity

The tablet porosity was calculated as described in Section 3.2.4.2, using the 10 tablets weighed and measured in Section 5.2.5.1 (prior to the tensile strength measurement measurement) for each formulation at each timepoint and condition.

5.2.5.3 Dynamic Contact Angle

Dynamic contact angle measurements were taken and processed according to Section 3.2.4.3. For each batch, condition and timepoint, contact angle measurements were performed on 2 tablets.

The data collected during the dynamic contact angle measurements were also modelled to provide information about the liquid absorption and swelling kinetics, which is discussed by Markl *et al.* (2021) for tablets of each filler combination with CCS.

5.2.5.4 Disintegration time

Disintegration testing was performed as described in Section 3.2.4.4 for 6 tablets per timepoint, condition and formulation.

5.2.5.5 Statistical analysis

Pearson correlation coefficients were calculated using GraphPad Prism 9 (version 9.0.2, GraphPad Software LLC, San Diego) to identify correlations between physical tablet properties and the storage conditions. Correlations were considered significant for $p < 0.05$.

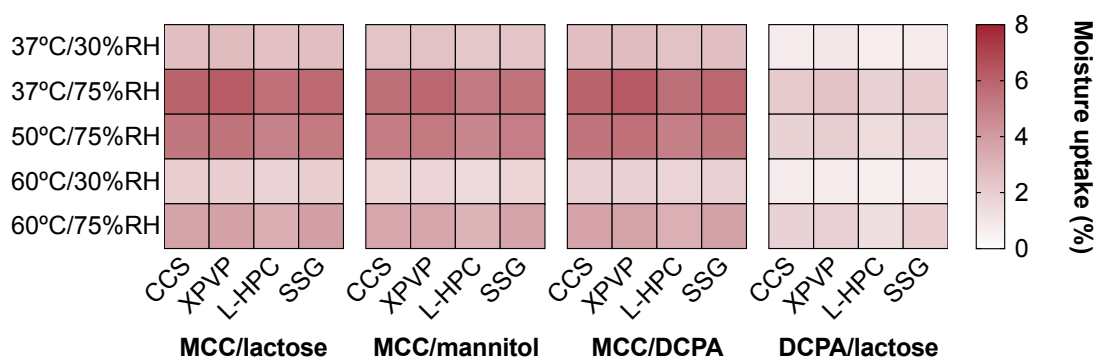


Figure 5.1: The theoretical moisture uptake for each formulation (%), based on the individual moisture sorption of each excipient.

5.3 Results

5.3.1 Moisture Sorption

The moisture sorption of each excipient was measured to simulate the conditions used in this study, with the exception of 70°C conditions. Due to temperature limits of the instrument, 60°C was used to replace 70°C. The results of the moisture uptake are shown in Fig 5.1. Formulations containing MCC (MCC/mannitol, MCC/lactose, and MCC/DCPA) experienced increased moisture uptake at high humidity conditions, whilst 30% RH conditions showed smaller increases in moisture uptake. DCPA/lactose-based tablets only showed small changes in moisture uptake for all conditions. The individual moisture sorption isotherms for each excipient at 25°C were shown in Chapter 4, and these profiles indicate that the main excipients contributing towards moisture uptake is MCC and the disintegrants.

5.3.2 Tensile strength

The change in tensile strength for each batch during the stability study is shown in Figure 5.2A. For tablets composed of MCC/lactose, there is little change in tensile strength for samples stored at low humidity. However, at high humidity, there is a decrease of around 40-60%. Tablets containing MCC/mannitol generally decreased in tensile strength after storage at all conditions. MCC/mannitol-based tablets with XPVP,

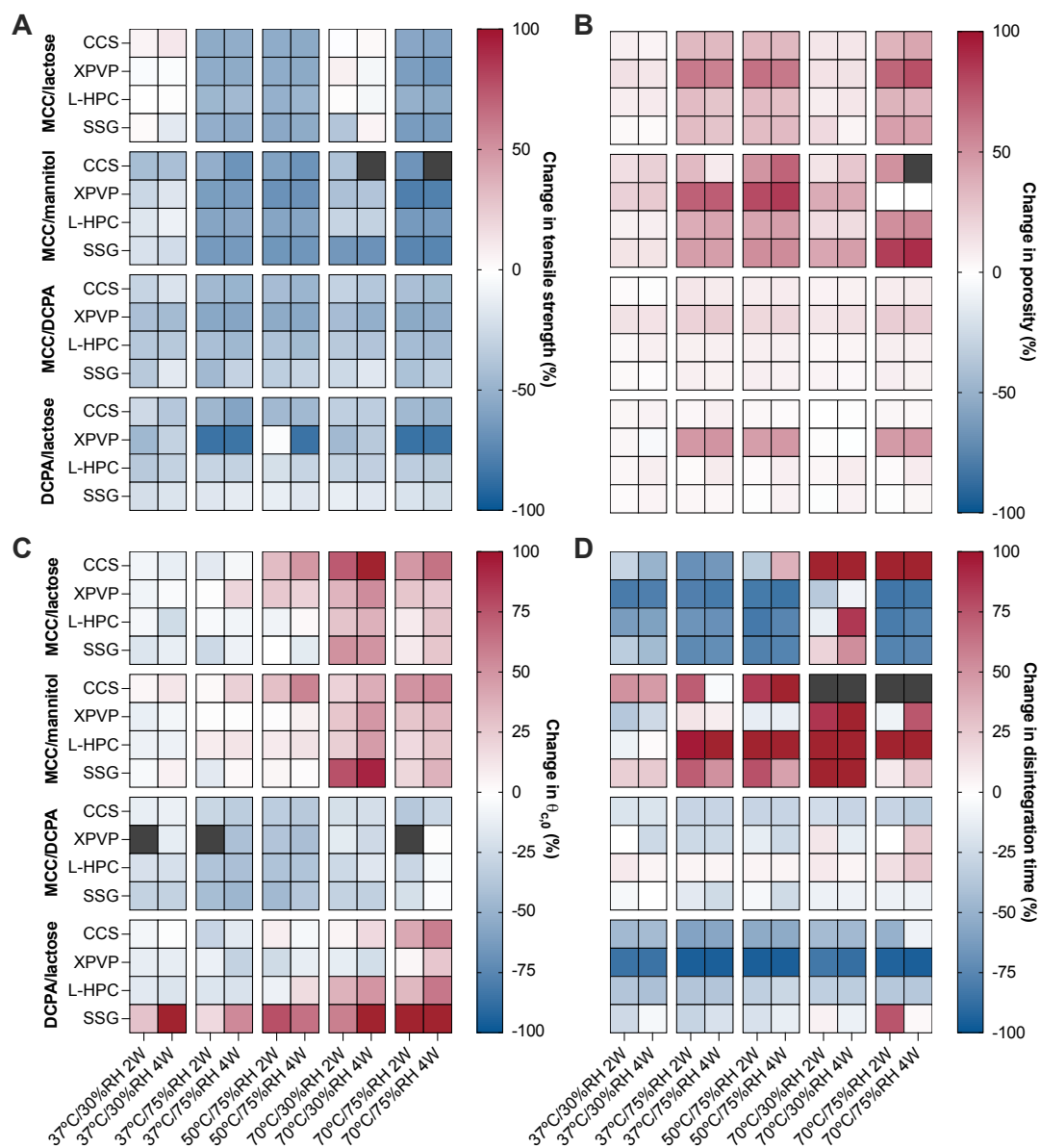


Figure 5.2: The change in (A) tensile strength, (B) porosity, (C) $\theta_{c,0}$, and (D) disintegration time for all batches after storage under accelerated conditions. Grey data points represent points where no data is available.

L-HPC and SSG as the disintegrant experienced a slightly larger decrease in tensile strength after storage at high humidity compared to storage at low humidity. DCPA-based tablets (MCC/DCPA and DCPA/lactose) also decreased in tensile strength after storage. The changes for these batches were generally smaller than those shown by other filler combinations with the exception of DCPA/lactose tablets containing XPVP, which decreased the most out of all batches tested. The changes in tensile strength for DCPA-based tablets were also more uniform across different conditions compared to the other filler combinations. The full data sets for tensile strength during storage are shown in Figures E1 - E4 in Appendix E. In most cases, changes in tensile strength occurred between the 0 and 2 week timepoints, after which point the tensile strength seemed to have reached a plateau.

5.3.3 Porosity

The changes in porosity during storage for all batches are shown in Figure 5.2B. Tablets composed of MCC/mannitol and MCC/lactose show a slight increase in porosity after storage at 30% RH and a larger increase for tablets stored at 75% RH. At high humidity conditions, hygroscopic excipients such as MCC and the disintegrants can absorb moisture from the air (as shown by the moisture uptake data in Fig 5.1), resulting in particle expansion (often termed "disintegrant pre-activation") (Berardi *et al.*, 2021). After removal from storage, the absorbed moisture will subsequently be lost and enlarged or swollen particles will shrink to their original size, however, the changes to the microstructure caused by this particle expansion will be irreversible.

For MCC/mannitol and MCC/lactose the initial porosity (around 13%) is much lower than that of the MCC/DCPA and DCPA/lactose batches (around 23% and 19%, respectively, as shown in Chapter 4). In the case of DCPA-based tablets, it was previously demonstrated that increases in porosity did not significantly affect the disintegration time due to the swelling-controlled disintegration mechanism of this batch (see Chapter 4). The disintegration time of swelling-controlled tablets is less influenced by changes in the tablet microstructure than the wettability- or dissolution-controlled tablets, and so the increase in porosity associated with disintegrant pre-activation during storage is

less significant for the DCPA-based batches.

Within each filler combination, the largest increases in porosity are found with the batch containing XPVP as a disintegrant. This could indicate that the different mechanism of action of the disintegrants influences the stability of the formulation. Alternatively, the larger changes observed for these batches could be attributed to the higher moisture sorption capacity of XPVP (see Chapter 4), or the premature release of energy by strain recovery for this disintegrant.

Profiles of tablet porosity during storage are shown in Figures E5 - E8 in Appendix E. Similarly to the tensile strength profiles, these figures demonstrate that the porosity of the tablets generally exhibits the most change between 0 and 2 weeks, then remaining relatively constant between 2 and 4 weeks.

5.3.4 Contact angle

The changes in initial contact angle for each formulation during the stability study is shown in Figure 5.2C. The individual plots of $\theta_{c,0}$ at each timepoint are shown in Fig E9 - E12 in Appendix E. The changes in contact angle appear to vary within each of the filler combinations used in this study.

MCC/mannitol- and MCC/lactose-based tablets generally show large increases in $\theta_{c,0}$ after storage at high temperature, particularly at 70°C. For tablet stored at 37°C there are only small changes in $\theta_{c,0}$. These results suggest that increasing temperature results in decreased wettability for these batches.

When MCC/DCPA is used as the filler combination instead, $\theta_{c,0}$ generally decreased for all batches by around 20-40% of the initial value. For these tablets, the change in $\theta_{c,0}$ occurs between the initial and 2 week timepoint, and then remains constant between the 2 and 4 week timepoint.

The behaviour of tablets composed of DCPA/lactose vary depending on the disintegrant used. A large increase in $\theta_{c,0}$ can be observed for tablets containing SSG across all timepoints and conditions. Tablets with CCS and L-HPC as the disintegrant only show a slight increase in $\theta_{c,0}$ at high temperatures. When XPVP was used as a disintegrant, $\theta_{c,0}$ generally decreased slightly for all conditions and timepoints except for

tablets stored at 70°C/75% RH for 4 weeks.

5.3.5 Disintegration time

The changes in disintegration time on stability are shown in Figure 5.2D. The full stability profiles for tablet disintegration time are found in Figures E13 - E16 in Appendix E.

MCC/lactose-based tablets generally showed a decrease in disintegration time for tablets stored at every condition except 70°C/30% RH for tablets with CCS, L-HPC and SSG as the disintegrant. For the batch which used CCS as disintegrant, there was also an increase in disintegration time at 70°C/75% RH.

When MCC/mannitol was used as the filler combination, there were large increases in disintegration time for most storage conditions. For tablets containing CCS and SSG, the disintegration time increased for every storage condition. In particular, tablets with CCS as the disintegrant, storage at 70°C resulted in tablets which did not fully disintegrate even after 20 minutes, and instead formed a gel-like consistency. The disintegration time of tablets containing L-HPC as the disintegrant increased at all conditions except 37°C/30% RH. The MCC/mannitol batch least affected by storage was the batch containing XPVP as the disintegrant, which experienced an increased disintegration time at 70°C/30% RH (2 weeks and 4 weeks) and 70°C/75% RH (4 weeks).

For tablets containing DCPA, changes in disintegration time were generally much smaller. The exception is tablets containing DCPA/lactose with XPVP, which showed a consistent decrease in disintegration time at all conditions. It should also be noted that for tablets containing MCC/DCPA and DCPA/lactose, the initial disintegration time was already short (<60 s (see Chapter 4)), and so even moderate relative changes in disintegration time are only a few seconds in real-time.

5.3.6 Effects of Storage Time

The changes in tensile strength, porosity, initial contact angle and disintegration time over time can be found in Appendix E. In most cases, changes in the physical properties

of the tablets occur within the first 2 weeks of storage, and then there is little change between the 2 and 4 week timepoints. This suggests that temperature- or humidity-induced changes are generally occurring within the 2 weeks of storage before reaching a constant state, which could mean that the changes are only dependent on storage conditions and would not occur during long-term storage at ambient conditions. There are some exceptions to this, for example, the disintegration time of MCC/lactose/L-HPC tablets stored at 70°C/30% RH, and MCC/mannitol/XPVP tablets stored at 70°C/75% RH, which demonstrated little change in the first 2 weeks and a significant increase between 2 and 4 weeks. Conversely, the disintegration times of MCC/mannitol/CCS tablets stored at 37°C/75% RH increased within the first 2 weeks, before returning to the initial disintegration time after 4 weeks.

5.3.7 Correlation between temperature, humidity and physical tablet properties

The correlation coefficients for physical tablet properties with storage temperature and humidity are depicted in Figures 5.3A and B, respectively. Only statistically significant correlations ($p \geq 0.05$) are shown here.

There is a strong correlation (≥ 0.80) between storage temperature and dynamic contact angle for all MCC/lactose-based tablets, most MCC/mannitol-based tablets (except those containing CCS) and most DCPA/lactose-based tablets (except those containing XPVP). This correlation suggests that for those batches, an increase in temperature results in an increase in $\theta_{c,0}$, indicating a decrease in wettability. The wettability of a surface is influenced by three factors – porosity, surface roughness and surface energy. Comparing the porosity and contact angle, it seems that porosity changes are mainly based on humidity, whereas the contact angle is changing in response to storage temperature instead (Fig 5.2). When we consider surface roughness, we can assume that the surface roughness is not decreasing during storage, however, it may increase slightly as a result of premature swelling of some particles and the changes in porosity. If surface roughness increases, the contact angle for these samples would be expected to decrease (Wenzel, 1936). This suggests that the only property left which

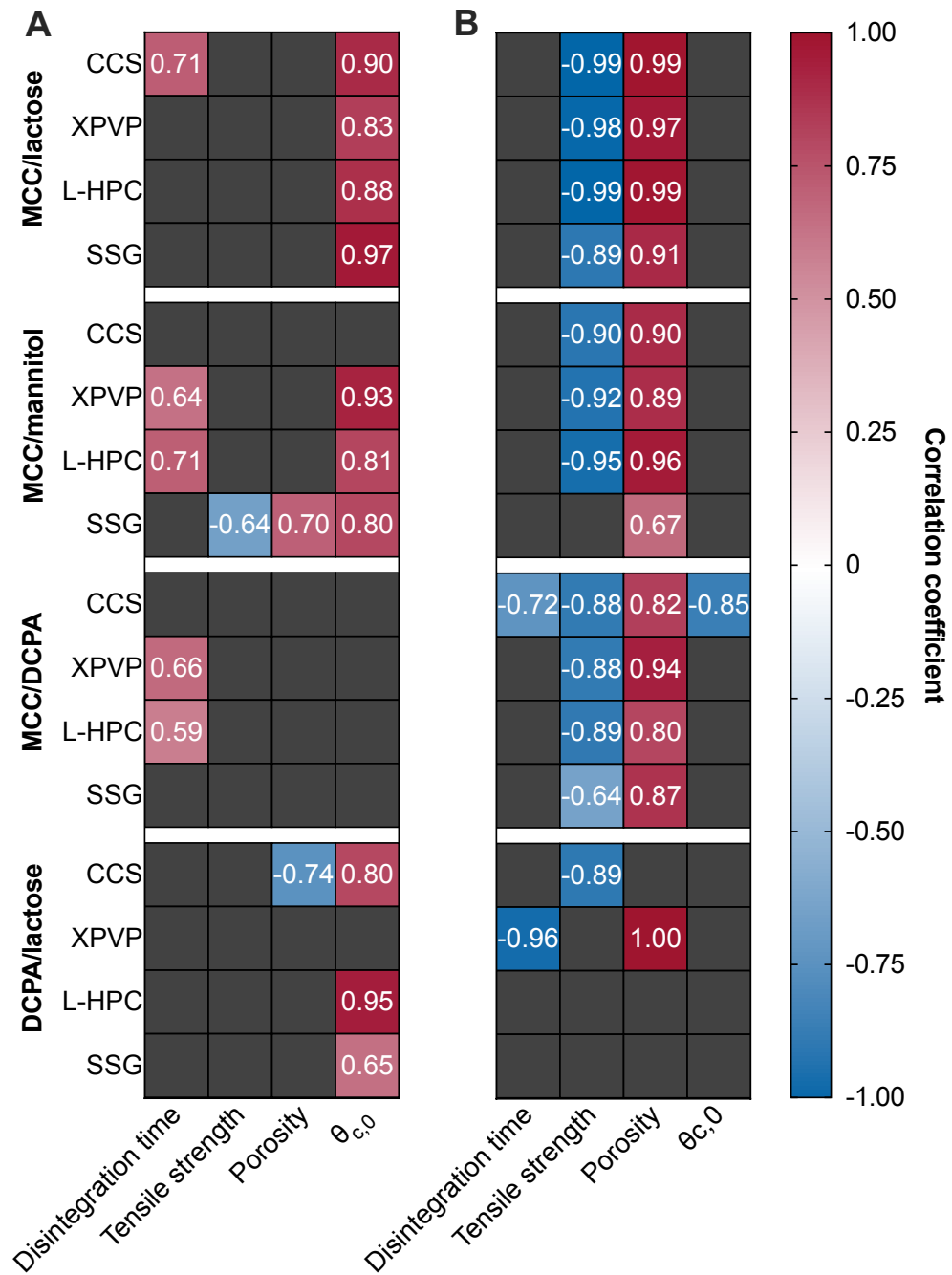


Figure 5.3: Pearson correlation coefficient between (A) storage temperature and (B) storage humidity with physical tablet properties. Only significant correlations ($p < 0.05$) are shown.

could be influencing the contact angle is a change in surface energy, or possibly surface chemistry, which is driven by high temperatures.

In some cases, this decrease in wettability is also reflected by an increase in disintegration time (MCC/lactose-based tablets with CCS and MCC/mannitol-based tablets with XPVP and L-HPC) with increasing storage temperature, however in most cases only the $\theta_{c,0}$ correlates with temperature. For all MCC/DCPA-based tablets, there is no correlation between porosity, tensile strength and $\theta_{c,0}$ with storage temperature. For tablets containing XPVP and L-HPC with MCC/DCPA, the disintegration time positively correlates with the storage temperature – indicating that an increase in storage temperature results in slower disintegration. This correlation between disintegration time and storage temperature can also be observed for a few other formulations, specifically MCC/mannitol-based tablets with XPVP and L-HPC, and MCC/lactose tablets with CCS.

Correlation coefficients indicate that for most formulations (particularly those containing MCC), tensile strength and porosity have strong correlations with relative humidity (Figure 5.3B). The positive correlation with porosity suggests that when stored at high relative humidity, the porosity of tablets would increase, whilst tensile strength would generally decrease (as shown in Figures 5.2B and 5.2A, respectively). This can be explained by considering the effect of premature swelling of excipients such as MCC or the disintegrants. During storage at elevated humidity conditions, water is absorbed by hygroscopic, swelling particles, and after removal from storage this additional water is gradually lost. As water is absorbed, the pore space expands and remains permanently altered even after the loss of moisture. As the pore space expands, the bonds between the particles are weakened, resulting in the decreased tensile strength observed in most batches. These correlations are strongest in batches containing MCC, in which both MCC and the disintegrant may undergo premature swelling. For tablets containing DCPA/lactose, these correlations are generally not significant, with the exception of porosity for tablets containing XPVP and tensile strength for tablets containing CCS tablets. For these batches, premature swelling only occurs for the disintegrant particles as DCPA and lactose are not capable of swelling.

5.3.8 Correlation between physical tablet properties and disintegration time

The correlation coefficient between disintegration time and the physical tablet properties (porosity, tensile strength and $\theta_{c,0}$) are denoted in Figure 5.4. Tablets composed of MCC/lactose (with the exception of CCS) show a significant correlation between both porosity and tensile strength with disintegration time. The correlation between porosity and disintegration time is negative, indicating that an increase in porosity is associated with a decrease in disintegration time. For tensile strength, there is a positive correlation with disintegration time. This suggests that as tensile strength decreases, disintegration time also decreases. These results can be explained by considering the absorption of moisture and subsequent swelling described previously. The disintegration performance of MCC/lactose was categorised as wettability-limited (see Chapter 4). In this case, the increase in porosity can result in faster liquid penetration, which improves the rate of wetting and in turn facilitates faster disintegration.

The disintegration times of MCC/mannitol-based tablets show a strong positive correlation (> 0.8) with $\theta_{c,0}$ for each disintegrant. The disintegration mechanism of MCC/mannitol tablets were previously described as dissolution controlled (see Chapter 4). For these tablets (except those containing CCS), the contact angle is shown to increase with increased storage humidity (Figure 5.3B). This increase in contact angle is also associated with an increase in disintegration time. The increase in $\theta_{c,0}$ indicates a decrease in wettability, which could contribute toward slower wetting of mannitol particles, and thus, slower dissolution of mannitol from the tablet matrix. As this was previously determined to be the performance-limiting mechanism for disintegration, it follows that disintegration slows down after storage.

DCPA-based tablets (MCC/DCPA and DCPA/lactose) were previously classified as swelling-controlled, based primarily on the rapid disintegration times and high porosity. For these batches, initial disintegration time was rapid and changes during storage were generally small. For this reason, correlations between disintegration time and the physical tablet properties are generally low.

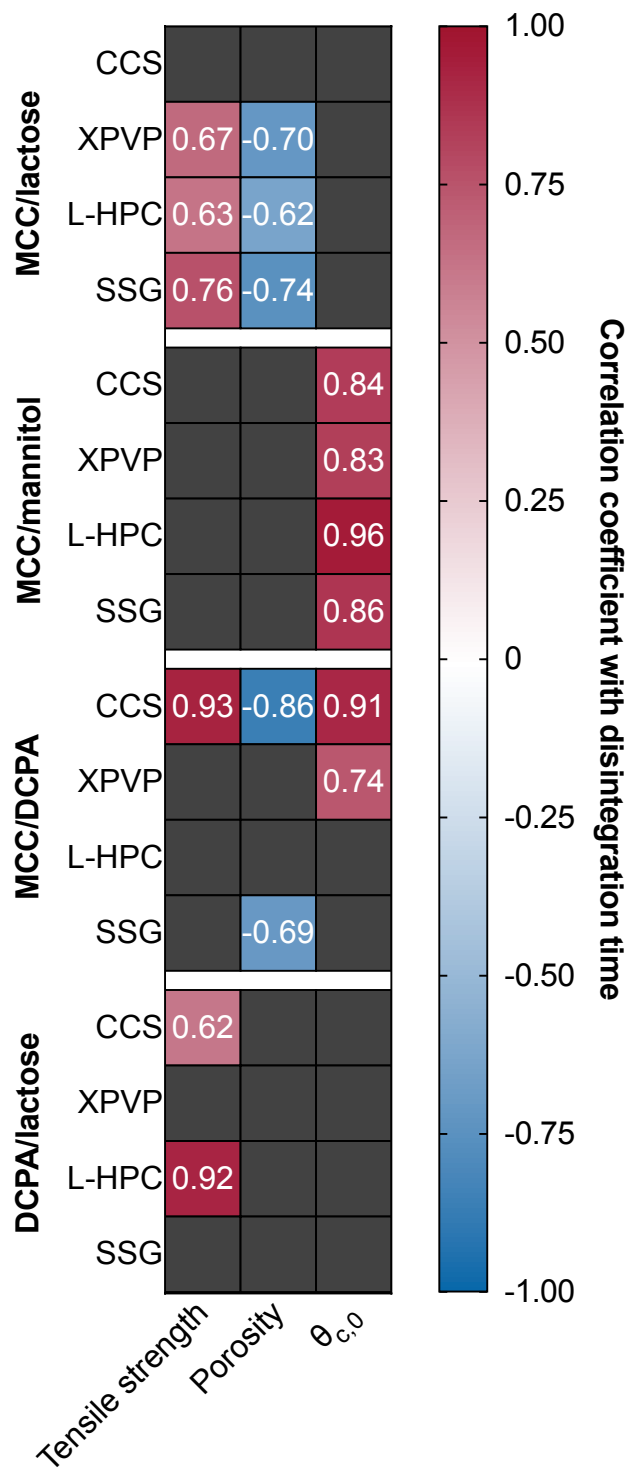


Figure 5.4: Pearson correlation coefficient between the disintegration time and the tensile strength, porosity and initial contact angle of all tablet during storage. Only significant correlations ($p < 0.05$) are shown.

5.4 Discussion

5.4.1 MCC/lactose tablets

MCC/lactose-based tablets were previously classified as wettability controlled (see Chapter 4). For these tablets at the initial timepoint, disintegration is slow due to a combination of the low porosity of the tablets and the slow dissolution of lactose from the tablet matrix. Changes in $\theta_{c,0}$ of MCC/lactose-based tablets do not significantly correlate with disintegration time, suggesting that although $\theta_{c,0}$ is shown to change based on the storage conditions, this does not necessarily influence the disintegration time for these tablets. Instead, increases in porosity and decreases in tensile strength are the key changes which result in decreases in disintegration time. This can be attributed to improved wettability due to increases porosity, and a lower force (due to reduced interparticle bonding strength) being required to break the tablet apart. This confirms the classification of MCC/lactose-based tablets as wettability controlled, as the disintegration at initial was limited by the low porosity (low liquid uptake) and the slow dissolution of lactose.

After storage at high temperature $\theta_{c,0}$ generally increases for these tablets, indicated by the strong correlation coefficient between storage temperature and $\theta_{c,0}$ (Figure 5.3A). Figure 5.3B shows that there is also strong correlations between the relative humidity during storage and porosity with tensile strength. After storage at elevated humidity, tablets expand due to premature swelling of MCC and the disintegrants, resulting in increased porosity and lower tensile strength.

5.4.2 MCC/mannitol tablets

Previously, these MCC/mannitol tablets were classified as dissolution controlled as the disintegration was primarily driven by the rapid dissolution of mannitol from the tablet matrix (see Chapter 4). This resulted in an increase in pore space, increased liquid penetration and thus rapid disintegration. The results of this study demonstrate that the disintegration time of these tablets is primarily correlated with $\theta_{c,0}$, which indicates that changes in disintegration time on stability can be associated primarily with changes

to the wettability of the tablet. If the wettability of the tablet decreases during storage – specifically accelerated temperatures – then the dissolution of mannitol could be slowed due to slower wetting of the mannitol particles (Lu *et al.*, 2014).

5.4.3 DCPA-based tablets

The correlation coefficients of tablets composed of MCC/DCPA or DCPA/lactose must be interpreted with caution. For these batches, the initial disintegration time is so rapid (<30 s for MCC/DCPA tablets and <60 s for DCPA/lactose tablets) that although changes in disintegration time can be seen in Figure 5.2D, these changes are actually only a few seconds for each condition. Due to the relatively low change in disintegration time, it is difficult to draw conclusions based on the apparent correlations shown in Fig 5.4.

However, for these tablets we observe that there are very small changes in the porosity, presumably as the porosity is already higher for DCPA-based tablets compared to MCC/mannitol or MCC/lactose. We also see slight changes in tensile strength, however these changes are more consistent at all storage conditions, unlike batches composed of MCC/mannitol or MCC/lactose, which show a more distinct difference depending on the storage humidity.

5.4.4 Effect of Disintegrant Choice

These results have primarily highlighted trends in the stability behaviour within each filler combination, as these are the most clear observations based on the data. However, disintegrant choice is also an integral part of the formulation selection. In this study, tablets containing XPVP tended to show the largest increases in porosity compared to tablets containing the same filler combination formulated with other disintegrants. This could be due to the increased moisture uptake capacity of XPVP (demonstrated by the moisture sorption data shown in Fig 5.1), leading to increased swelling during the disintegrant pre-activation. Aside from this observation, the change in other physical properties appears to be primarily driven by the fillers and disintegration mechanism.

5.5 Conclusions

This study investigated the effects of accelerated storage conditions on the physical properties of directly compressed placebo tablets. In terms of humidity, most formulations displayed increases in porosity and decrease in tensile strength after storage at high humidity. This can be explained by the premature expansion of swelling components (specifically MCC and disintegrants) as moisture is absorbed during storage. As a result, the microstructure of the tablet is permanently changed, even after removal from storage. The influence of storage temperature on the physical properties of tablets varied based on the formulation, however, the property most affected by storage was the initial contact angle. This suggests that high temperatures could affect the surface wettability of tablets during storage. For each batch studied, the initial performance-controlling mechanism could be considered to understand the changes observed after storage.

The focus of this study was to investigate the effects of different excipients and disintegration mechanisms on physical ageing. As such, uncoated tablets without an active pharmaceutical ingredient were used for this work. However, in a commercial setting most tablets would be coated during the manufacturing process. Tablet coating can offer several advantages, and can provide a slight lag in moisture uptake affects by forming an additional barrier to dissolution or disintegration of the tablet core. Having an understanding of the effects of storage on the core tablet components could inform the selection of coating and packaging materials.

It should also be noted that the scale of these changes in disintegration time (for example, a few minutes) would not generally be of concern in a commercial setting, and in fact, some of these changes (particularly those which occurred at the highest temperature and humidity conditions) may not occur during storage or stability studies performed under traditional ICH conditions. However, understanding the physical properties causing these changes can provide valuable mechanistic insight into the effects of these excipients and, consequently, provide a basis for excipient selection during formulation development. These physical changes could also have implications in a clin-

ical setting, for example, to identify potential changes for patients who live in humid climates, or when medication is stored in bathroom cabinets where moisture absorption is likely. Finally, future studies with additional timepoints within the first 2 weeks of the study would provide more information on the shape of the stability profiles for each property, and therefore facilitate modelling of these changes.

Chapter 6

Assessing the Dissolution Stability of Directly Compressed Tablet Formulations with Griseofulvin

Chapter Summary

In this chapter, accelerated stability studies were used to evaluate the effects of storage on tablets containing griseofulvin as a model API. Three of the 16 formulations from the placebo studies (Chapters 4 and 5) were brought forwards as the basis for griseofulvin-containing tablets, allowing for comparisons to be made between the physical stability and performance of tablets with and without the presence of an API. Dissolution profiles for the long-term storage of tablets were predicted using the dissolution stability approach proposed by Scrivens (2019).

6.1 Introduction

Stability studies are used to ensure a product is safe and effective throughout its lifetime. These studies are performed throughout drug product development, and are used in the determination of a product's shelf life and packaging selection, as well as informing formulation design and drug load in the early stages of development. Chemical stability focuses on identifying and quantifying the formation of chemical degradants, as well as identifying the potential degradation pathways. Studying the physical stability of a product ensures that in addition to being safe, the performance and efficacy of a product is consistent throughout its shelf life.

The ICH maintain a series of technical guidelines which define the requirements of pharmaceuticals in terms of safety, quality and efficacy. The ICH Q1A(R2) guideline outlines the design and implementation of stability studies for the registration of new drug substances and products (ICH, 2003). These guidelines suggest storage conditions of 25°C/60%RH (long-term), 30°C/65%RH (intermediate), and 40°C/75%RH (accelerated) for the stability assessment of drug products intended to be stored at room temperature. Traditional ICH studies are used throughout the pharmaceutical industry, however, an increasing number of companies are implementing APS approaches alongside these traditional studies (Williams *et al.*, 2017).

Most APS techniques utilise a moisture-modified version of the Arrhenius equation to estimate the rate of degradation under long-term storage conditions (Qiu, 2018a; Waterman, 2011). Whilst this approach is well-suited to predicting chemical degradation, it is unclear whether these approaches are applicable to predicting changes in physical stability. The underlying mechanisms of change in physical tablet properties are not guaranteed to follow Arrhenius behaviour as expected with chemical degradation, and as such, several studies have investigated the application of these approaches to physical properties such as dissolution during storage.

Li *et al.* (2016) used the ASAP*prime*[®] software to accurately predict whether there would be long-term changes in dissolution rate for two different API using data collected during an accelerated stability program. ASAP*prime*[®] is a stability modelling software

which is based on the Accelerated Stability Assessment Program (ASAP) proposed by Waterman *et al.* (2007). ASAP studies rely on the determination of the 'time to failure' for a range of different storage conditions in order to predict the point at which specification failure would occur during long-term stability studies.

Another approach to the prediction of long-term dissolution performance was proposed by Scrivens (2019). In this approach, an "acceleration factor" (AF) is determined to act as a single parameter which describes the change in a full dissolution profile. The acceleration factor is expressed as a function of time, and then a combination of curve-fitting and regression is used to determine the influence of temperature, humidity, and storage time on the dissolution performance. This approach offers the benefit of considering the dissolution profile in full, rather than selecting a single-point (e.g. the percentage of drug dissolved at 20 min), which could lead to inaccurate predictions.

Tsunematsu *et al.* (2020) applied a non-linear model which focused on the use of changes in surface area as a predictor for changes in dissolution performance after storage. Tsunematsu *et al.* (2020) were able to accurately predict the dissolution performance of tablets stored at 40°C/75%RH for 6 months using data collected over the course of a 7-week accelerated stability program.

Whilst these approaches can provide accurate predictions, the empirical nature of the models mean that they are often only applicable to the batch under investigation. These current approaches do not address the underlying mechanisms which cause the observed changes in product performance. This is a topic in which there is a lack of understanding, in part due to the wide range of influencing factors including both formulation selection and manufacturing processes. By shifting to a mechanistic approach to understanding physical stability, it could be possible to use the same models across a range of formulations.

The objective of this study is to assess the dissolution performance of tablets containing three different tablet formulations of griseofulvin before and after storage under accelerated conditions, and evaluate the relationship between the environmental conditions (temperature, humidity), the storage time, and the physical properties of the tablets (e.g. porosity, tensile strength, disintegration, and dissolution performance).

Changes in the tablet properties are compared against the corresponding placebo tablets with respect to the performance-controlling mechanisms. Finally, the predictive model proposed by Scrivens (2019) is applied to the dissolution of griseofulvin tablets to determine the long-term stability behaviour of each formulation.

6.2 Materials and Methods

6.2.1 Materials

All materials are described in Section 3.1.

6.2.2 Raw Material Characterisation

The characterisation of each excipient used in this study is detailed in Chapter 4. The model API, griseofulvin, was characterised by DVS (as described in Section 3.2.1.1 to determine its hygroscopicity and moisture sorption properties, and by gas pycnometry (as described in Section 3.2.1.3) to measure its true density.

6.2.3 Tablet Manufacture

In this study, three different formulations were used to prepare tablets. Each blend contained 30% w/w griseofulvin. A drug loading of 30% was selected with an aim of clearly distinguishing any effects of the API on physical stability without compromising the ability to manufacture the tablets by direct compression. Each formulation also contained a combination of two fillers (32% w/w each), CCS (5% w/w), and magnesium stearate (1% w/w). The filler combinations used in this study were based on three filler combinations used in the placebo study – MCC/mannitol, MCC/lactose, and MCC/DCPA. These filler combinations were selected to represent the three performance-controlling mechanisms described in Chapter 4, however, it should be noted that the performance-controlling mechanism may be affected by the addition of griseofulvin at 30% w/w. Given that both MCC/DCPA and DCPA/lactose shared the swelling controlled mechanism and displayed similar performance throughout Chapters 4 and 5, MCC/DCPA was selected to represent the swelling controlled batch for the griseofulvin study. The

disintegrant and lubricant concentrations were fixed to replicate the placebo batches tested in Chapters 4 and 5. The filler ratio was fixed at 1:1, but the concentrations lowered to accommodate the addition of griseofulvin. The blends were prepared by mixing griseofulvin, both fillers, and CCS in a Pharmatech AB-015 bin blender for 20 min, with a blend speed of 20 rpm and an agitator speed of 200 rpm. After 20 min, the lubricant was added and the powder was blended for a further 5 min. Tablets were then compacted with a 9 mm flat round die using a single punch automated tablet press (FlexiTab, Bosch Packaging Technology Ltd, Merseyside, UK) with a compression force of 10 kN for all batches.

6.2.4 Sample Storage

During the course of the stability study, samples were stored under accelerated conditions as described in Section 3.2.3. Based on the results presented in Chapter 5, an additional timepoint was added at 1 week to give more information on the rate of change of the physical properties during storage, and the highest temperature condition was lowered from 70°C to 60°C. The stability study design is outlined in Table 6.1.

Table 6.1: Accelerated stability study design for griseofulvin-containing tablets.

| Temperature | Humidity | Timepoints |
|-------------|----------|-------------------|
| 37°C | 30%RH | 1, 2, and 4 weeks |
| 37°C | 75%RH | 1, 2, and 4 weeks |
| 50°C | 75%RH | 1, 2, and 4 weeks |
| 60°C | 30%RH | 1, 2, and 4 weeks |
| 60°C | 75%RH | 1, 2, and 4 weeks |

Clear glass jars were used for the sample storage, and as such, the tablets were not protected from the effects of light. During storage, samples stored in the controlled temperature rooms (37°C and 50°C) may have been exposed to light while the controlled temperatures rooms were in use, however samples stored in the 60°C oven were not exposed to light during storage. After removal from storage, samples were kept in the dark in cupboards until needed for testing.

At each storage condition, a DS1923 Hygrochron iButton Temperature/Humidity

logger (Measurement Systems Ltd, Berkshire, UK) was added to one of the sample jars to confirm the target storage conditions were maintained throughout the storage time. Each datalogger recorded the temperature and humidity within the jar every 600 s. Samples were allowed to equilibrate to room temperature for 2 weeks after removal from the accelerated storage condition, allowing any relaxation effects to occur prior to testing.

6.2.5 Tablet Characterisation

The sampling plan for the stability studies is outlined in Table 6.2. Details on each of the methods are given in Chapter 3, under the specific references given in Table 6.2.

Table 6.2: Sampling plan for the accelerated stability study of griseofulvin-containing tablets, including the number of tablets tested at initial (n_{initial}) and at each stability timepoint (n_t).

| Test | Method | n_{initial} | n_t |
|-----------------------|-----------------|----------------------|-------|
| Weight & dimensions | Section 3.2.4.1 | All | 14 |
| Tensile strength | Section 3.2.4.1 | 10 | 4 |
| Porosity | Section 3.2.4.2 | All | 14 |
| Dynamic contact angle | Section 3.2.4.3 | 4 | 4 |
| Disintegration | Section 3.2.4.4 | 3 | 3 |
| Dissolution | Section 3.2.4.5 | 3 | 3 |

6.2.6 Predicting Dissolution after Long-Term Storage

Scrivens (2019) described an approach to model the shift in dissolution profiles on stability by calculating an acceleration factor (AF) for the dissolution rate. This approach is based on the observation that adjustment of the x-axis (i.e. the dissolution sampling time) allows the dissolution curves from different storage times and conditions to overlap. An overview of this approach is given in Figure 6.1.

Firstly, the dissolution profile is fitted to a Weibull curve, to extract a dissolution rate constant, k_d , as shown in Eq 6.1:

$$y = 100 \cdot (1 - \exp(-(x \cdot k_d)^b)) \quad (6.1)$$

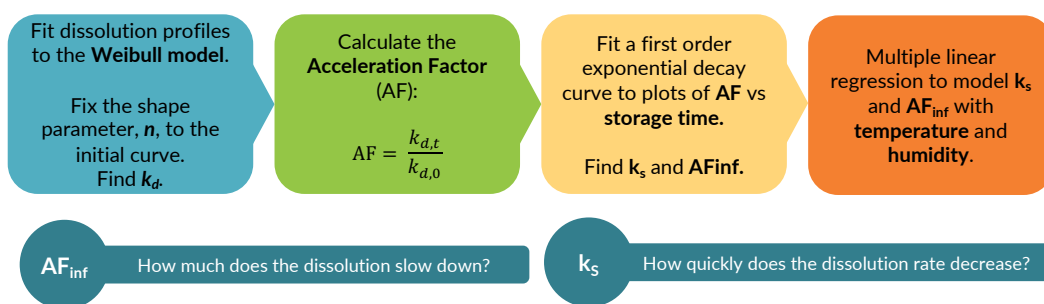


Figure 6.1: A summary of the accelerated dissolution stability modelling approach proposed by Scrivens (2019).

where y is the percentage of the final dose dissolved at time x , k_d is the dissolution rate constant, and b is the shape parameter for the dissolution curve.

This approach assumes that the dissolution profiles after storage will overlap with the initial dissolution curve once the time is adjusted, and so the shape parameter, b , is fixed as the shape parameter of the initial dissolution curve, b_0 .

For each dissolution curve, k_d was obtained by fitting the Weibull curve using b_0 as the shape parameter for all dissolution profiles. The AF was then calculated using the values of k_d as shown in Eq 6.2 (Scrivens, 2019):

$$AF = \frac{k_{d,t}}{k_{d,0}} \quad (6.2)$$

where $k_{d,0}$ is the dissolution rate constant for samples at the initial timepoint, and $k_{d,t}$ is the dissolution rate of samples tested after storage at each condition. An AF value of 1 suggests that there is no change in the dissolution rate, whilst values >1 indicate an increase in the dissolution rate, and values <1 indicate a decrease in the dissolution rate relative to the initial profile.

In general, Scrivens (2019) observed that for each condition, the AF as a function of time could be approximated by a first-order exponential decay curve. By fitting the profiles of AF to an exponential decay curve, it is therefore possible to determine a rate constant for the change in AF, k_s , and the plateau at infinite time, AF_{inf} . These two properties are helpful in describing both the maximum change in dissolution rate that we would expect (AF_{inf}), and the speed at which this change in dissolution rate occurs,

(k_s).

Scrivens (2019) then performed multiple linear regression using these properties to determine coefficients for both temperature and humidity. Several empirical models were assessed, but the best fit for both k_s and AF_{inf} could be obtained by the following equations (Eq 6.4):

$$k_s = \exp \left(C_{0,k} + C_{1,k} \frac{1}{T} + C_{2,k} \ln(RH) \right) \quad (6.3)$$

$$AF_{inf} = \exp \left(C_{0,AF} + C_{1,AF} \frac{1}{T} + C_{2,AF} \ln(RH) \right) \quad (6.4)$$

where C_0 is a coefficient for the intercept; C_1 is the coefficient of temperature, T; and C_2 is the coefficient for the relative humidity, RH.

To predict the amount of drug dissolved, D_t , for different sampling times and storage conditions, the equations of k_s and AF_{inf} are combined as shown in Eq 6.5 (Scrivens, 2019):

$$D_t = D_{inf} \cdot \left\{ 1 - \exp \left[- \left(\{ AF_0 + (AF_{inf} - AF_0) \cdot (1 - \exp[-k_s \cdot t_s]) \} k_d \cdot t_d \right)^b \right] \right\} \quad (6.5)$$

where D_{inf} is the amount of drug dissolved at an infinite sampling time (assumed to be 100%); AF_0 is the acceleration factor after 0 weeks of storage (i.e. 1); t_s is the storage time (in weeks); t_d is the dissolution sampling time (in min); and k_d and b are the rate and shape parameters (respectively) of the Weibull fit for the dissolution curve at initial.

6.3 Results

6.3.1 Weight and Dimensional Analysis

The weight and dimensions of all tablets prior to storage under accelerated conditions is given in Table 6.3. The differences in mass across the batches was a result of varying excipients For each formulation, the relative standard deviation was less than 5% across the weight of the full batch. The diameter of the tablets was consistent in all cases at

9.02 mm. The thickness of the tablet varied similarly to the weight, with variability of approximately 3.9 to 5%.

Table 6.3: The initial weight and dimensions of each batch, showing mean and relative standard deviation (%). All tablets were measured prior to storage, n = 330 per batch.

| Batch | Weight (mg) | Diameter (mm) | Thickness (mm) |
|--------------|------------------|----------------|----------------|
| MCC/Mannitol | 268.03 (4.91) | 9.02 (0.04) | 3.22 (5.09) |
| MCC/Lactose | 229.04 (4.10) | 9.02 (0.04) | 3.24 (4.28) |
| MCC/DCPA | 306.25 (3.86) | 9.02 (0.06) | 3.31 (3.95) |

6.3.2 Tensile Strength

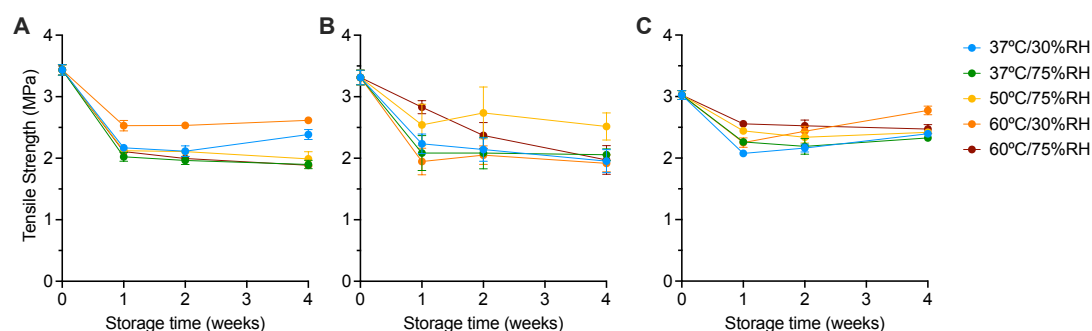


Figure 6.2: The tensile strength of (A) MCC/lactose-, (B)MCC/mannitol-, and (C) MCC/DCPA-based tablets containing griseofulvin before and after storage under accelerated temperature and humidity conditions (mean \pm standard deviation, n = 4).

The tensile strength of tablets after storage is shown in Fig 6.2. For each batch, the tensile strength decreased within the first week or storage at each condition. In most cases, the tensile strength remained relatively constant after the first week, with a few exceptions including MCC/mannitol tablets stored at 60°C/75%RH which continued to decrease throughout the duration of the study, and 50°C/75%RH which increased slightly at the 2 week timepoint. In some cases, there was a slight recovery of tensile strength after the 1 week timepoint, for example, MCC/DCPA tablets stored at 30%RH and MCC/lactose tablets stored at 37°C/30%RH.

6.3.3 Porosity

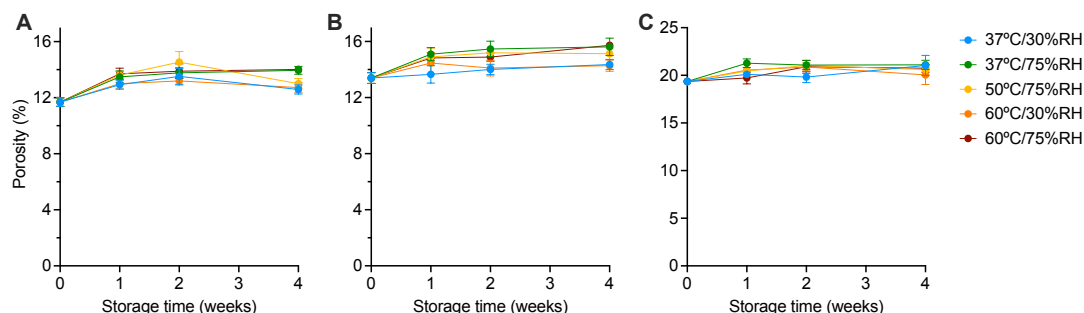


Figure 6.3: The porosity of (A) MCC/lactose-, (B) MCC/mannitol-, and (C) MCC/DCPA-based tablets containing griseofulvin before and after storage under accelerated temperature and humidity conditions (mean \pm standard deviation, $n = 210$ at 0 weeks, and $n = 14$ at subsequent timepoints).

The porosity of each batch is shown in Fig 6.3. In Fig 6.4, the relative change in porosity for each tablet before and after storage is summarised.

At the initial timepoint, MCC/mannitol and MCC/lactose have a porosity of approximately 13% and 11%, respectively. MCC/DCPA tablets have a higher porosity of around 20%, which is due to the higher intraparticle porosity of DCPA (as described in Chapter 4).

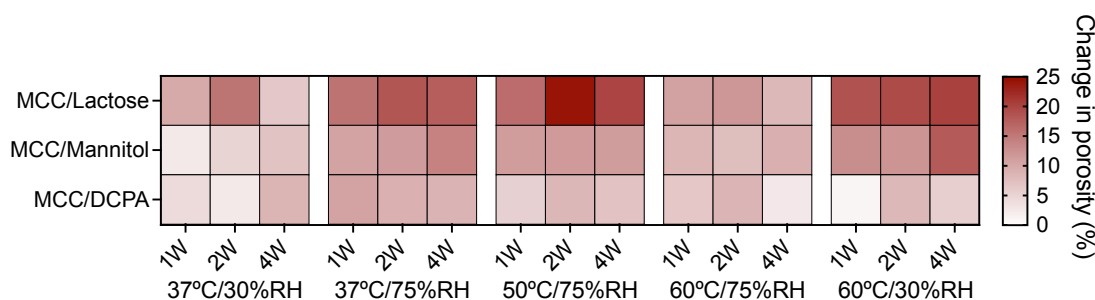


Figure 6.4: The mean relative change in porosity for tablets containing griseofulvin after storage under accelerated temperature and humidity conditions.

After storage, small increases in porosity are observed for tablets composed of MCC/mannitol and MCC/lactose stored at 30%RH. On the other hand, tablets stored at 75%RH show much higher increases in porosity, with increases of up to 25% of the

initial tablet porosity for MCC/lactose. These observations are attributed to the premature activation of swelling particles in the formulations. During storage, particularly at high humidity conditions, swelling particles such as MCC and CCS may prematurely expand due to the presence of moisture in the atmosphere. After removal from storage there is an equilibration period in which this moisture evaporates, however, changes to the microstructure are permanent and are not reversed. These effects may be less pronounced in the case of MCC/DCPA due to the higher starting porosity, meaning that the pore space is sufficiently high to accommodate the premature swelling without significantly altering the microstructure of the tablet.

6.3.4 Contact Angle

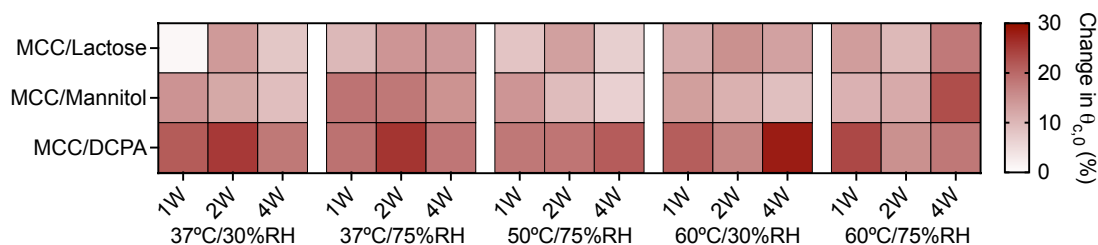


Figure 6.5: The relative change in $\theta_{c,0}$ after 1, 2 and 4 weeks storage at accelerated temperature and humidity conditions (mean of $n = 4$).

The change in $\theta_{c,0}$ of each batch is shown in Fig 6.5. In general, the contact angle increases during storage (with the exception of MCC/lactose stored at 37°C/30%RH for 1 week, which shows little change). Increases in the initial contact angle suggest decreases in the surface wettability of the tablets. Tablets composed of MCC/DCPA generally showed the largest increases in $\theta_{c,0}$, whilst those containing MCC/mannitol and MCC/lactose showed slightly less change.

6.3.5 Disintegration Time

The disintegration times of each batch before and after storage are shown in Fig 6.6. In general, tablets composed of MCC/mannitol and MCC/lactose showed little change during storage, with the exception of the 60°C/75%RH condition which resulted in

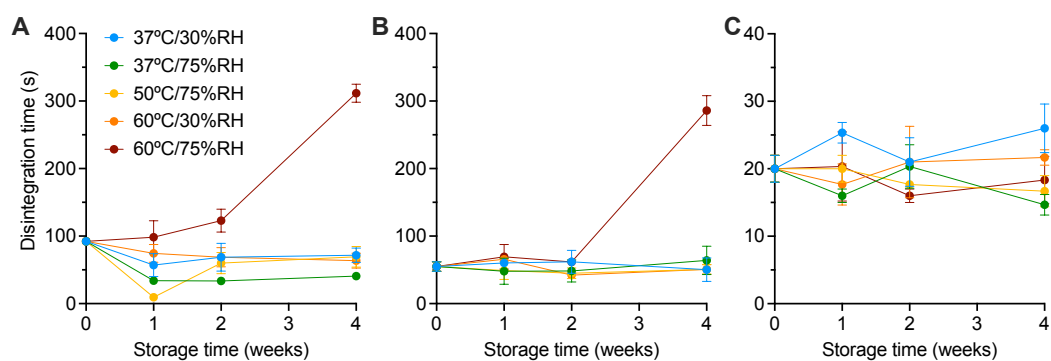


Figure 6.6: The disintegration time of griseofulvin tablets containing (A) MCC/lactose, (B) MCC/mannitol, and (C) MCC/DCPA after storage under accelerated conditions (mean \pm standard deviation, $n = 3$).

significantly slower disintegration of MCC/mannitol and MCC/lactose tablets after 4 weeks of storage. Interestingly, the disintegration times of MCC/mannitol tablets showed little change in the first 2 weeks of storage at this condition, and MCC/lactose tablets also showed only slight increases prior to the 4 week timepoint. In the case of MCC/DCPA-based tablets, which showed much faster disintegration times at initial (approximately 20 s, compared to 55 s for MCC/mannitol and 92 s for MCC/lactose), there was no clear trend observed for changes in disintegration time after storage – even for the highest temperature and humidity conditions.

6.3.6 Dissolution

For each formulation, dissolution testing was performed during method development to assess whether the dissolutions profiles were affected by coning (as described in Section 3.2.4.5). The results of testing at paddle speeds of 50 and 75 rpm are shown in Fig 6.7. The profiles indicate that MCC/DCPA tablets are significantly affected by coning, with only approx 50% of the final dose being released after 60 mins. Coning is often associated with high density materials such as DCPA. As a result of this comparison, all dissolution testing was performed at 75 rpm.

The dissolution profiles of tablets stored under accelerated conditions for 4 weeks are shown in Fig 6.8. To compare the dissolution profiles, dissolution is plotted as a

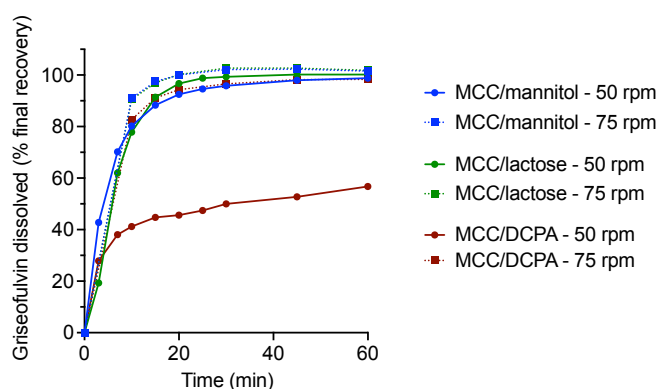


Figure 6.7: The dissolution profiles of griseofulvin from tablets composed of MCC/mannitol, MCC/lactose, and MCC/DCPA with paddle speeds of 50 and 75 rpm, shown as a percentage of the final release of griseofulvin after a 30 min infinity spin at 200 rpm.

percentage of the final mass of griseofulvin released from the tablet (i.e. the mass of griseofulvin after completion of the infinity spin).

As shown in Fig 6.8, the dissolution rate of each of these batches is affected by storage. In particular, storage at 60°C/75% RH appears to cause the biggest slow-down in dissolution rate for MCC/mannitol and MCC/lactose. In the case of MCC/DCPA-based tablets, storage at 60°C/30% RH and 60°C/75% RH appears to have resulted in the typical dissolution curve being distorted and displaying increased variability. For these conditions, spare MCC/DCPA-based tablets were tested (giving n=6 instead of the original n=3) to confirm that the changes in dissolution profile was not the result of a measurement error.

The acceleration factor was calculated for each storage condition and timepoint, as described by Scrivens (2019). In order to adequately fit a first-order exponential decay curve, additional AF values were interpolated from the calculated values at 0.5, 1.5 and 3 weeks to allow adequate fitting of the curve. The AFs and first-order exponential decay curves are shown in Fig 6.9. In the case of MCC/mannitol (Fig 6.9B), the 37°C/30% condition was excluded from further modelling, as the curve plateau, AF_{inf} , could not be determined for this condition.

For each condition, the parameters obtained from the curve, k_s and AF_{inf} , were

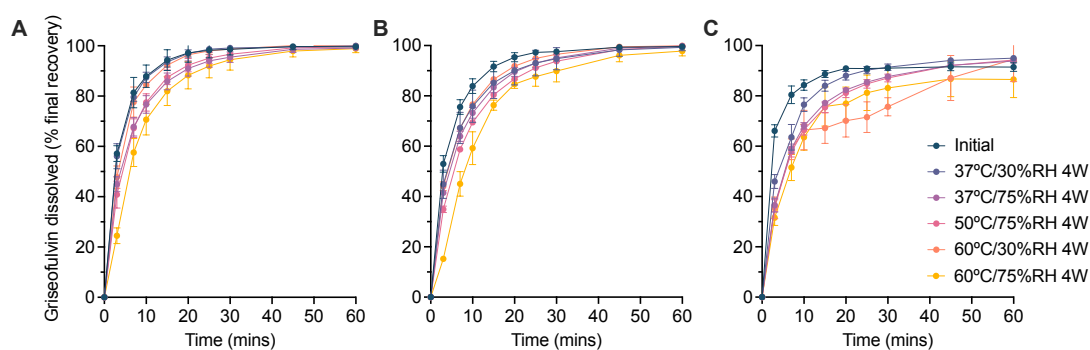


Figure 6.8: Dissolution profiles of (A) MCC/lactose-, (B) MCC/mannitol-, and (C) MCC/DCPA-based tablets containing griseofulvin before and after 4 weeks of storage under accelerated temperature and humidity conditions (mean \pm standard deviation, $n = 3$ with the exception of the 60°C/30%RH and 60°C/75%RH condition for MCC/DCPA for which $n=6$).

modelled by multiple linear regression to determine coefficients for temperature and humidity for each formulation. Finally, the resultant equations from the multiple linear regression were combined with the original Weibull dissolution equation, to allow predictions of long term dissolution rates as described in Section 6.2.6.

The model was assessed by comparing the experimental values collected during dissolution studies of each batch with the values predicted by the predictive model for each formulation (shown in Fig 6.10).

The Scrivens model was used to estimate the expected dissolution profiles of tablets of each batch if they were stored for 2 years, 1 year, and 6 months at ICH-defined conditions for long-term, intermediate, and accelerated storage, respectively. The predicted profiles are shown in Fig 6.11.

6.4 Discussion

6.4.1 Comparison of Placebo and Griseofulvin Tablets

The physical properties of the griseofulvin tablets are compared with the corresponding placebo tablets (as discussed in Chapter 4) in Figure 6.12.

The disintegration of tablets composed of MCC/lactose was classified as wettabil-

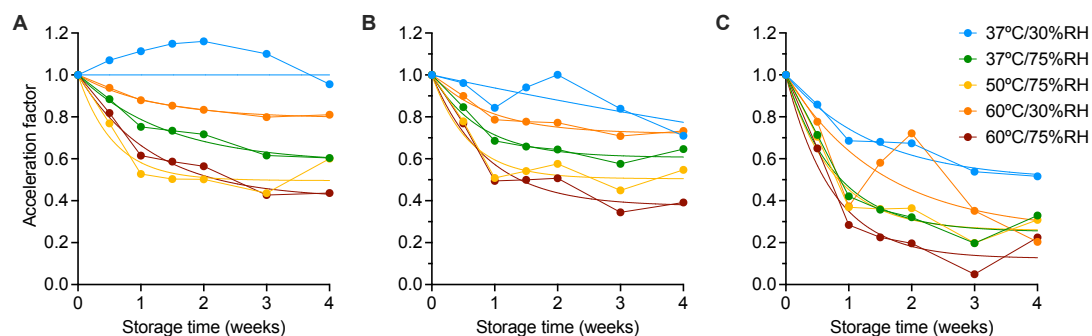


Figure 6.9: The acceleration factors of (A) MCC/lactose, (B) MCC/mannitol, and (C) MCC/DCPA, using experimental values (0, 1, 2, and 4 weeks) and values imputed by spline interpolation (0.5, 1.5, and 3 weeks), including the fit of a first-order exponential decay curve for each condition.

ity controlled in the placebo studies (Chapter 4). When griseofulvin is added to the formulation, tablets show decreased porosity and wettability when manufactured under the same process conditions. The disintegration of tablets is faster for those containing griseofulvin, suggesting that reduction of the fillers (decrease of 15% wt. each of MCC and lactose) with griseofulvin could change the performance-controlling mechanism such that tablet disintegration is no longer limited by the slow liquid penetration and wetting of the tablet.

MCC/mannitol- and MCC/DCPA-based batches do not show significant differences in disintegration time when griseofulvin is added to the formulation, despite decreases in porosity and wettability for both formulations.

Tablets containing MCC/mannitol were previously described as being dissolution controlled, whereby rapid dissolution of mannitol occurred during the disintegration process, resulting in faster liquid penetration and therefore rapid disintegration. In Chapter 4, placebo tablets containing MCC/mannitol were also manufactured at a higher porosity, which resulted in slower disintegration, which is attributed to the loss of efficiency of swelling particles.

The porosity of MCC/DCPA tablets is most affected by the addition of griseofulvin to the formulation, due to the reduction in DCPA which has a high intraparticle porosity (as discussed in Chapter 4). Placebo tablets composed of MCC/DCPA were described

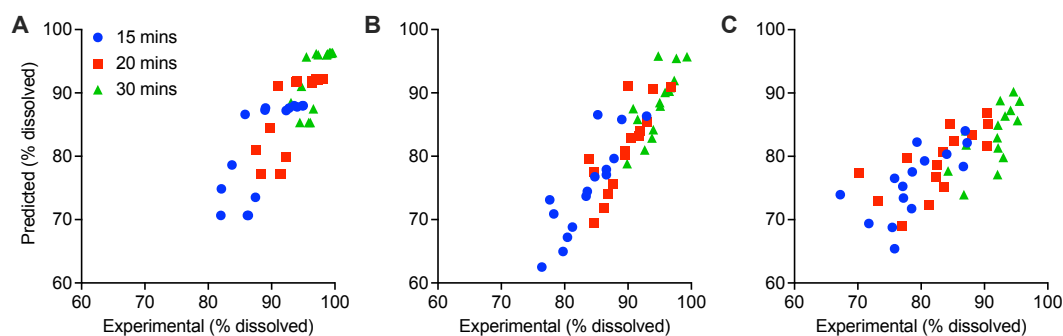


Figure 6.10: The predicted and experimental values for griseofulvin dissolution at 15, 20, and 30 min at each condition for (A) MCC/lactose, (B) MCC/mannitol and (C) MCC/DCPA tablets.

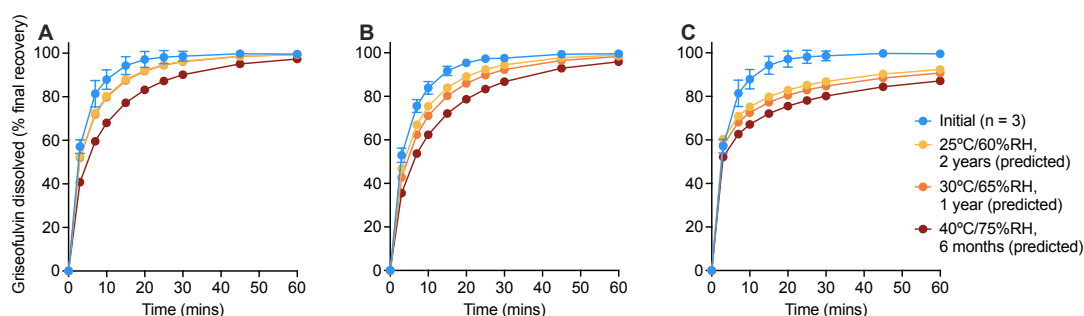


Figure 6.11: The predicted dissolution profiles for (A) MCC/lactose, (B) MCC/mannitol, and (C) MCC/DCPA tablets containing griseofulvin after storage under ICH long-term (25°C/60%RH), intermediate (30°C/65%RH), and accelerated (40°C/75%RH) storage conditions.

as swelling-controlled, as they were not significantly affected by changes in porosity, and are mainly dependent on the swelling efficiency of the disintegrant against the insoluble matrix. In the case of tablets containing griseofulvin, the disintegration time is not significantly altered compared to the placebo tablets.

6.4.2 The Effects of Temperature and Humidity

Correlations between temperature, humidity and physical changes in tablet properties are shown in Fig 6.13.

There are few correlations between the temperature and the physical tablet prop-

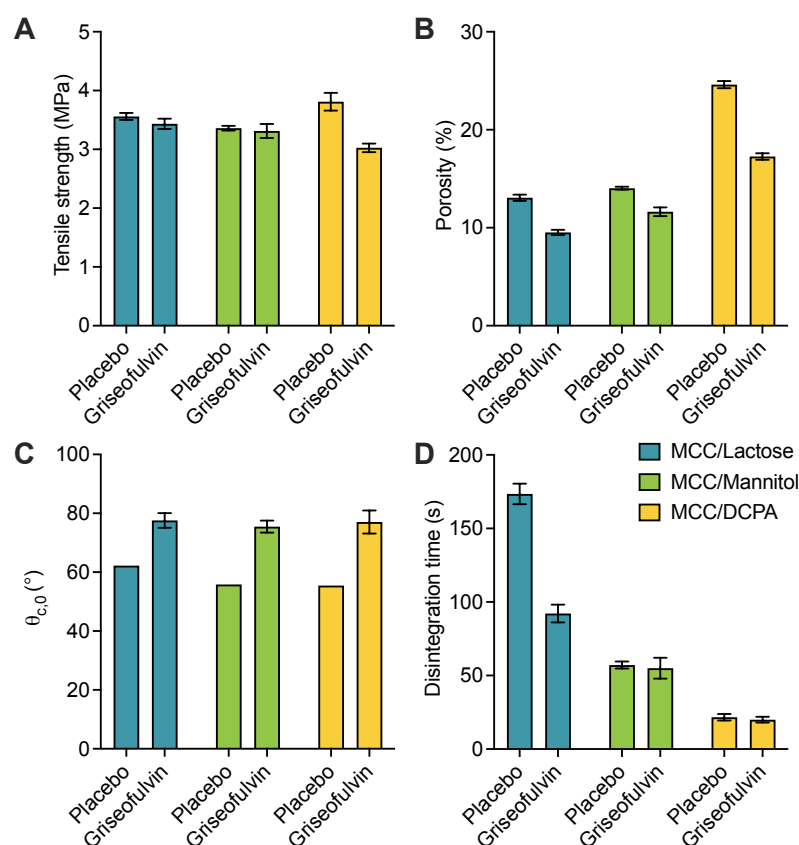


Figure 6.12: The (A) tensile strength, (B) porosity, (C) initial contact angle ($\theta_{c,0}$) and (D) disintegration time of placebo tablets (see Chapter 4) and griseofulvin tablets prior to storage (mean \pm standard deviation, except for (C) where $n = 2$ for placebo tablets and so no standard deviation is shown).

erties, with the exception of the dissolution curve parameter, b , for MCC/lactose, and the tensile strength for MCC/DCPA.

In terms of humidity, we see several different properties which correlate to the storage humidity. Firstly, all batches show a correlation between humidity and the dissolution rate, k_d , indicating that storage at high humidity leads to decreases in the dissolution rate for all formulations. This suggests that during storage, changes in dissolution performance are mainly driven by the humidity, i.e. the presence of moisture in the atmosphere.

The correlations between physical tablet properties and humidities also suggest dif-

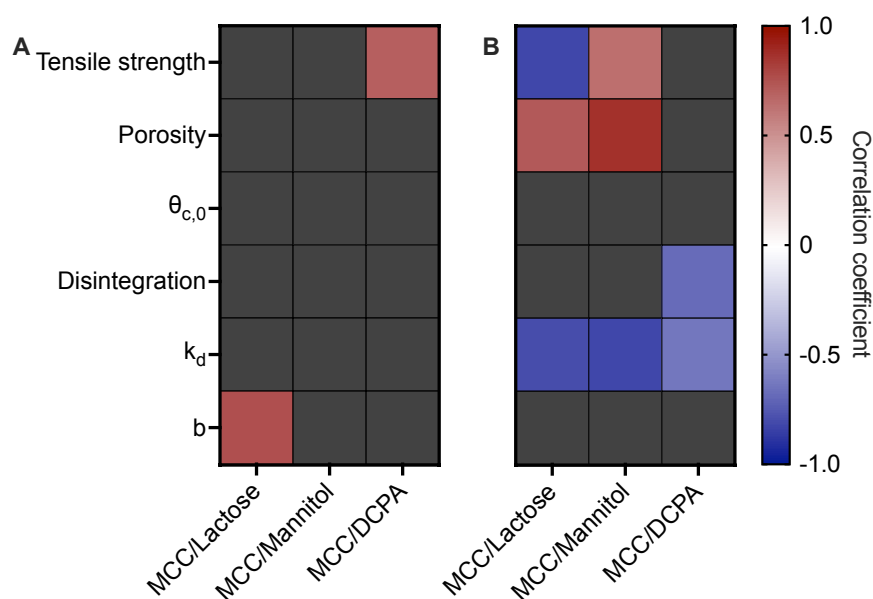


Figure 6.13: Pearson correlation coefficients between (A) temperature and (B) humidity with the change in physical tablet properties during storage. Only significant correlations ($p < 0.05$) are shown.

ferent mechanisms of change in each formulation. For example, both MCC/lactose and MCC/mannitol show positive correlations between humidity and porosity, indicating that high humidity leads to increased porosity after storage. This is likely due to the premature swelling of MCC and CCS upon exposure to high humidity, and the subsequent loss of moisture after removal from storage. Overall, the expansion of particles results in permanent change in the microstructure, which is reflected in the change in tablet porosity. This is discussed in Chapter 5, where porosity changes were strongly correlated with the storage humidity for all MCC-based formulations.

In addition to correlations with porosity, storage humidity is also correlated with tensile strength for both MCC/lactose and MCC/mannitol tablets. However, unlike porosity, the correlations with tensile strength differ between the formulations. For MCC/lactose, we observe a negative correlation with tensile strength, indicating that higher humidity conditions are associated with decreased tensile strength. This is consistent with the results of the MCC-based formulations used in the placebo study (Chapter

5). These decreases in tensile strength were attributed to increased porosity reducing the contact between particles within the tablet, leading to weaker interparticle bonds.

On the other hand, the tensile strength of tablets composed of MCC/mannitol show a positive correlation with humidity, which suggests that storage at high humidity results in stronger interparticle bonds between tablets. Although this was not observed in the placebo studies (Chapter 5), this has been demonstrated for various formulations in the literature (Chowhan, 1980b; Molokhia *et al.*, 1982). In these studies, increasing tensile strength was attributed to the partial dissolution and recrystallisation of soluble fillers, leading to the formation of solid bridges. Although we see overall reduced tensile strength of MCC/mannitol tablets after storage at all conditions (as shown in Fig 6.2), the positive correlation between humidity and tensile strength suggests that both mechanisms (preactivation of swelling particles and the partial dissolution and recrystallisation of soluble particles) may be occurring simultaneously and therefore both mechanisms are having a competing influence on the tensile strength of MCC/mannitol tablets.

The final formulation, MCC/D CPA, shows a negative correlation with humidity for the disintegration time. This would imply that increased humidity is associated with lower dissolution times, however, as discussed in Chapter 5, the absolute changes in disintegration time are very small (<10 s), and so correlations with this property should be interpreted with caution.

It is also noted that in the study of placebo tablets, most formulations containing MCC/lactose and MCC/mannitol demonstrated strong correlations between temperature and the contact angle, which are not observed in the study of griseofulvin tablets.

Further studies of these formulations manufactured with a range of drug loadings (e.g. 5%, 10%, and 20% wt. griseofulvin) could provide further insight into these changes in correlations, however, the performance of stability studies on multiple formulations with multiple levels of drug loading would result in a large volume of samples to be stored and analysed, and as such, the use of an automated dissolution system would be essential.

A schematic summary of the mechanisms of change during storage is shown in Fig

6.14.

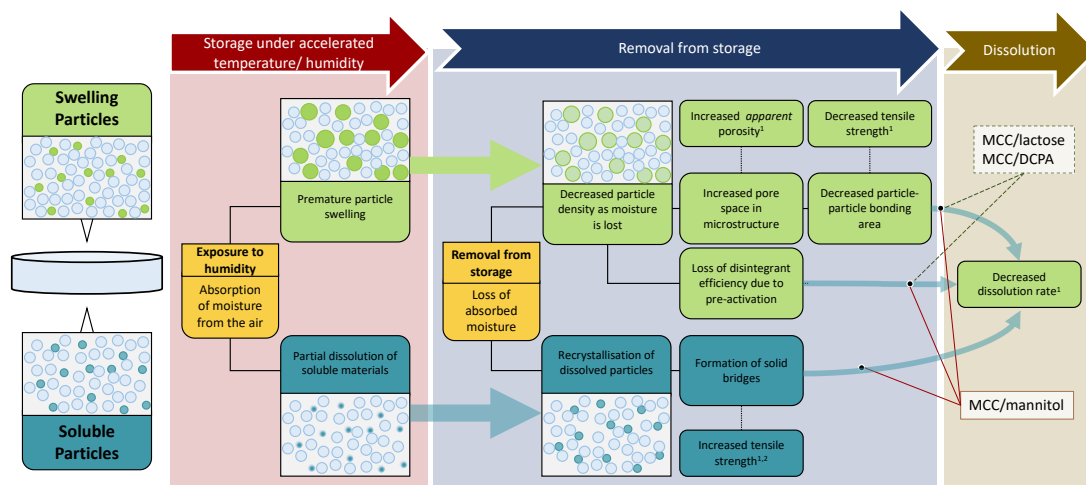


Figure 6.14: A summary of the potential mechanisms of physical change during the storage of tablets under accelerated conditions, including the expected effects on the physical tablet properties.

6.4.3 The Effects of Storage on Product Performance

Correlation coefficients were also calculated for each property with the Weibull dissolution parameters for rate, k_d , and shape, b , as shown in Fig 6.15.

In general, there are few significant correlations with the dissolution shape parameter, b (Fig 6.15). MCC/lactose tablets show correlations between the dissolution rate and humidity, porosity and b . Decreasing dissolution rate is associated with increases in humidity and porosity, as described for Fig 6.13 in Section 6.4.2. Similarly to MCC/lactose, the dissolution rate of tablets containing MCC/mannitol show correlations with humidity, porosity and tensile strength. MCC/DCPA-based tablets show correlations between the tensile strength, humidity, and disintegration time with tablet dissolution rate.

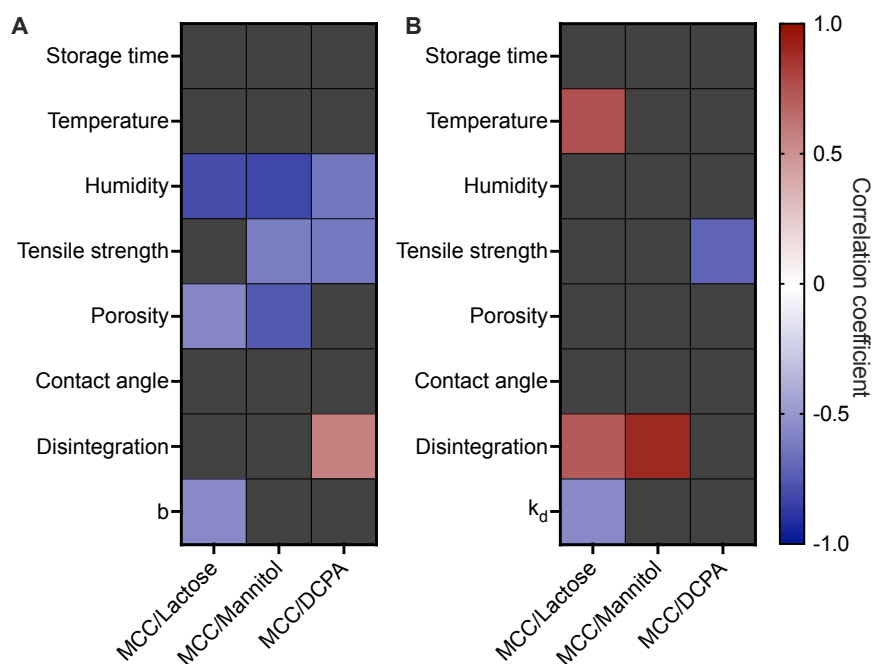


Figure 6.15: Pearson correlation coefficients between the Weibull dissolution parameters, (A) k_s and (B) b , with the change in physical tablet properties during storage. Only significant correlations ($p < 0.05$) are shown.

6.4.4 Prediction of Long-Term Dissolution Changes

Using the approach described by Scrivens (2019) allows the prediction of long-term dissolution profiles using data collected by following an accelerated stability protocol. This approach has been applied to data collected from tablets griseofulvin with three different formulations. To validate these predictions, long-term data would be required, which is not within the scope of this study. However, this approach and the predictions still provide an insight into the temperature- and humidity- dependence of the formulations, as well as potential stability changes which may occur. For example, the predicted profiles for each formulation shown in Fig 6.11 suggest that large decreases in dissolution performance may be observed for the tablets composed of MCC/DCPA, even after storage at the long-term condition of 25°C/60%RH, with only 80% of the total dose released after 60 min. Decreases in the rate of dissolution are also observed for long-term storage of MCC/lactose and MCC/mannitol (Fig 6.11A and B, respectively),

although these changes are smaller. For all formulations, storage at 40°C/75%RH for 6 months is predicted to cause a much larger drop in dissolution rate, which is supported by the decrease in dissolution rate that we observed after storage for 4 weeks at the similar condition of 37°/75%RH (Fig 6.8). In these cases, where dissolution performance is affected, careful packaging selection may be employed to mitigate these affects. For example, the use of a desiccant or moisture-protective blisters may be required to prevent changes in dissolution rate during the shelf-life of a product.

To generate accurate predictions using this approach, it is important that there are enough timepoints to sufficiently define both the curve shape and the plateau level for plots of AF over the storage time. In an ideal scenario, the stability study would be flexible in terms of storage timepoints, such that timepoints are adjusted during the course of the study based on the rates of change in these properties. For dissolution studies, this level of flexibility could be achieved through the use of automated systems and on-line UV sample analysis, which would allow dissolution profiles to be produced and analysed rapidly. In practice, there are several factors which may contribute towards limited flexibility. In cases where automated dissolution baths are not available, semi-automated or manual baths must be used; UV analysis is not always suitable, for example, batches with low drug loading may present difficulty achieving the required sensitivity for quantification; and finally, large volumes of samples can increase the turn-around time for results, resulting in delays to the feedback cycle.

Another factor in the accuracy of predictions is the number of storage conditions used. In this study, we include 5 conditions which span 3 temperature (from 37° to 60°C), and 2 humidity conditions (30 and 75%RH). The addition of further storage conditions provides additional data for the multiple linear regression to find temperature and humidity coefficients for k_s and AF_{inf} , however, each additional condition will raise the number of samples as multiple timepoints will be required, as described above.

6.5 Conclusions

This study has applied an accelerated stability study design to assess the physical stability of griseofulvin tablets composed of three different filler combinations – MCC/lactose, MCC/mannitol, and MCC/DCPA. The results of this study contribute towards improved understanding of the mechanism of change of certain properties during storage, and can also be compared with previous chapters in which the same formulations were studied without the presence of griseofulvin (Chapters 4 and 5). The results of this study demonstrate that for all formulations tested, decreases in dissolution rate correlate with increased storage humidity. In addition to dissolution rate, the tensile strength and porosity of MCC/mannitol and MCC/lactose also correlate with storage humidity. On the other hand, the storage temperature shows few correlations with the physical properties of these tablets.

Finally, the dissolution performance of the tablets was assessed by applying the predictive model proposed by Scrivens (2019) to generate predictions of the dissolution performance which might be expected after long-term storage. In this study, predictions were generated for storage at the long-term (25°C/60%RH), intermediate (30°C/65%RH), and accelerated (40°C/75%RH) conditions, as defined by the ICH. These profiles suggested that the dissolution rate of MCC/mannitol and MCC/lactose tablets would be slightly lower after long-term storage, whilst predictions of MCC/DCPA showed significant changes in the performance, even after storage at the milder condition of 25°/60%RH. These predictions must be validated through the collection of long-term stability data, however, the predictions may still offer an insight into potential stability issues which could be investigated further.

Chapter 7

Conclusions & Future Outlook

7.1 General Conclusions

This work has focused on the application of accelerated stability techniques for the assessment of physical tablet stability, in particular, *in vitro* performance attributes such as disintegration and dissolution performance. As industry leaders and regulatory authorities work together to improve the regulatory guidance around the use of APS techniques to predict and monitor chemical degradation in regulatory submissions, it seems appropriate that an increasing volume of research is now also directed towards developing equivalent approaches which can suitably assess the critical quality attributes which are likely to affect product performance on stability.

In this project, 16 different placebo formulations containing different combinations of fillers and disintegrants were characterised and classified based on the performance-controlling mechanism. These mechanisms were explored in order to determine the critical formulation or manufacturing parameters which must be controlled in order to optimise tablet disintegration. This was summarised in the form of a simple workflow, which can be used to identify the performance-controlling mechanism of a given formulation.

The formulations discussed above were then subjected to an accelerated stability study, using five different temperature and humidity conditions, with analysis after 2 and 4 weeks of storage. The physical properties of each batch were assessed during the study,

to determine changes in tensile strength, porosity, wettability, and disintegration time. These physical changes were considered with respect to the performance-controlling mechanisms proposed earlier, and the key mechanisms of change with temperature and humidity were discussed.

Finally, tablets were manufactured with a model API using a selection of the base formulations assessed during the placebo study. The addition of an API, griseofulvin, allowed for the addition of dissolution testing throughout the stability program. Changes in dissolution performance were compared with changes in other physical properties in order to identify relationships between the different physical properties for each formulation. As well as investigating the mechanisms of change in performance, the dissolution data was also modelled using a predictive approach described by Scrivens (2019) to predict the dissolution performance after long-term storage.

7.2 Future Work

This project forms a starting point for a range of future work, in terms of both disintegration mechanisms and stability testing. Specifically, the following proposals would be of interest.

7.2.1 Further Development of the Workflow for Classifying the Performance-Controlling Disintegration Mechanisms

In Chapter 4, we proposed a workflow which could determine the performance-controlling disintegration mechanism of directly compressed tablets. Whilst this workflow is well-supported by the data herein to guide classification of formulations, further work could be performed to improve the workflow in terms of making it robust and flexible for a wider range of formulations and properties. With this further work to validate the workflow and define the decision points, this workflow could then be incorporated into the formulation design stages in industry to speed up development times for new formulations.

Define Criteria for the Decision Points. The workflow proposed in Chapter 4 features several decision points which guide the classification of tablets. These decision points were identified by comparing all formulations studied herein, however, using the current data it was unclear where the true limits of these decision points lie. For example, we do not have sufficient data to define whether a raw materials intrinsic dissolution rate is 'fast' or 'slow'. To identify the tolerances of these decision points, further studies would be required to target the wider design space and to include materials with a wider range of properties. This may be a challenging task, given the vast number of different excipients and materials which are used across the pharmaceutical industry.

Validate and Refine with Further Variables. This workflow was developed based on the data collected for 16 different placebo formulations. In order to improve the workflow, data should be collected from a wider range of excipients, encompassing different manufacturing settings (e.g. compression forces) and containing varying ratios of excipients, i.e. different quantities of disintegrants and fillers. In doing so, the workflow would become a more robust tool for use by formulators. Additionally, the application of this workflow to tablets containing API of varying physicochemical properties would also aid in refining the decision points and tolerances.

7.2.2 Advancing Current Accelerated Stability Approaches for Physical Stability

Validate Predictions by the Collection of Long-Term Stability Data. In this thesis, we apply the Acceleration Factor approach described by Scrivens (2019) to predict the dissolution rates of tablets after long-term storage. In order to validate these predictions, long-term data would need to be collected over the course of several years. This data could be used not only to validate these approaches, but also to confirm or improve our current understanding of the underlying mechanisms causing a shift in tablet dissolution.

Assessment of Impact of Alternative Formulation and Manufacturing Conditions. In this study, the application of these approaches was considered for directly

compressed tablets with a selection of 9 different excipients and 1 API. In order to further assess the reliability of these accelerated stability models across a wider range of products, these studies should be performed with a range of different formulations and manufacturing processes (for example, tablets manufactured with a wet or dry granulation step). Additional APIs should also be assessed to determine the effect of varying physicochemical properties of the API. For example, these studies should be repeated with APIs of different hygroscopicity or solubility to distinguish the effects of these properties.

Development of Mechanistic Models for the Assessment of Dissolution Stability. Current approaches for the assessment of dissolution changes during stability focus on empirical models, with no real mechanistic basis. Whilst these approaches can provide accurate predictions and information on the rate of change of dissolution, further development of the literature around the underlying mechanisms of change could allow for better control and design of the dissolution characteristics of a tablet during the formulation and manufacturing development process.

Appendices

Appendix A

Selected Conference Abstracts

Compaction Simulation Forum (2018):

The Effect of Accelerated Temperature and Humidity Conditions on the Physical Stability of Direct Compression Formulations

N. Maclean, I. Khadra, G. Halbert, D. Markl, J. C. Mann and H. Williams

Stability studies are crucial to ensure a drug product will remain safe and effective throughout its assigned shelf life. It is imperative that chemical degradation is monitored to ensure that specification limits are not exceeded by the rate of degradation product formation. Moreover, it is also crucial that the physical stability of the tablet is not compromised, as changes in dissolution rate may alter the release characteristics and bioavailability of the drug.

Recently, industrial interest in predictive techniques has grown. Whilst regulatory acceptance has increased for the use of these techniques to predict chemical stability, their application to physical changes remains deficient. For example, the Accelerated Stability Assessment Program (ASAP) predicts degradation product formation using a moisture-corrected Arrhenius equation. This approach is suitable for chemical degradation where reactions follow Arrhenius behaviour, however this method is not suitable for predicting the dissolution behaviour as a response to the storage conditions, i.e.

temperature and humidity of the storage environment.

The complex interdependencies between characteristic properties of a tablet, such as hardness, porosity and swelling kinetics, renders the prediction of the dissolution performance during and after storage highly difficult. Currently, dissolution changes are generally attributed to excipient-related issues such as disintegrant pre-activation or the formation of a moisture layer on the tablet surface upon exposure to increased humidity. The ability to assign the reason for dissolution changes using predictive techniques would result in a more cost-effective development process with rapid formulation screening and fewer surprise failures during stability testing, ultimately decreasing the time for new drug products to reach patients.

This poster will provide a review of the current understanding of dissolution stability and analytical techniques that could be used to investigate these changes.

AstraZeneca PhD Day (2019): The Effect of Accelerated Storage Conditions on the Physical Properties of Tablets

N. Maclean, I. Khadra, D. Markl, H. Williams and J. Mann

Background: Accelerated predictive stability techniques have become increasingly more common for the prediction of chemical degradation rates during pharmaceutical development, and these approaches have become more widely accepted by regulatory bodies [1]. These techniques can allow for accurate shelf-life determinations in a matter of weeks, as opposed to traditional stability approaches which can take years to complete [2]. Whilst these techniques are becoming well-established for chemical stability, more evidence is required to support the prediction of physical stability properties, such as dissolution performance. Accurate stability predictions rely on a fundamental understanding of the relationship between the physical tablet properties and the disintegration/dissolution performance at accelerated storage conditions. As such, this study aims to characterise the effects of accelerated storage conditions on the physical properties of tablets.

Methods: Tablets containing microcrystalline cellulose, mannitol, croscarmellose sodium and magnesium stearate were manufactured using compression forces of 10, 13 and 16 kN. Prior to the stability study, the weight and dimensions of each tablet were recorded. Tablets were stored at 40°C/75%RH, 50°C/75%RH and 70°C/75%RH for 4 weeks. After 2 and 4 weeks, tablets were tested in order to ascertain the tensile strength, disintegration time and contact angle. In addition to this, tablet weights and dimensions were measured to analyse changes in weight, volume and porosity.

Results: Immediately after removal from storage, tablets had increased in weight, volume and porosity. After a 2 day equilibration period, increases in weight appeared to be largely reversed. Tablet volume decreased slightly after the equilibration period, however it did not return to the initial volume. Consequently, the porosity of the

tablet did not return to the initial value. Tablet tensile strength appeared to decrease significantly after exposure to accelerated conditions, and only a small portion of the original tensile strength was recovered after 2 days at ambient conditions. Changes in disintegration time varied depending on the batch compression force and storage conditions.

Conclusion: This study revealed that the tensile strength, disintegration time and porosity of the tablets changed after exposure to accelerated storage conditions. Whilst some of these changes were reversible (e.g. tablet weight), other properties were altered permanently after storage (e.g. porosity). Further work is required to investigate the validity of the accelerated results in comparison to long-term samples, in addition to the effect of different formulations and the addition of active pharmaceutical ingredients (APIs) with different physicochemical properties. However, accelerated stability techniques have the potential to reduce the time and resources required for drug product development if they can be suitably applied to the physical properties of a drug product.

References: [1] Stephens D. et al. (2018) *Pharmaceutical Technology*, 42, 8, 42 – 47.
[2] Waterman K. C. and Adami R. C. (2005) *Int. J. Pharm.*, 293, 1 – 2, 101 – 125.

**PSSRC 14th Annual Meeting (2020):
Exploring the Stability-Controlling Tablet Disintegration Mechanisms**

N. Maclean, I. Khadra, H. Williams, J. C. Mann and D. Markl

PURPOSE Stability testing is a crucial process in the development of all drug products. The development of predictive stability approaches has reduced the time required to accurately predict chemical degradation,⁽¹⁾ however, these methods are not applicable to physical changes such as tablet disintegration and dissolution. Changes in the formulation and storage conditions influence the disintegration mechanisms such as the rate the tablet takes up liquid and swells. In this study, a systematic approach was adopted to investigate the effect of different excipients on the physical properties of directly compressed tablets, and the stability of these tablets when exposed to a range of temperatures and humidities following an accelerated stability assessment program.⁽¹⁾ The focus of this study was to explore the performance- and stability-controlling disintegration mechanisms as a function of the raw material properties, tablet properties and the tablet's storage history.

METHODS A total of 16 different placebo formulations (4 different fillers and 4 different disintegrants) were manufactured by direct compression, where each formulation was composed of two fillers (47 wt.% each), a disintegrant (5 wt.%) and a lubricant (magnesium stearate, 1 wt.%). Tablets were stored for 2 and 4 weeks (2 timepoints) at 37°C/30%RH, 37°C/75%RH, 50°C/75%RH, 70°C/30%RH and 70°C/75%RH. The weight, dimensions and hardness of tablets were measured at each timepoint. The porosity was calculated using the weight, dimensions and true density. The disintegration time and dynamic contact angle were both measured.

RESULTS There are several processes which can limit the disintegration process – wetting, swelling of particles, and/or the dissolution of soluble components in the tablet. This study demonstrates a workflow which can be used to identify the disintegration

mechanism using raw material and tablet properties. The impact of storage on tablet disintegration varied with the disintegration mechanism. For tablets which are wettability limited, increases in porosity during storage result in a decrease in disintegration time. In contrast, tablets which are swelling-limited do not appear to be affected by storage.

CONCLUSION The performance-limiting disintegration mechanism of each formulation can be identified by considering the raw material and tablet properties. The physical changes which occur during stability are influenced by both the disintegration mechanism and the storage condition.

CHALLENGES The grand challenge of this project is to develop a model that considers the complex interactions of raw material properties, tablet properties and environmental properties (e.g. storage temperature and humidity) and is capable of predicting changes in disintegration time after storing the tablet for a certain period of time.

REFERENCES 1. Waterman, K.C. The Application of the Accelerated Stability Assessment Program (ASAP) to Quality by Design (QbD) for Drug Product Stability, AAPS PharmSciTech, 12, 923-927 (2011).

**PBP 12th World Meeting (2021):
Exploring the Performance and Stability-Controlling Tablet
Disintegration Mechanisms**

N. Maclean, E. Walsh, M. Soundaranathan, I. Khadra, A. Abbott, H. Mead, H. Williams, J. Mann and D. Markl

INTRODUCTION Stability testing is a crucial process in the development of all drug products. Any chemical degradation must be assessed in order to ensure product safety throughout the duration of the shelf-life. Furthermore, changes in performance-controlling characteristics such as tablet disintegration and dissolution must be monitored to prevent a change in product performance. Traditional stability testing is performed over three years. However, the development of predictive stability approaches for chemical degradation has reduced the time required for accurate stability predictions to a matter of weeks (Waterman, 2011), however a gap exists for physical stability. Changes in the formulation and storage conditions particularly influence tablet disintegration mechanisms such as the take up of physiological fluid and the swelling which eventually causes the tablet to break up.

In this study, a systematic approach was adopted to investigate the effect of different excipients on the physical properties of direct compression tablets, and the stability of these tablets when exposed to accelerated temperature and humidity. The focus of this study was to explore performance- and stability-controlling disintegration mechanisms as a function of the raw material properties and the tablet's storage history.

METHODS Microcrystalline cellulose (MCC) (Avicel® PH-102, FMC International), mannitol (Pearlitol® 200 SD, Roquette), lactose (FastFlo® 316, Foremost Farms USA) and dibasic calcium phosphate anhydrous (DCPA) (Anhydrous Emcompress®, JRS Pharma) were used as fillers for the tablet formulations. Disintegrants included croscarmellose sodium (CCS) (FMC International), crospovidone (XPVP) (Kollidon® CL, BASF), low-substituted hydroxypropyl cellulose (L-HPC) (Shin-Etsu Chemical Co.)

and sodium starch glycolate (SSG) (Primojel®), DFE Pharma). Magnesium stearate (Mallinckrodt) was used as a lubricant. All excipients were provided by AstraZeneca (Macclesfield, UK).

Each formulation comprised two fillers (47% w/w each), a disintegrant (5% w/w) and magnesium stearate (1% w/w). Tablets were compressed at 10 kN (MCC/mannitol, MCC/lactose and MCC/DCPA formulations) and 16 kN (DCPA/lactose formulations) to a target weight of 350 mg and tensile strength >2.5 MPa. Tablets were stored in airtight glass jars at 37°C/30%RH, 37°C/75%RH, 50°C/75%RH, 70°C/30%RH and 70°C/75%RH. Samples were tested at three timepoints: 1) after compression and after storage for 2) two and 3) four weeks at the aforementioned conditions.

The weight and dimensions of tablets were recorded at each timepoint (n = 10). Tablet hardness was measured using a Copley TBF 1000 hardness tester (n = 10) (Copley Scientific Ltd, Nottingham, UK). Tablet porosity was calculated using the true density of the excipients in addition to the tablet weight and dimensions. The disintegration time was measured using a Copley DTG 2000 disintegration tester (n = 6) (Copley Scientific Ltd, Nottingham, UK). The dynamic contact angle was measured using a Krüss DSA 30 goniometer (n = 2) (Krüss GmbH, Hamburg, Germany). Video recordings were taken as a droplet of deionized water was dispensed onto the tablet surface. MATLAB (MathWorks, Natick, Massachusetts) was then used to calculate the contact angle between the tablet surface and the droplet of water.

Partial Least Squares (PLS) regression was used to model the stability data for each formulation. First, the change in disintegration time was converted to a percentage change relative to the initial disintegration time. PLS was performed using SIMCA (Umetrics, Sartorius Stedim, Umeå, Sweden), with change in disintegration time as the response variable. Both environmental factors (timepoint, temperature and humidity) and measured values (tensile strength, porosity, moisture content and initial contact angle) were used as predictor variables.

RESULTS AND DISCUSSION Formulations containing MCC/lactose showed the longest disintegration times for each disintegrant (see Figure 2). This is in agreement

with previous studies which showed that higher matrix solubility resulted in slower disintegration (Johnson et al., 1991). For MCC/lactose, the increased disintegration times provide a clear distinction between each disintegrant. This suggests that the disintegration is limited by the liquid-uptake for this filler combination.

For MCC/lactose formulations, the batch containing XPVP had the fastest disintegration time, followed by CCS, SSG and then L-HPC. This supports the order of disintegrant efficiency described by Quodbach et al. (2014) after assessing disintegrant action using MRI analysis.

The use of DCPA results in a very high tablet porosity in the MCC/DCPA and DCPA/lactose batches compared to the tablets from the other batches with similar weight and tensile strength. MCC/lactose and MCC/mannitol batches had a porosity of 13%, whilst batches containing DCPA had porosity of 30%. The high porosity of DCPA-based formulations resulted in a rapid liquid uptake. For these formulations, the choice of filler plays the primary role in determining the disintegration behaviour. Specifically, the disintegration time of the MCC/DCPA formulations is the fastest which is attributed to the fact that MCC also exhibits a swelling action.

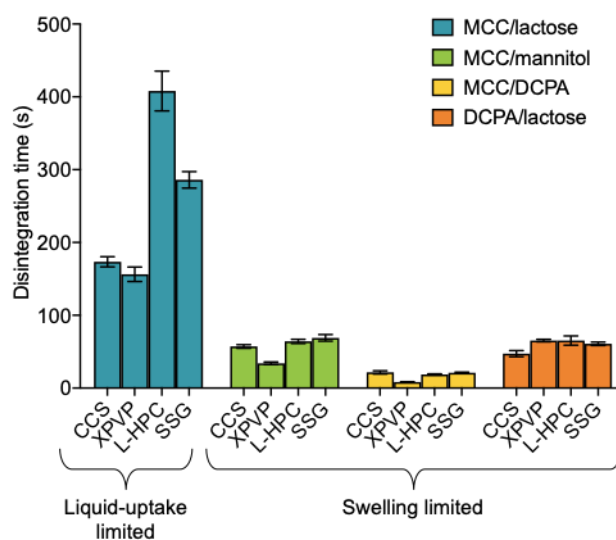


Figure A.1: Disintegration time (s) of each filler and disintegrant combination (showing mean and standard deviation).

The results of PLS regression are shown for MCC/mannitol, MCC/lactose and

MCC/DCPA. The loading values for each batch are given in Figure 3. These results show that an increase in storage temperature causes an increase in initial contact angle ($\theta_{c,0}$) and contributes towards an increase in disintegration time, with the exception of MCC/DCPA with CCS. Similarly, storage at high humidity leads to an increase in porosity and moisture content. Therefore, disintegration time decreases.

Low values for the contact angle indicate that the surface has high wettability and therefore water can spread and penetrate the tablet easily. For this reason, it is clear that initial contact angle would have a strong and positive impact on the disintegration time, which is reflected in these data.

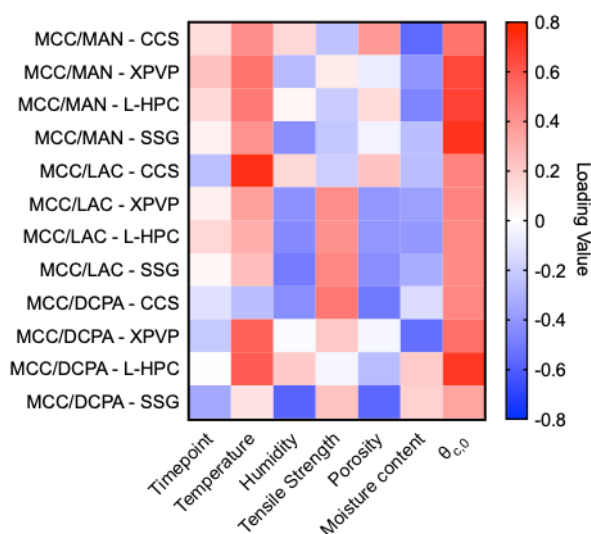


Figure A.2: Loading values from the PLS analysis of MCC/mannitol, MCC/lactose and MCC/DCPA formulations with each disintegrant. $\theta_{c,0}$ is the initial contact angle.

CONCLUSIONS These results provide the basis of a formulation guideline by exploring the differences between physical properties for tablets composed of common filler and disintegrant combinations and considering the physical stability of each formulation. This study has also applied the framework of accelerated stability studies to investigate the complex relationships between different tablet properties and identify the key factors which influence changes in disintegration time. These results show that the performance- and stability-influencing properties vary based on the filler and disin-

tegrants used. Future work aims to incorporate API into these model formulations in order to assess the impact of the physicochemical properties of the drug on the overall tablet stability.

REFERENCES

1. Waterman, K. C. The Application of the Accelerated Stability Assessment Program (ASAP) to Quality by Design (QbD) for Drug Product Stability, *AAPS PharmSciTech*, 12, 932-937 (2011)
2. Johnson, J. R.; Wang, L. H.; Gordon, M. S., Chowhan, Z. T. Effect of Formulation Solubility and Hygroscopicity on Disintegrant Efficiency in Tablet Prepared by Wet Granulation in Terms of Dissolution, *Journal of Pharmaceutical Sciences*, 80, 469-471 (1991)
3. Quodbach, J.; Kleinebudde, P. A New Apparatus for Real-Time Assessment of the Particle Size Distribution of Disintegrating Tablets, *Journal of Pharmaceutical Sciences*, 103, 3657-3665 (2011)

PSSRC 15th Annual Meeting (2021): The Role of Disintegration Mechanism in Physical Tablet Stability

N. Maclean, I. Khadra, A. Abbott, H. Williams, H. Mead, J. Mann and D. Markl

PURPOSE The objective of this work is to identify the links between storage conditions and physical tablet properties such as disintegration time, porosity, hardness and contact angle. Previously, the formulations used in this study were classified based on the performance-controlling mechanism^[1]. By studying the role of disintegration mechanism, we can identify the key properties which are likely to affect the performance of a product after storage under different conditions.

METHODS Placebo tablets were prepared by direct compression for 16 different formulations. Four different filler combinations (microcrystalline cellulose(MCC)/mannitol, MCC/lactose, MCC/dibasic calcium phosphate anhydrous (DCPA) and DCPA/lactose) were used with four different disintegrants (croscarmellose sodium (CCS), crospovidone (XPVP), low-substituted hydroxypropylcellulose (L-HPC) and sodium starch glycolate (SSG)). Tablets were stored for 2 and 4 weeks at 37°C/30%RH, 37°C/75%RH, 50°C/75%RH, 70°C/30%RH and 70°C/75%RH. At each timepoint, the porosity, disintegration time, breaking force and initial contact angle^[2] were measured.

RESULTS The stability results show that generally, for all formulations an increase in humidity resulted in an increase in tablet porosity and a decrease in tensile strength. For tablets composed of MCC/mannitol and MCC/lactose, storage at high temperature generally resulted in an increase in initial contact angle. For MCC/DCPA and DCPA/lactose, changes in disintegration time were very low. For MCC/mannitol and MCC/lactose, the disintegration time changes appear to be influenced by the disintegrant choice, as well as filler-combination.

CONCLUSIONS Generally, storage at accelerated humidity conditions results in increased tablet porosity and decreased tensile strength, likely due to premature swelling of some excipients after exposure to moisture. The effects of temperature vary based on the formulation, however tablets composed of MCC/mannitol and MCC/lactose generally show increases in initial contact angle after storage, indicating decreased wettability. Disintegration time was least affected for tablets composed of MCC/DCPA and DCPA/lactose, where initial disintegration times were already rapid.

CHALLENGES The biggest challenge in this study is identifying the key property changes and inter-relationships which ultimately influence the tablet performance, and finding a method of modelling these changes.

REFERENCES

1. Maclean N, Walsh E, Soundaranathan M, Khadra I, Mann J, Williams H and Markl D. Exploring the performance-controlling tablet disintegration mechanisms for direct compression formulations. *International Journal of Pharmaceutics*. 2021;599:120221. doi:10.1111/jphp.12276.
2. Markl D, Maclean N, Mann J, Williams H, Abbott A, Mead H and Khadra I. Tablet disintegration performance: effect of compression pressure and storage conditions on surface liquid absorption and swelling kinetics. *International Journal of Pharmaceutics*. 2021;120382. doi:10.1016/j.ijpharm.2021.120382.

Appendix B

Study Design and COVID-19 Implications

The study outline shown in Fig B.1 shows the original study design, which comprised four different filler combinations, four different disintegrants, three different levels of compression forces and four APIs. For the placebo characterisation and stability, only one compression force was used to reduce the amount of samples and testing required to ensure enough time remained for the study of API-containing batches.

The COVID-19 pandemic had a direct impact on this work, resulting in delays to practical work due to laboratory closures during lockdowns, access and equipment limitations due to capacity limits upon re-opening of the laboratories, and self-isolation time. To mitigate these delays, the study design of the API-containing batches was reduced from the original aim of testing 4 API with varying physicochemical properties to the selection of just 1 API. Additionally, the number of filler combinations was reduced from 4 to 3, such that there was still one formulation to represent each of the performance-controlling mechanisms identified during the placebo studies.

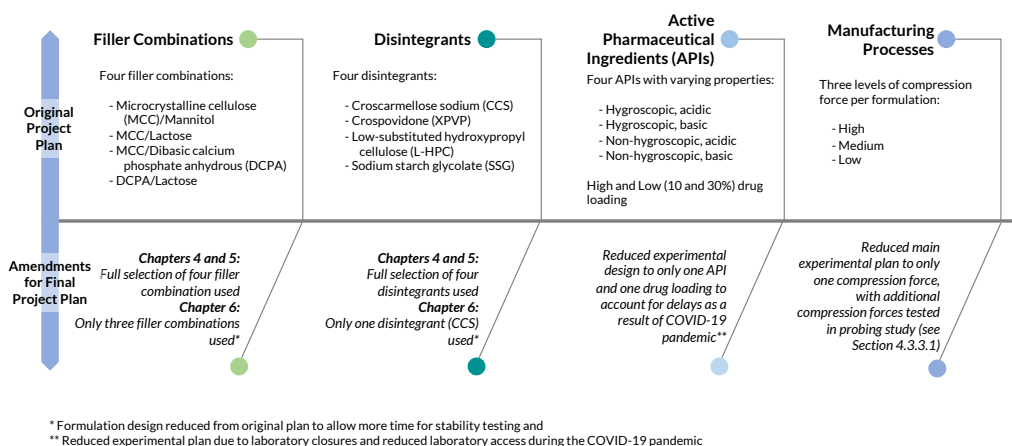


Figure B.1: The original study design (top) and the actual study design (bottom), including the justification for changes to the testing plan.

Appendix C

Material Data Sheets

Summary

This appendix provides the material data sheets and certificates of analysis (where available) for the excipients and griseofulvin used in this study.

8516112961

FOREMOST FARMS USA CERTIFICATE OF ANALYSIS

Sold To:

Attn:

Code Number:

Directive:

Other:

Fax:

Manufacturing Site: 10202 Foremost Dr, PO Box 98
 Rothschild, WI 54474 US ✓

Manufacturing Phone: (715) 359-0534

Date of Manufacture: 29-NOV-2016 ✓

Re-Evaluation Date: 29-NOV-2017

Expiration Date: 29-NOV-2019 ✓

Product: NF Lactose Hydrate Mod Spry Dry Fast Flo ✓ WL10405316 **CAS No.:** 64044-51-5

Lot Number: 8516112961 ✓ **Container Size:** 75kg **Order No.:**

Description: White crystalline powder, spray-dried mixture of crystalline and amorphous lactose (JP Lactose Monograph Description: Granulated Powder) **Date:**

| NF Monograph Analysis | Foremost Laboratory Result | Specification |
|---|----------------------------|-------------------------------|
| Microbial | | |
| Escherichia coli | Absent | Absent |
| Total Aerobic Microbial Count | † | 100 CFU/g maximum |
| Total Combined Mold and Yeast | † | 50 CFU/g maximum |
| Gen App/Organoleptic | | |
| Absorbance @ 400nm | 0.00 | 0.04 @ 400nm maximum |
| Clarity and Color of Solution | Clear & Colorless | Clear & Nearly Colorless |
| Identification Tests | | |
| Identification A | *Meets Specification | * Complies With Specification |
| Identification B | *Meets Specification | * Complies With Specification |
| Physical & Chemical | | |
| Acidity/Alkalinity | 0.0 | 0.4 mL 0.1N NaOH maximum |
| Acidity/Alkalinity Color | Solution = Colorless | Solution is Colorless |
| Heavy Metals | *Meets Specification | * Complies With Specification |
| Loss on Drying | 0.4 | 1.0 % maximum |
| PLAI Absorbance @ 210-220nm | 0.04 | 0.25 @ 210-220 nm maximum |
| PLAI Absorbance @ 270-300nm | 0.02 | 0.07 @ 270-300 nm maximum |
| Residue on Ignition | 0.02 | 0.10 % maximum |
| Specific Rotation | 55.0 | 54.4-55.9 deg_angle |
| Water | 4.8 | 4.5-5.5 % |
| Non NF Analysis | | |
| Appearance of Solution - EP method | Acceptable | Acceptable |
| Density-Bulk g/ml | 0.61 | 0.50 g/mL minimum |
| Density-Tapped g/ml | 0.70 | 0.60 g/mL minimum |
| Enterobacteriaceae-Bile Tolerant Organism | Absent | Absent |
| Pseudomonas | Negative per 10g | Negative per 10g |
| Salmonella per 100g | Negative per 100g | Negative per 100g |
| Staphylococcus aureus | Negative per 10g | Negative per 10g |
| Particle Size-RoTap | | |
| Particle Size % on #60/250um | 0.0 | 2.0 % maximum |
| Particle Size % on #140/106um | 49.1 | 20.0 % minimum |
| Particle Size % on #200/75um | 77.5 | 50.0 % minimum |

*Specified Limit Guaranteed: This Lot Not Tested

The above lot number has been manufactured, processed, held in accordance with United States cGMP's and tested according to procedures as stated in the NF lactose monohydrate monograph and conforms to the same monograph specifications. This lot meets the current USP/NF BP, EP, and JP lactose monohydrate/lactose granulated powder monograph and subsequent supplements at the time of manufacture. This lot number conforms to FDA guidelines regarding BSE/TSE. The USA is the origin of the bovine used in producing this lot number. We have no knowledge of any other impurity in this lot number which is present at a level of 0.1 % or greater. This lot number complies with the ICH Guideline on Residual Solvents (CPMP/ICH/283/95) in that no class 1, 2, 3, or any other solvents are used in our process or likely to be present in the lactose. Storage conditions: Protect from moisture and excessive heat.

Signed by:  12-DEC-2016
 Quality Control Supervisor Date
 Abby Lundgren

Anhydrous Emcompress®

Dibasic Calcium Phosphate Anhydrous, USP, Calcium Hydrogen Phosphate Anhydrous, Ph. Eur.,
 Anhydrous Dibasic Calcium Phosphate, JP

CERTIFICATE OF ANALYSIS

Batch No.: **452711**
 Re-evaluation date: 12/2018
 Manufacturing date: 04/2016

Manufacturing Site: Chicago Heights, IL., USA

| Description | |
|-------------|--|
| Appearance | White or almost white, crystalline powder |
| Solubility | practically insoluble in cold water and in ethanol. It dissolves in dilute hydrochloric acid and in dilute nitric acid |

| Characteristics | Specification | Lot Result | Test Reference |
|---------------------------|--|------------|-------------------|
| Identification I*) | White precipitate is formed | Conforms | USP, Ph. Eur., JP |
| Identification II*) | Yellow precipitate is formed | Conforms | USP, Ph. Eur., JP |
| Loss on ignition | 6.6 – 8.5 % | 8.0 % | USP, Ph. Eur. |
| Carbonate*) | No effervescence occurs | Passes | USP, Ph. Eur., JP |
| Chloride*) | Not more than 0.248 % | < 0.248 % | USP, Ph. Eur., JP |
| Sulfate*) | Not more than 0.48 % | < 0.48 % | USP, Ph. Eur., JP |
| Arsenic*) | Not more than 2 ppm | < 2 ppm | USP, Ph. Eur., JP |
| Barium*) | No turbidity is produced within 10 minutes | Passes | USP, Ph. Eur., JP |
| Heavy metals*) | Not more than 0.003 % | < 0.003 % | USP, Ph. Eur., JP |
| Acid insoluble substances | Not more than 0.2% | < 0.2 % | USP, Ph. Eur., JP |
| Fluoride*) | Not more than 0.005 % | < 0.005 % | USP, Ph. Eur. |
| Assay | 98.0 – 103.0 % | 98.4 % | USP, Ph. Eur., JP |
| Lead*) | Not more than 0.25 ppm | < 0.25 ppm | T273F |
| Iron | Not more than 400 ppm | < 400 ppm | Ph. Eur. |
| Particle Size by Ro-Tab® | 40.0 – 80.0 % retained on #100 mesh sieve (150 µm) | 57.9 % | T271F |
| | Not more than 5 % passes through #325 mesh sieve (45 µm) | 3.2 % | |

Identification I/II tests: Results reported are expected results based on historical data.

*) reduced testing schedule

The raw materials, manufacturing process and product do not contain any of the solvents listed in Residual Solvents (USP <467>, Ph.Eur. <5.4>).

This lot was re-evaluated for loss on ignition in December 2017.

2017-12-08
 Ref: Rettenmaier UK Ltd

Zemcanhp01b_JP

Stefanie Henker
Stefanie Henker
QUALITY ASSURANCE
 Pharmaceutical and Food Excipients

Worldwide headquarters
JRS PHARMA GMBH & CO. KG

73494 Rosenberg (Germany) · Holzmühle 1
 Phone: + 49 (0) 7967 / 152 312
 Fax: + 49 (0) 7967 / 152 345
 info@jrspharma.de · www.jrspharma.de · www.jrs.de
Customer Service: + 49 (0) 7967 / 152 312

USA + Canada
JRS PHARMA LP

2981 Route 22, Suite 1 · Patterson, NY 12563-2359, USA
 Toll-Free (USA): + 1 (800) 431 2457
 Phone: + 1 (845) 878 3414 · Fax: + 1 (845) 878 3484
 info@jrspharma.com · www.jrspharma.com
Customer Service: + 1 (845) 878 3414

FMC International
 Health and Nutrition
 Wallingstown, Little Island
 Co. Cork, Ireland
 Customer Service: + 353-21-435-4133
 Fax: + 353-21-451-7210

FMC

Certificate of Analysis

Avicel® Microcrystalline Cellulose, NF, Ph. Eur, JP

Type : PH-102

Lot No : 71744C

Manufacturing Date: 31-Oct-2017

Reevaluation Date: 30-Oct-2021

Customer Material number: 394703300

Customer Purchase Order : 3500150598

Delivery Number : 80739817

| Standard | Specification | Lot Analysis |
|---|------------------------|--------------|
| Loss on Drying, % | 3.0 - 5.0 | 3.6 |
| Loose Bulk Density, g/cc | 0.28 - 0.33 | 0.30 |
| DP ,units (ID B USP,EP)(ID 3 JP) | NMT 350 | 222 |
| P.S.D.,Malvern LD, μm ,d10 (FRC, Ph.eur) | 15 - 55 | 34 |
| P.S.D.,Malvern LD, μm ,d50 (FRC, Ph.eur) | 80 - 140 | 114 |
| P.S.D.,Malvern LD, μm ,d90 (FRC, Ph.eur) | 170 - 283 | 238 |
| Identification A(USP,EP, JP 1) | PASS | Pass |
| Identification 2 (JP) | PASS | Pass |
| pH | 5.5 - 7.0 | 6.7 |
| Conductivity, $\mu\text{S}/\text{cm}$ | NMT 75 | 36 |
| Residue on Ignition, % | NMT 0.050 | 0.000 |
| Water Soluble Substances, mg/5g | NMT 12.5 | 7.4 |
| Water soluble substances, % | NMT 0.25 | 0.15 |
| Heavy Metals, % | NMT 0.001 | Pass |
| Sol.in Cu Tetramine Hydroxide | Soluble | Pass |
| Ether Soluble Substances,mg/10g | NMT 5.0 | 0.0 |
| Air Jet Particle Size, wt. % + 60Mesh | NMT 8.0 | 1.1 |
| Air Jet Particle Size, wt. % + 200Mesh | NLT 45.0 | 61.7 |
| Total Aerobic Microbial Count, cfu/gram | NMT 100 | Pass |
| Total Yeast and Mold Count, cfu/gram | NMT 20 | Pass |
| Salmonella Species | Absent in a 10g sample | Pass |
| Escherichia coli | Absent in a 10g sample | Pass |
| Staphylococcus aureus | Absent in a 10g sample | Pass |
| Pseudomonas aeruginosa | Absent in a 10g sample | Pass |
| Coliform species | Absent in a 10g sample | Pass |

Storage Conditions: Store at ambient conditions, keep containers sealed, material is hygroscopic.

We certify that as of the date of shipment the product conforms with the current USP / NF, Ph.Eur & JP specifications on the date of manufacture. This product is manufactured in accordance to GMP as detailed in IPEC GMP guide for Bulk Excipients. Our test methods are used when the test is not listed in the Pharmacopeia.

The Product meets the requirement for Residual Solvents USP < 467 > and ICH Guide Q3C.

ISO 9001:2008 Certified Quality System. Refer to package label for Kosher status.

FRC.s (Ph.Eur) Hausner Ratio Typical values: For all Avicel PH grades: 1.18 - 1.45.

Degree of Crystallinity Typical Values: For all Avicel PH grades, approximately 80% by Intensity and 66% by Area.

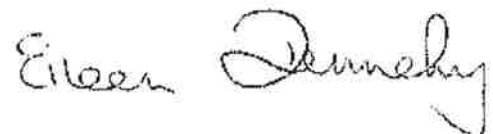
Typical Degree of Polymerization range for Avicel PH Microcrystalline Cellulose is 100 to 300.

Expiry date: None, but we recommend retesting for Loss on Drying after re-evaluation date listed above.

MT-More than, NMT-Not more than, LT-Less than, NLT-Not less than.

Manufactured under GMPs and Issued by:

FMC International
 Health and Nutrition
 Wallingstown, Little Island,
 Co. Cork, Ireland



Eileen Dennehy
 Quality Manager

Certificate of Analysis

Shin-Etsu Chemical Co., Ltd.
 Naoetsu Plant Quality Assurance Department
 28-1, Nishifukushima, Kubiki-ku,
 Joetsu-shi, Niigata



Product Name L-HPC
 (Low-Substituted Hydroxypropyl Cellulose, NF)
 Grade LH-21
 Lot Number 6121512
 Quantity 20kg
 Manufacture Date 2016/12/22
 Recommended Re-Evaluation Date * 2019/12/21
 Analysis Date 2016/12/27
 Issue No. D5120170304584002-1-01

Remark

This product complies with the specifications described in the current NF, EP and JP.

This product is manufactured in accordance with GMP.

* Shin-Etsu Chemical recommends that the customer's quality control unit may re-evaluate the quality of this material on its own responsibility prior to use after the Recommended Re-Evaluation date.

Storage Conditions: Store containers sealed and in a dry place. Keep away from heat or sunlight.

| Test Item | Unit | Test Result | Specification | Method |
|-------------------------------------|------|---------------------|---------------------|--------|
| Description | | Conforms | Conforms | JP/NF |
| Identification (1)/A | | Conforms | Conforms | JP/NF |
| Identification (2)/B | | Conforms | Conforms | JP/NF |
| Identification (3)/C | | Conforms | Conforms | JP/NF |
| pH | | 6.6 | 5.0 - 7.5 | JP |
| Chloride | % | Not more than 0.355 | Not more than 0.355 | JP/NF |
| Heavy metals | ppm | Not more than 10 | Not more than 10 | JP |
| Heavy metals | % | Not more than 0.001 | Not more than 0.001 | NF |
| Arsenic | ppm | Not more than 2 | Not more than 2 | JP |
| Loss on drying | % | 1.7 | Not more than 5.0 | JP/NF |
| Residue on ignition | % | 0.15 | Not more than 0.5 | JP/NF |
| Hydroxypropoxy content | % | 11.3 | 10.0 - 12.9 | JP/NF |
| Particle size: Average (D50) | μm | 49.1 | 35 - 55 | SEC |
| Particle size: 90% cumulation (D90) | μm | 135.1 | 100 - 150 | SEC |

E. Machida

Eiichi Machida
 General Manager, Q. A. Dept.

Shin-Etsu No. : 67027603-01-01

Issue:
 Shin-Etsu Chemical Co., Ltd.
 Cellulose Department
 6-1, Ohtemachi 2-chome, Chiyoda-ku, Tokyo, Japan
 TEL 81-3-3246-5261 FAX 81-3-3246-5372

Judgment:
 Shin-Etsu Chemical Co., Ltd.
 Naoetsu Plant Quality Assurance Department
 28-1, Nishifukushima, Kubiki-ku,
 Joetsu-shi, Niigata, Japan



Product group: Superdisintegrants
Brand name: Primojel®
Product description: Sodium Starch Glycolate

Document No.: PD-0279 Page 1 of 3

Material Safety Data Sheet

This product is not a "dangerous" product according to the applicable EU-rules. The MSDS is provided as a service to our customers and there is no legal obligation to provide it in your national language and in the legally defined format.

This document should be read in conjunction with the Ingredient Declaration and the Product Specification for the relevant product or product category.

1. Identification of the substance/preparation and of the company/undertaking

Product name: Primojel®
Manufacturer/supplier identification: See Footer

2. Composition/information on ingredients

See Ingredient Declaration and the Product Specification
CAS No.: 9063-38-1
EC index No.: N.A.
EINECS No.: N.A.

3. Risk (Health Hazards)

No hazardous product as specified in the current EU legislation.

4. First aid measures

After inhalation: fresh air
After skin contact: wash off with plenty of water.
After eye contact: rinse out with water.
After swallowing (large amounts): get medical attention.

5. Hazards Fire-fighting measures

This product will burn. Suitable extinguishing media: water, powder, spray foam, CO₂
In adaptation to materials stored in the immediate neighborhood.

6. Precautions

Avoid generation of dusts

7. Handling and storage

Store in tightly closed packing protected from solvents. Dry preferable at + 5°C to +25°C.

DMV-Fonterra Excipients GmbH & Co. KG

Klever Strasse 187
47574 Goch, Germany
P.O. Box 20 21 20
47568 Goch, Germany
T +49 2823 9288 770
F +49 2823 9288 7799
Stat. seat: Goch
Amtsgericht Kleve HRA 3232

Bank:
The Royal Bank of Scotland
BLZ 502 304 00
Account 1809898005
BIC: ABNADEFFRA
IBAN DE85502304001809898005
VAT DE 246736318

General partner: DMV-Fonterra
Excipients Verwaltungs-GmbH
Directors: Jan Jongsma
Richard Whiteman
pharma@dfepharma.com
www.dfepharma.com
Stat. seat Goch
Amtsgericht Kleve HRB 8945

All offers for the sale and purchase of
products by DMV-Fonterra Excipients
GmbH & Co KG, and all agreements with
respect thereto, are subject to the general
conditions of DMV-Fonterra Excipients
GmbH & Co KG. A copy of these conditions
will be sent upon request and can be
consulted at www.dfepharma.com

Edition No.: 4 - Issue date: 01 Sep 2015 - Valid until: 01 Sep 2018



Product group: Superdisintegrants
Brand name: Primojel
Product description: Sodium Starch Glycolate

Document No.: PD-0279 Page 2 of 3

8. Exposure controls/personal protection

Respiratory protection required when dusts are generated. Eye protection is required. The use of hand protection is recommended. Wash hands after working with substance.

9. Physical and chemical properties

For chemical and physico-chemical data see the Product Specification.

10. Stability and reactivity

Like any other powdered product, there is a risk of explosion in a confined cloud.

Table with 4 columns: LEL g/m³, Pmax Bar, Kst bar.m/s, MIE mJ. Row 1: 125, 7,2, 56, >8700. Row 2: MIT °C, Smoulder °C, Dust Explosion class. Row 3: 360, 310/320, ST1.

LEL= Lower explosion limit; Pmax= Maximum explosion pressure; Kst=Maximum rate of pressure rise; MIE= Minimum ignition energy; MIT= Determination of the minimum ignition temperature; Smoulder= Smoulder temperature

11. Toxicological information

No toxic effects are to be expected when the product is handled appropriately.

12. Ecological information

No ecological problems are to be expected when the product is handled and used with due care and attention.

13. Disposal considerations

Products and Packaging

There are no uniform EC Regulations for the disposal of chemicals or residues. Chemical residues generally count as special waste. The disposal of the latter is regulated in the EC member countries through corresponding laws and regulations. We recommend that you contact either the authorities in charge or approved waste disposal companies which will advise you on how to dispose of special waste.

14. Transport information

Not subject to transport regulations.

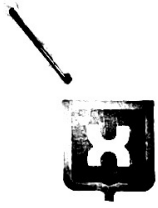
DMV-Fonterra Excipients GmbH & Co. KG

Klevert Strasse 187
47574 Goch, Germany
P.O. Box 20 21 20
47568 Goch, Germany
T. +49 2823 9288 770
F. +49 2823 9288 7799
Stat. seat: Goch
Amtsgericht Kleve HRA 3232

Bank:
The Royal Bank of Scotland
BLZ 502 304 00
Account 1809898005
BIC: ABNADEFFRA
IBAN: DE85502304001809898005
VAT DE 246736318

General partner: DMV-Fonterra
Excipients Verwaltungs-GmbH
Directors: Jan Jongsma
Richard Whiteman
pharma@dfepharma.com
www.dfepharma.com
Stat. seat: Goch
Amtsgericht Kleve HRB 8945

All offers for the sale and purchase of products by DMV-Fonterra Excipients GmbH & Co. KG, and all agreements with respect thereto, are subject to the general conditions of DMV-Fonterra Excipients GmbH & Co. KG. A copy of these conditions will be sent upon request and can be consulted at www.dfepharma.com



DFE pharma

MSDS

Product group: Superdisintegrants
Brand name: Primojel[®]
Product description: Sodium Starch Glycolate

Document No.: PD-0279

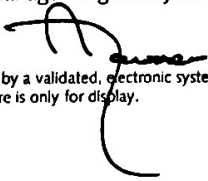
Page 3 of 3

15. Regulatory information

Labeling according to EC directives
Keep away from sources of ignition – No smoking

14. Other information

none

Name : Armand M. Janssen
Job title : Manager Regulatory Affairs
Signature : 

This document is controlled by a validated, electronic system and is valid without signature.
The above facsimile signature is only for display.

The information given in this document is based on our current knowledge and experience, however without any obligation and without any assumption of liability on our part. The information may be used at your discretion and risk. It does not relieve you from carrying out your own precautions and tests. You must comply with all applicable laws, rules and regulations and observe all third party rights.

18 951-0714

DMV-Fonterra Excipients GmbH & Co. KG

Klevert Strasse 187
47574 Goch, Germany
PO Box 20 21 20
47568 Goch, Germany
T +49 2823 9288 770
F +49 2823 9288 7799
Stat. seat: Goch
Amtsgericht Kleve HRA 3232

Bank:
The Royal Bank of Scotland
BLZ 502 304 00
Account 1809898005
BIC: ABNADEFFRA
IBAN DE85502304001809898005
VAT DE 246736318

General partner: DMV-Fonterra
Excipients Verwaltungs-GmbH
Directors: Jan Jongmsma
Richard Whiteman
pharma@dfepharma.com
www.dfepharma.com
Stat. seat: Goch
Amtsgericht Kleve HRB 8945

All offers for the sale and purchase of products by DMV-Fonterra Excipients GmbH & Co. KG, and all agreements with respect thereto, are subject to the general conditions of DMV-Fonterra Excipients GmbH & Co. KG. A copy of these conditions will be sent upon request and can be consulted at www.dfepharma.com

Edition No.: 4 Issue date: 01 Sep 2015 Valid until: 01 Sep 2018

Section 1: Identification of the Substance/Mixture and of the Company Undertaking SDS number: M0230

Product Name: MAGNESIUM STEARATE
Product Codes: Item code: 1277, 1726, 1729, 2254, 2255, 2256, 2257, 2279, 3508, 4024, 5705, 5712, 5716, 5774, 5777, Item code 6504, 7205, 7807
Synonym: STEARIC ACID, MAGNESIUM SALT * Octadecanoic acid, magnesium salt
Manufacturer MSDS Number: SDS number: M0230
Product Uses: Recommended use: Laboratory reagent or process chemical.
Product Restrictions: Recommended restrictions: None known.
Manufacturer Name: Mallinckrodt
Business Phone: Not available.
Customer Service Phone: 888-744-1414
Emergency Phone: 24 Hour Emergency: 314-654-1600
Business Email: Not available.
Distributor: Mallinckrodt
Distributor Address 1: 675 McDonnell Blvd.
 Hazelwood, MO 63042
Chemtrec: CHEMTREC Numbers: For emergencies in the US, call CHEMTREC: 800-424-9300
Revision Date: 03-19-2015
Notes from Section 1: CAS #: 557-04-0

Section 2: Hazards Identification

SDS number: M0230

Precautionary Statements: P264 - Wash hands after handling.
 P501 - Dispose of contents/container in accordance with local/regional/national/international regulations.

Product:

Note: #: This substance has been assigned Community workplace exposure limit(s).

Notes from Section 2:

Physical hazards: Not classified.
 Health hazards: Not classified.
 Environmental hazards: Not classified.
 OSHA defined hazards: Combustible dust
 *Hazards not stated here are "Not classified", "Not applicable" or "Classification not possible".
 Labeling
 Contains: MAGNESIUM STEARATE
 Label elements
 Hazard symbol: None.
 Signal word: Warning
 Hazard statement: May form combustible dust concentrations in air.
 Precautionary statement
 Prevention: Observe good industrial hygiene practices. Dust accumulation from this product may present Prevention an explosion hazard in the presence of an ignition source.
 Response: Wash hands after handling. Response
 Storage: Store away from incompatible materials. Storage
 Disposal: Dispose of contents/container in accordance with local/regional/national/international regul Disposal ations.
 Hazard(s) not otherwise classified (HNOC): None known.
 Supplemental information: None.

MAGNESIUM STEARATE:

Note: Common name and synonyms : STEARIC ACID, MAGNESIUM SALT
 Octadecanoic acid, magnesium salt

Section 3: Composition/Information on Ingredients

SDS number: M0230

Molecular Formula: C18-H36-O2.1/2Mg

Molecular Weight: 591.27 g/mol

| Ingredient Name | CAS Number | Ingredient Percent | EC Number | Comments |
|--------------------|------------|--------------------|-----------|----------|
| MAGNESIUM STEARATE | 557-04-0 | 100% | | |

Product:

Comments: #: This substance has been assigned Community workplace exposure limit(s).

MAGNESIUM STEARATE:

Comments: Common name and synonyms : STEARIC ACID, MAGNESIUM SALT
 Octadecanoic acid, magnesium salt

Section 4: First Aid Measures

SDS number: M0230

Inhalation: If dust from the material is inhaled, remove the affected person immediately to fresh air. Oxygen or artificial respiration if needed. Call a POISON CENTER or doctor/physician if you feel unwell.

Skin Contact: Remove contaminated clothing. Wash off with soap and water. Wash clothing separately before reuse. Get medical attention if irritation develops and persists.

Eye Contact: Rinse cautiously with water for several minutes. Remove contact lenses, if present and easy to do. Continue rinsing. Get medical attention if irritation develops and persists.

Ingestion: IF SWALLOWED: Call a POISON CENTER or doctor/physician if you feel unwell. Never give anything by mouth to a victim who is unconscious or is having convulsions. Do not induce vomiting without advice from poison control center. Rinse mouth thoroughly. If vomiting occurs, keep head low so that stomach content doesn't get into the lungs.

Notes from Section 4: Most important symptoms/effects, acute and delayed: Dusts may irritate the respiratory tract, skin and eyes.
 Indication of immediate medical attention and special treatment needed: Provide general supportive measures and treat symptomatically. In case of shortness of breath, give oxygen.
 General information: Call a POISON CENTER or doctor/physician if you feel unwell. Ensure that medical General information personnel are aware of the material(s) involved, and take precautions to protect themselves.

Section 5: Firefighting Measures

SDS number: M0230

Fire: Flammable properties: This product is not flammable. Dust may form explosive mixture with air.
 General fire hazards: May form combustible dust concentrations in air.

Flash Point: Not available.

Auto Ignition Temperature: Not available.

Upper Flammable Limit: Not available.
 Explosive limit (%): Not available.

Lower Flammable Limit: Not available.
 Explosive limit (%): Not available.

Extinguishing Media: Water spray. Alcohol foam. Dry chemical powder. Carbon dioxide (CO₂). Ad Suitable extinguishing media dition of water or foam to the fire may cause frothing.

Unsuitable Media: Not available.

Fire Fighting Instructions: Firefighters must use standard protective equipment including flame retardant coat, helmet with face shield, gloves, rubber boots, and in enclosed spaces, SCBA. In the event of fire, cool tanks with water spray. Move containers from fire area if you can do so without risk. As in any fire, wear self-contained breathing apparatus pressure-demand, MSHA/NIOSH (approved or equivalent) and full protective gear.

Protective Equipment: Firefighters must use standard protective equipment including flame retardant coat, helmet with face shield, gloves, rubber boots, and in enclosed spaces, SCBA.

Fire Fighting Equipment: In the event of fire, cool tanks with water spray. Move containers from fire area if you can do so without risk. As in any fire, wear self-contained breathing apparatus pressure-demand, MSHA/NIOSH (approved or equivalent) and full protective gear.

Notes from Section 5: Specific hazards arising from the chemical: Melted fatty acid can give "grease" type fire. Explosion hazard: Avoid generating dust; fine dust dispersed in air in sufficient concentrations and in the presence of an ignition source is a potential dust explosion hazard.
 Specific methods: In the event of fire and/or explosion do not breathe fumes. Cool containers exposed Specific methods to flames with water until well after the fire is out.

Section 6: Accidental Release Measures

SDS number: M0230

Personnel Precautions: Personal precautions, protective equipment and emergency procedures: Ensure adequate ventilation. Keep unnecessary personnel away. Do not touch damaged containers or spilled material unless wearing appropriate protective clothing. Wear appropriate protective equipment and clothing during clean-up. Avoid inhalation of dust from the spilled material. Wear a dust mask if dust is generated above exposure limits. Ventilate closed spaces before entering them.

Environmental Precautions: No special environmental precautions required.

Methods for Containment:

Stop the flow of material, if this is without risk. ELIMINATE all ignition sources (no smoking, flares, sparks or flames in immediate area). Collect spillage. If sweeping of a contaminated area is necessary use a dust suppressant agent which does not react with the product. Sweep up or vacuum up spillage and collect in suitable container for disposal. Avoid dust formation. Collect dust using a vacuum cleaner equipped with HEPA filter. Use only non-sparking tools. Following product recovery, flush area with water. For waste disposal, see section 13 of the SDS.

Methods for Cleanup:

Stop the flow of material, if this is without risk. ELIMINATE all ignition sources (no smoking, flares, sparks or flames in immediate area). Collect spillage. If sweeping of a contaminated area is necessary use a dust suppressant agent which does not react with the product. Sweep up or vacuum up spillage and collect in suitable container for disposal. Avoid dust formation. Collect dust using a vacuum cleaner equipped with HEPA filter. Use only non-sparking tools. Following product recovery, flush area with water. For waste disposal, see section 13 of the SDS.

Section 7: Handling and Storage

SDS number: M0230

Handling:

Precautions for safe handling: Do not use in areas without adequate ventilation. DO NOT handle, store Precautions for safe handling or open near an open flame, sources of heat or sources of ignition. Protect material from direct sunlight. Avoid breathing dust. Keep formation of airborne dusts to a minimum. Provide appropriate exhaust ventilation at places where dust is formed. Take precautionary measures against static discharges. All equipment used when handling the product must be grounded. Ground and bond containers when transferring material. Use personal protective equipment as required. Avoid contact with skin and eyes. Do not ingest. Use non-sparking tools and explosion-proof equipment. Wash thoroughly after handling. When using, do not eat, drink or smoke. Handle and open container with care.

Storage:

Conditions for safe storage, including any incompatibilities: Keep container tightly closed. Store in a well-ventilated place. Keep at temperature not exceeding 40°C. Guard against dust accumulation of this material. Keep away from heat and sources of ignition. This material can accumulate static charge which may cause spark and become an ignition source. Prevent electrostatic charge build-up by using common bonding and grounding techniques. Use care in handling/storage. Store in accordance with local/regional/national/international regulation.

Hygiene Practices:

General hygiene considerations: When using, do not eat, drink or smoke. Avoid breathing dust. Avoid contact with eyes. Avoid contact with skin. Wash hands after handling and before eating. Handle in accordance with good industrial hygiene and safety practice.

Section 8: Exposure Controls/Personal Protection

SDS number: M0230

Engineering Controls:

Appropriate engineering controls: Explosion-proof general and local exhaust ventilation. Good general ventilation (typically 10 air changes per hour) should be used. Ventilation rates should be matched to conditions. If applicable, use process enclosures, local exhaust ventilation, or other engineering controls to maintain airborne levels below recommended exposure limits. If exposure limits have not been established, maintain airborne levels to an acceptable level. Ventilation should be sufficient to effectively remove and prevent buildup of any dusts or fumes that may be generated during handling or thermal processing. If engineering measures are not sufficient to maintain concentrations of dust particulates below the Occupational Exposure Limit (OEL), suitable respiratory protection must be worn. If material is ground, cut, or used in any operation which may generate dusts, use appropriate local exhaust ventilation to keep exposures below the recommended exposure limits. Ensure adequate ventilation, especially in confined areas.

Eye Protection:

Use tight fitting goggles if dust is generated. Provide eyewash station and safety shower.

| | |
|-------------------------|---|
| Face Protection: | Use tight fitting goggles if dust is generated. Provide eyewash station and safety shower. |
| Other Protective: | Wear suitable protective clothing. |
| Respiratory Protection: | Wear respirator with dust filter. If airborne concentrations are above the applicable Respiratory protection licable exposure limits, use NIOSH approved respiratory protection. |
| Hand Protection: | Wear protective gloves. |
| Hygiene Practices: | General hygiene considerations: When using, do not eat, drink or smoke. Avoid breathing dust. Avoid contact with eyes. Avoid contact with skin. Wash hands after handling and before eating. Handle in accordance with good industrial hygiene and safety practice. |
| Exposure limit: | Biological limit values: No biological exposure limits noted for the ingredient(s). |
| Notes from Section 8: | Thermal hazards: Wear appropriate thermal protective clothing, when necessary. |

Exposure Guidelines - Ingredient Based:**MAGNESIUM STEARATE:**

| | |
|----------------------|--|
| Exposure Guidelines: | U.S. - OSHA Type: PEL Value: 5 mg/m ³ Form: Respirable fraction for nuisance dusts |
| | ACGIH Type: TWA Value: 10 mg/m ³ |
| | US. ACGIH Threshold Limit Values Type: TWA Value: 10 mg/m ³ |

Section 9: Physical and Chemical Properties

SDS number: M0230

| | |
|---------------------------|---|
| Physical State: | Solid. Appearance: Powder Form: Powder. |
| Color: | White or Yellow. |
| Odor: | Slight. |
| Odor Threshold: | Not available. |
| pH: | Not available. |
| Melting Temperature: | 302 - 338 °F (150 - 170 °C) |
| Boiling Temperature: | Not available. |
| Flash Point: | Not available. |
| Evaporation Rate: | Not applicable. |
| Flammability (Solid/Gas): | Not available. |
| Upper Flammable Limit: | Not available. Explosive limit (%): Not available. |
| Lower Flammable Limit: | Not available. Explosive limit (%): Not available. |
| Vapor Pressure: | Not available. |
| Vapor Density: | Not available. |
| Density: | Relative density: 1.028 g/cm ³ |

| | |
|-------------------------------|---|
| Solubility In Water: | Insoluble in water. |
| Octanol Water Partition Coef: | Not available. |
| Auto Ignition Temperature: | Not available. |
| Decomposition Temperature: | Not available. |
| Viscosity: | Not available. |
| Freezing Temperature: | 302 - 338 °F (150 - 170 °C) |
| Specific Gravity: | 1.03 |
| Molecular Formula: | C18-H36-O2.1/2Mg |
| Molecular Weight: | 591.27 g/mol |
| Note from Section 9: | Dust Electrostatic Properties Minimum Ignition Energy (Cloud): 3 - 10 mJ Dust Explosion Properties dP/dT: 955 bar/s Kst: 259 bar.m/s Limiting Oxygen Concentration: 12 - 13 % Minimum Explosible Concentration: 20 - 30 g/m3 Minimum Ignition Temperature-Cloud: 824 - 860 °F (440 - 460 °C) Minimum Ignition Temperature-Layer: 716 - 734 °F (380 - 390 °C) Moisture: 1 % Particle Size: 8 µm Pmax: 7.6 bar |

Section 10: Stability and Reactivity

SDS number: M0230

| | |
|-----------------------------------|---|
| Reactivity: | The product is stable and non-reactive under normal conditions of use, storage and transport. Possibility of hazardous reactions: Hazardous polymerization does not occur. |
| Chemical Stability: | Material is stable under normal conditions. |
| Conditions To Avoid: | Avoid dust formation. Avoid dispersal of dust in the air (i.e., clearing dust sur Conditions to avoid faces with compressed air). Heat, flames and sparks. Contact with incompatible materials. |
| Incompatible Materials: | Strong oxidizing agents. Acids. |
| Hazardous Decomposition Products: | Carbon monoxide. May include oxides of magnesium. |

Section 11: Toxicological Information

SDS number: M0230

| | |
|----------------------------|--|
| Product: | |
| Acute Toxicity: | Not applicable. |
| Sensitization: | Respiratory sensitization: Due to lack of data the classification is not possible. Skin sensitization: Not a skin sensitizer. |
| Mutagenicity: | No data available to indicate product or any components present at greater than 0.1% are mutagenic or genotoxic. |
| Reproductive Toxicity: | This product is not expected to cause reproductive or developmental effects. |
| STOT SE: | Due to lack of data the classification is not possible. |
| STOT RE: | Due to lack of data the classification is not possible. |
| MAGNESIUM STEARATE: | |
| ACGIH Carcinogen: | A4 Not classifiable as a human carcinogen. |

| | |
|---------------------------|--|
| Aspiration Hazard: | Due to lack of data the classification is not possible |
| Product: | |
| Route of Exposure: | Information on likely routes of exposure Ingestion: No significant adverse effects are expected upon ingestion of the product. Inhalation: Inhalation of dusts may cause respiratory irritation. Coughing. Difficulty in breathing. Skin contact Health injuries are not known or expected under normal use. Eye contact Dust or powder may irritate eye tissue. |
| Chronic Toxicity: | Chronic effects: Inhalation of powder/dust may cause lung edema. |
| Carcinogenicity: | This product is not considered to be a carcinogen by IARC, ACGIH, NTP, or OSHA. |
| Irritation: | Skin corrosion/irritation: Due to lack of data the classification is not possible. Skin corrosion/irritation Serious eye damage/eye irritation: Due to lack of data the classification is not possible. |
| Sign and Symptoms: | Symptoms related to the physical, chemical and toxicological characteristics: Dusts may irritate the respiratory tract, skin and eyes. |

Section 12: Ecological Information

SDS number: M0230

| | |
|---|--|
| Product: | |
| Ecotoxicity: | This product has no known eco-toxicological effects |
| Biodegradation: | No data is available on the degradability of this product. |
| BioAccumulation: | Not established. |
| Mobility In Environmental Media: | Mobility in soil : Not available. |
| Notes from Section 12: | Other adverse effects: An environmental hazard cannot be excluded in the event of unprofessional handling or disposal. |

Section 13: Disposal Considerations

SDS number: M0230

| | |
|--------------------------------|--|
| Waste Disposal: | Disposal instructions: Dispose in accordance with all applicable regulations. Waste from residues / unused products: Not available. |
| Waste Code: | Hazardous waste code: Not regulated. |
| Contaminated Packaging: | Empty containers should be taken to an approved waste handling site for recycling or disposal. |

Section 14: Transport Information

SDS number: M0230

| | |
|------------------------|---|
| Transportation: | Transport in bulk according to Annex II of MARPOL 73/78 and the IBC Code: This substance/mixture is not intended to be transported in bulk. |
| DOT: | Not regulated as dangerous goods. |
| IMDG: | Not regulated as dangerous goods. |
| IATA: | Not regulated as dangerous goods. |

Section 15: Regulatory Information

SDS number: M0230

Regulatory - Product Based:

US federal regulations:

This product is a "Hazardous Chemical" as defined by the OSHA Hazard Communication Standard, 29 CFR 1910.1200.
All components are on the U.S. EPA TSCA Inventory List.
TSCA Section 12(b) Export Notification (40 CFR 707, Subpt. D): Not regulated.
CERCLA Hazardous Substance List (40 CFR 302.4): Not listed.
SARA 304 Emergency release notification: Not regulated.
OSHA Specifically Regulated Substances (29 CFR 1910.1001-1050): Not listed.
CERCLA (Superfund) reportable quantity: None

Superfund Amendments and Reauthorization Act of 1986 (SARA):

Hazard categories: Immediate Hazard - No
Delayed Hazard - No
Fire Hazard - Yes
Pressure Hazard - No
Reactivity Hazard - No
SARA 302 Extremely hazardous substance: Not listed.
SARA 311/312 Hazardous chemical: Yes

Other federal regulations:

Clean Air Act (CAA) Section 112 Hazardous Air Pollutants (HAPs) List: Not regulated.
Clean Air Act (CAA) Section 112(r) Accidental Release Prevention (40 CFR 68.130): Not regulated.
Safe Drinking Water Act (SDWA): Not regulated.
Food and Drug Administration (FDA): Total food additive
Direct food additive
GRAS food additive

US state regulations:

California Safe Drinking Water and Toxic Enforcement Act of 1986 (Proposition 65): This material is not known to contain any chemicals currently listed as carcinogens or reproductive toxins.
US. Massachusetts RTK - Substance List: Not regulated.
US. New Jersey Worker and Community Right-to-Know Act: Not listed.
US. Pennsylvania Worker and Community Right-to-Know Law: Not listed.
US. Rhode Island RTK: Not regulated.
US. California Proposition 65: Not Listed.

International Inventories:

Country(s) or region: Australia
 Inventory name: Australian Inventory of Chemical Substances (AICS)
 On inventory (yes/no)*: Yes

Country(s) or region: Canada
 Inventory name: Domestic Substances List (DSL)
 On inventory (yes/no)*: Yes

Country(s) or region: Canada
 Inventory name: Non-Domestic Substances List (NDSL)
 On inventory (yes/no)*: No

Country(s) or region: China
 Inventory name: Inventory of Existing Chemical Substances in China (IECSC)
 On inventory (yes/no)*: Yes

Country(s) or region: Europe
 Inventory name: European Inventory of Existing Commercial Chemical Substances (EINECS)
 On inventory (yes/no)*: Yes

Country(s) or region: Europe
 Inventory name: European List of Notified Chemical Substances (ELINCS)
 On inventory (yes/no)*: No

Country(s) or region: Japan
 Inventory name: Inventory of Existing and New Chemical Substances (ENCS)
 On inventory (yes/no)*: Yes

Country(s) or region: Korea
 Inventory name: Existing Chemicals List (ECL)
 On inventory (yes/no)*: Yes

Country(s) or region: New Zealand
 Inventory name: New Zealand Inventory
 On inventory (yes/no)*: Yes

Country(s) or region: Philippines
 Inventory name: Philippine Inventory of Chemicals and Chemical Substances (PICCS)
 On inventory (yes/no)*: Yes

Country(s) or region: United States & Puerto Rico
 Inventory name: Toxic Substances Control Act (TSCA) Inventory
 On inventory (yes/no)*: Yes

*A "Yes" indicates that all components of this product comply with the inventory requirements administered by the governing country(s)

A "No" indicates that one or more components of the product are not listed or exempt from listing on the inventory administered by the governing country(s).

Section 16: Additional Information

SDS number: M0230

Revision Date: 03-19-2015

Revision Notes: Revision Information: Product and Company Identification: Synonyms
 Exposure Controls / Personal Protection: OELs
 Physical & Chemical Properties: Multiple Properties
 Regulatory Information: United States
 GHS: Classification

Version Number: 01

Disclaimer: Mallinckrodt provides the information contained herein in good faith but makes no representation as to its comprehensiveness or accuracy. This document is intended only as a guide to the appropriate precautionary handling of the material by a properly trained person using this product. Individuals receiving the information must exercise their independent judgment in determining its appropriateness for a particular purpose. MALLINCKRODT MAKES NO REPRESENTATIONS OR WARRANTIES, EITHER EXPRESS OR IMPLIED, INCLUDING WITHOUT LIMITATION ANY WARRANTIES OF MERCHANTABILITY, FITNESS FOR A PARTICULAR PURPOSE WITH RESPECT TO THE INFORMATION SET FORTH HEREIN OR THE PRODUCT TO WHICH THE INFORMATION REFERS. ACCORDINGLY, MALLINCKRODT WILL NOT BE RESPONSIBLE FOR DAMAGES RESULTING FROM USE OF OR RELIANCE UPON THIS INFORMATION.

Notes from Section 16: Further information: New US GHS SDS.
Refer to NFPA 654, Standard for the Prevention of Fire and Dust Explosions from the Manufacturing, Processing, and Handling of Combustible Particulate Solids, for safe handling.

Copyright © 1996-2018 Enviance Inc. All Rights Reserved.

Section 1: Identification of the Substance/Mixture and of the Company Undertaking

1.1 Product identifier

Product Name: Kollidon CL
 Synonym: Chemical name: 2-Pyrrolidinone, 1-ethenyl-, homopolymer
 Manufacturer MSDS Number: (ID no. 30034964/SDS_GEN_00/EN)

1.2. Relevant identified uses of the substance or mixture and uses advised against

Product Uses: Relevant identified uses of the substance or mixture and uses advised against
 Relevant identified uses: pharmaceutical excipient

1.3 Supplier's details

Manufacturer Name: BASF SE
 Business Email: EN-global-safety-data@basf.com
 Distributor: BASF SE
 Distributor Address 1: 67056 Ludwigshafen
 GERMANY
 Operating Division Nutrition and Health
 Distributor Phone: +49 621 60-48434

1.4 Emergency phone number

Emergency Phone: International emergency number: +49 180 2273-112
 Revision Date: 16.12.2015
 Notes from Section 1: BASF Safety data sheet according to UN GHS 4th rev.
 CAS Number: 9003-39-8

Section 2: Hazards Identification

(ID no. 30034964/SDS_GEN_00/EN)

2.1 Classification of the substance or mixture

2.1.1. Classification according to Regulation (EC) No 1272/2008 [CLP]

2.2 Label elements:

Labelling according to Regulation (EC) No 1272/2008 [CLP]

2.3 Other hazards

Emergency Overview: Classification of the substance or mixture
 According to UN GHS criteria
 No need for classification according to GHS criteria for this product.

Label elements

Globally Harmonized System (GHS)

The product does not require a hazard warning label in accordance with GHS criteria.

Other hazards

According to UN GHS criteria

The product is under certain conditions capable of dust explosion.

Section 3: Composition/Information on Ingredients

(ID no. 30034964/SDS_GEN_00/EN)

3.2 Mixtures:

| | | | | |
|--|--|--|--|--|
| | | | | |
|--|--|--|--|--|

| Ingredient Name | CAS Number | Ingredient Percent | EC Number | Comments |
|--|------------|--------------------|-----------|----------|
| 2-Pyrrolidinone, 1-ethenyl-, homopolymer | 9003-39-8 | NA | | |

Product:

Notes: Substances

Chemical nature : 2-Pyrrolidinone, 1-ethenyl-, homopolymer
CAS Number: 9003-39-8
crosslinked, Microgranule (MG)

Mixtures : Not applicable

Section 4: First Aid Measures

(ID no. 30034964/SDS_GEN_00/EN)

4.1 Description of first aid measures

Eye Contact: On contact with eyes: Wash affected eyes for at least 15 minutes under running water with eyelids held open.

Skin Contact: On skin contact: Wash thoroughly with soap and water.

Inhalation: If inhaled: Keep patient calm, remove to fresh air.

Ingestion: On ingestion: Rinse mouth and then drink plenty of water.

4.2 Most important symptoms and effects, both acute and delayed**4.3 Indication of immediate medical attention and special treatment needed**

Notes from Section 4: Description of first aid measures : Remove contaminated clothing.

Most important symptoms and effects, both acute and delayed
Symptoms: No significant symptoms are expected due to the non-classification of the product.

Indication of any immediate medical attention and special treatment needed
Treatment: Symptomatic treatment (decontamination, vital functions).

Section 5: Firefighting Measures

(ID no. 30034964/SDS_GEN_00/EN)

5.1 Extinguishing media

Extinguishing Media: Suitable extinguishing media : water spray, foam, dry powder

Unsuitable Media: Unsuitable extinguishing media for safety reasons: carbon dioxide

5.2 Special hazards arising from the substance or mixture**5.3 Advice for firefighters**

Fire Fighting Instructions: Advice for fire-fighters
Special protective equipment:
Wear a self-contained breathing apparatus.

Notes from Section 5: Special hazards arising from the substance or mixture
Carbon dioxide, cyanides, nitrogen oxides
The substances/groups of substances mentioned can be released in case of fire.

Further information:
Dispose of fire debris and contaminated extinguishing water in accordance with official regulations.

Section 6: Accidental Release Measures

(ID no. 30034964/SDS_GEN_00/EN)

6.1 Personal precautions, protective equipment and emergency procedures

Personnel Precautions: Personal precautions, protective equipment and emergency procedures : Avoid dust formation. Information regarding personal protective measures see, section 8.

6.2 Environmental precautions

Environmental Precautions: Do not discharge into drains/surface waters/groundwater.

6.3 Methods and materials for containment and cleaning up

Methods for containment: For small amounts: Sweep/shovel up.
For large amounts: Sweep/shovel up.
Dispose of absorbed material in accordance with regulations. Avoid raising dust.

Methods for cleanup: For small amounts: Sweep/shovel up.
For large amounts: Sweep/shovel up.
Dispose of absorbed material in accordance with regulations. Avoid raising dust.

6.4 Reference to other sections

Notes from Section 6: Reference to other sections : Information regarding exposure controls/personal protection and disposal considerations can be found in section 8 and 13.

Section 7: Handling and Storage

(ID no. 30034964/SDS_GEN_00/EN)

7.1 Precautions for safe handling

Handling: Precautions for safe handling
Handle in accordance with good industrial hygiene and safety practice. Avoid dust formation.

Protection against fire and explosion:
Avoid dust formation. The product is capable of dust explosion. Take precautionary measures against static discharges.

Dust explosion class: Dust explosion class 2 (Kst-value 200 up to 300 bar m s-1).

Hygiene Practices: General safety and hygiene measures : Handle in accordance with good industrial hygiene and safety practice. Handle in accordance with good industrial hygiene and safety practice.

7.2 Conditions for safe storage, including any incompatibilities

Storage: Conditions for safe storage, including any incompatibilities
Further information on storage conditions: Keep container tightly closed and dry. Keep at temperature not exceeding 25 °C.

7.3 Specific end use(s)

Notes from Section 7: Specific end use(s) : For the relevant identified use(s) listed in Section 1 the advice mentioned in this section 7 is to be observed.

Section 8: Exposure Controls/Personal Protection

(ID no. 30034964/SDS_GEN_00/EN)

8.1 Control parameters

Exposure limit: Components with occupational exposure limits
9003-39-8: 2-Pyrrolidinone, 1-ethenyl-, homopolymer

8.2 Exposure controls

Eye Protection: Safety glasses with side-shields (frame goggles) (e.g. EN 166)

Skin Protection: Body protection: Body protection must be chosen based on level of activity and exposure.

| | |
|-------------------------|--|
| Hand Protection: | Suitable chemical resistant safety gloves (EN 374) also with prolonged, direct contact (Recommended: Protective index 6, corresponding > 480 minutes of permeation time according to EN 374): E.g. nitrile rubber (0.4 mm), chloroprene rubber (0.5 mm), butyl rubber (0.7 mm) etc. Supplementary note: The specifications are based on tests, literature data and information of glove manufacturers or are derived from similar substances by analogy. Due to many conditions (e.g. temperature) it must be considered, that the practical usage of a chemical-protective glove in practice may be much shorter than the permeation time determined through testing. |
| Respiratory Protection: | Breathing protection if breathable aerosols/dust are formed. Particle filter with low efficiency for solid particles (e.g. EN 143 or 149, Type P1or FFP1) |
| Hygiene Practices: | General safety and hygiene measures : Handle in accordance with good industrial hygiene and safety practice. Handle in accordance with good industrial hygiene and safety practice. |

Section 9: PHYSICAL AND CHEMICAL PROPERTIES

(ID no. 30034964/SDS_GEN_00/EN)

9.1 Information on basic physical and chemical properties

PHYSICAL AND CHEMICAL PROPERTIES

| | |
|-------------------------------|--|
| Physical State: | Form: powder |
| Color: | white to cream |
| Odor: | faint specific odour |
| pH: | approx. 5 - 7 (1 %(m), 20 °C) (as aqueous suspension) |
| Melting Temperature: | >= 130 °C The substance / product decomposes. |
| Boiling Temperature: | not applicable |
| Flash Point: | not applicable, the product is a solid |
| Ignition Temperature: | approx. 440 °C (DIN 51794) |
| Lower Flammable Limit: | 30 g/m ³ (8,0 bar) (VDI 2263, air) |
| Upper Flammable Limit: | For solids not relevant for classification and labelling. |
| Decomposition Temperature: | Thermal decomposition: > 145 °C |
| Vapor Pressure: | dropped |
| Vapor Density: | Relative vapour density (air): not relevant |
| Density: | No data available. Relative density: Study does not need to be conducted. |
| Solubility: | insoluble |
| Solubility in Water: | (qualitative) solvent(s): organic solvents soluble |
| Evaporation Rate: | negligible |
| Odor Threshold: | not determined |
| Octanol Water Partition Coef: | (log Kow) : No data available., not determined |
| Dynamic Viscosity: | not applicable, the product is a solid |

9.2 Other information

Note from Section 9:

Flammability: not readily ignited

Flammability of Aerosol Products: not applicable, the product does not form flammable aerosoles

Self ignition:

Temperature: 195 °C No self ignition was observed up to the specified temperature.

Test type: Self-ignition at high temperatures.
(Method: VDI 2263, sheet 1, 1.4.1)

Explosion hazard: not explosive

Fire promoting properties: not fire-propagating

Other information

Minimum ignition energy: 10 - 30 mJ (1.013 hPa, 20 °C) Inductivity: 1 mH The product is capable of dust explosion.

(VDI 2263, sheet 1, 2.1.1)

Bulk density: approx. 330 kg/m³

Section 10: STABILITY AND REACTIVITY

(ID no. 30034964/SDS_GEN_00/EN)

10.1 Reactivity**Reactivity:**

Corrosion to metals: Corrosive effects to metal are not anticipated.

Formation of flammable gases: Remarks: Forms no flammable gases in the presence of water.

Possibility of hazardous reactions : No hazardous reactions when stored and handled according to instructions. Dust explosion hazard.

10.2 Chemical stability**Chemical Stability:**

The product is stable if stored and handled as prescribed/indicated.

10.3 Possibility of hazardous reactions**10.4 Conditions to avoid****Conditions To Avoid:**

Avoid dust formation. Avoid electro-static charge. Avoid all sources of ignition: heat, sparks, open flame.

10.5 Incompatible materials**Incompatible Materials:**

Substances to avoid : strong alkalies

10.6 Hazardous decomposition products:

No hazardous decomposition products if stored and handled as prescribed/indicated.

Section 11: TOXICOLOGICAL INFORMATION

(ID no. 30034964/SDS_GEN_00/EN)

11.1 Information on toxicological effects**Product:****Acute Toxicity:**

Assessment of acute toxicity:

Virtually nontoxic after a single ingestion. Virtually nontoxic by inhalation.

Experimental/calculated data:

LD50 rat (oral): > 2.000 mg/kg (BASF-Test)

LC50 rat (by inhalation): > 5,2 mg/l 4 h (OECD Guideline 403)

| | |
|-------------------------------|---|
| Chronic Toxicity: | Repeated dose toxicity and Specific target organ toxicity (repeated exposure) Assessment of repeated dose toxicity: No data available. |
| Target Organ Data: | Repeated dose toxicity and Specific target organ toxicity (repeated exposure) Assessment of repeated dose toxicity: No data available. |
| Carcinogenicity: | Assessment of carcinogenicity: In long-term animal studies in which the substance was given in high doses by feed, a carcinogenic effect was not observed. |
| Mutagenicity: | Germ cell mutagenicity Assessment of mutagenicity: The substance was not mutagenic in studies with mammals. |
| Irritation: | Assessment of irritating effects: Not irritating to the skin. Not irritating to the eyes. Experimental/calculated data: Skin corrosion/irritation rabbit: non-irritant (Draize test) Serious eye damage/irritation rabbit: non-irritant (Draize test) |
| Sensitization: | Respiratory/Skin sensitization Assessment of sensitization: No data available. |
| Other Toxicity: | Developmental toxicity Assessment of teratogenicity: No indications of a developmental toxic / teratogenic effect were seen in animal studies. |
| Notes from Section 11: | Aspiration hazard : No data available. |

Section 12: Ecological Information

(ID no. 30034964/SDS_GEN_00/EN)

12.1 Toxicity

Product:

Effect of Material On Aquatic: Assessment of aquatic toxicity:
There is a high probability that the product is not acutely harmful to aquatic organisms. The inhibition of the degradation activity of activated sludge is not anticipated when introduced to biological treatment plants in appropriate low concentrations.

Toxicity to fish:
LC50 (96 h) > 10.000 mg/l, *Leuciscus idus* (DIN 38412 Part 15, static)

Microorganisms/Effect on activated sludge:
EC20 (0,5 h) > 1.995 mg/l, activated sludge, industrial (OECD Guideline 209, aerobic)

12.2 Persistence and degradability

Product:

Biodegradation: Persistence and degradability
Assessment biodegradation and elimination (H2O): Poorly eliminated from water.
Elimination information:
< 10 % DOC reduction (15 d) (OECD Guideline 302 B) (aerobic, activated sludge, industrial) Poorly eliminated from water.

12.3 Bioaccumulative potential

Product:

BioAccumulation: Bioaccumulation potential:
Based on its structural properties, the polymer is not biologically available.
Accumulation in organisms is not to be expected.

12.4 Mobility in soil**Product:**

Mobility In Environmental
Media:

Mobility in soil

Assessment transport between environmental compartments:
Adsorption in soil: No data available.

Notes from Section 12:

Results of PBT and vPvB assessment

According to Annex XIV of Regulation (EC) No.1907/2006 concerning the Registration, Evaluation, Authorisation and Restriction of Chemicals (REACH): The product does not contain a substance fulfilling the PBT (persistent/bioaccumulative/toxic) criteria or the vPvB (very persistent/very bioaccumulative) criteria. Self classification

Other adverse effects : The substance is not listed in Regulation (EC) 1005/2009 on substances that deplete the ozone layer.

Section 13: DISPOSAL CONSIDERATIONS

(ID no. 30034964/SDS_GEN_00/EN)

13.1 Waste treatment methods

Waste Disposal:

Waste treatment methods : Observe national and local legal requirements.

Section 14: TRANSPORT INFORMATION

(ID no. 30034964/SDS_GEN_00/EN)

| | |
|------------------------|--|
| IATA Hazard Class: | Not applicable |
| IATA Packing Group: | Not applicable |
| IATA Other: | Environmental hazards: Not applicable Special precautions for user : None known |
| RID/ADR: | RID : Not classified as a dangerous good under transport regulations |
| RID/ADR Shipping Name: | Not applicable |
| RID/ADR UN Number: | Not applicable |
| RID/ADR Hazard Class: | Not applicable |
| RID/ADR Packing Group: | Not applicable |
| RID/ADR Other: | Environmental hazards: Not applicable Special precautions for user: None known |
| ICAO: | Not classified as a dangerous good under transport regulations |
| ICAO Shipping Name: | Not applicable |
| ICAO UN Number: | Not applicable |
| ICAO Packing Group: | Not applicable |
| ICAO Hazard Class: | Not applicable |
| ICAO Other: | Environmental hazards: Not applicable Special precautions for user : None known |

Section 15: REGULATORY INFORMATION

(ID no. 30034964/SDS_GEN_00/EN)

15.1 Safety, health and environmental regulations/legislation specific for the substance or mixture

Regulatory - Product Based:

Safety, health and environmental regulations/legislation specific for the substance or mixture:

If other regulatory information applies that is not already provided elsewhere in this safety data sheet, then it is described in this subsection.

15.2 Chemical Safety Assessment

Section 16: Additional Information

(ID no. 30034964/SDS_GEN_00/EN)

| | |
|------------------------|---|
| Revision Date: | 16.12.2015 |
| Revision Notes: | Vertical lines in the left hand margin indicate an amendment from the previous version. |
| Version Number: | 1.0 |
| Disclaimer: | The data contained in this safety data sheet are based on our current knowledge and experience and describe the product only with regard to safety requirements. The data do not describe the product's properties (product specification). Neither should any agreed property nor the suitability of the product for any specific purpose be deduced from the data contained in the safety data sheet. It is the responsibility of the recipient of the product to ensure any proprietary rights and existing laws and legislation are observed. |
| Notes from Section 16: | Any other intended applications should be discussed with the manufacturer. Corresponding occupational protection measurements must be followed. |



Copyright © 1996-2018 EnVance Inc. All Rights Reserved.

Appendix D

Additional Data for Chapter 4

Summary

This appendix provides the supporting information from the study of the performance-controlling tablet disintegration mechanisms in Chapter 4.

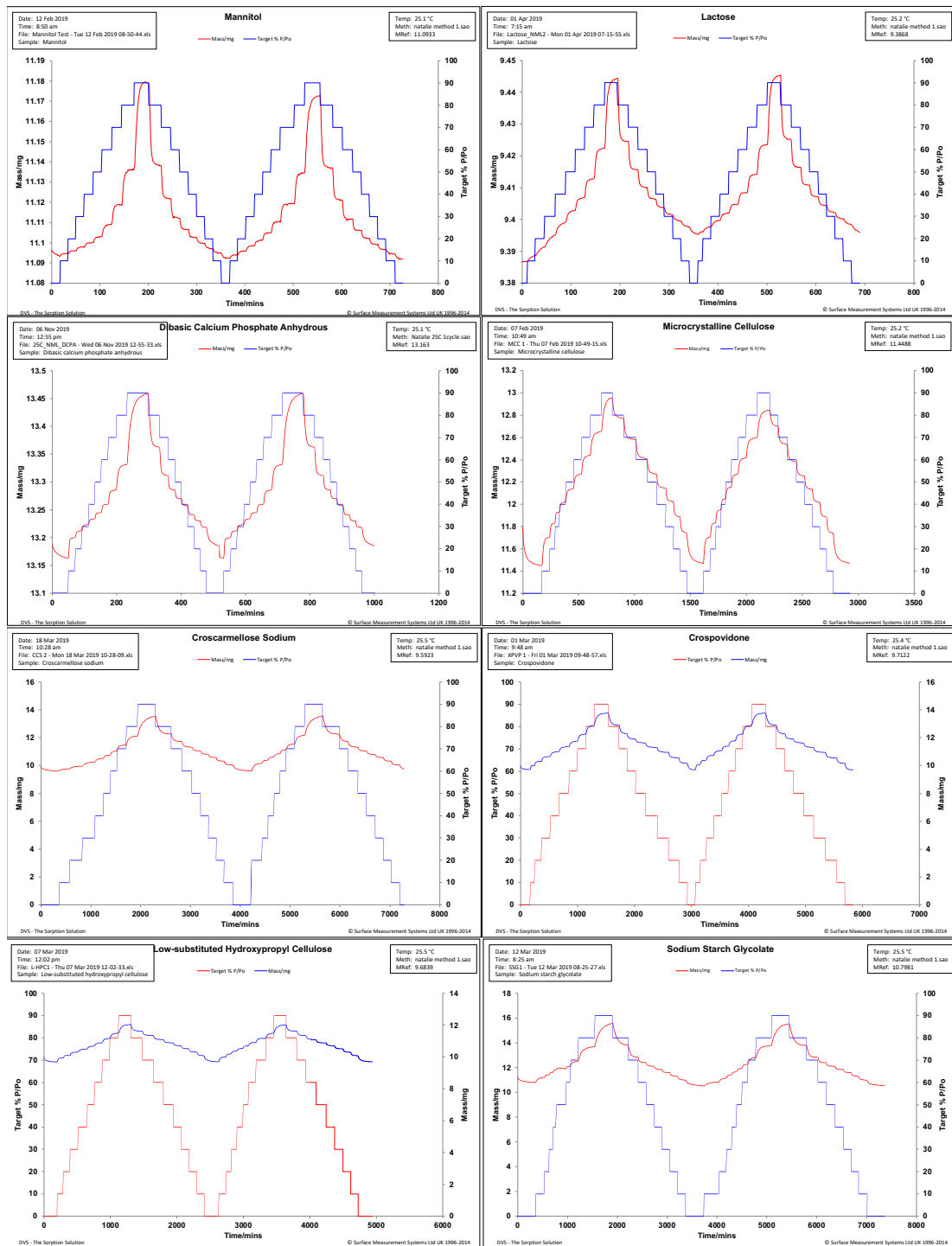


Figure D.1: Settling plots from the dynamic vapour sorption measurements of each filler and disintegrant.

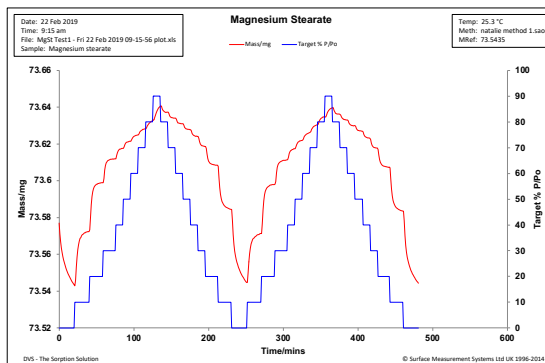


Figure D.2: Settling plot from the dynamic vapour sorption measurement of magnesium stearate.

Appendix E

Additional Data for Chapter 5

Summary

This appendix provides the supporting information for Chapter 5, giving the full data collected during the placebo stability studies.

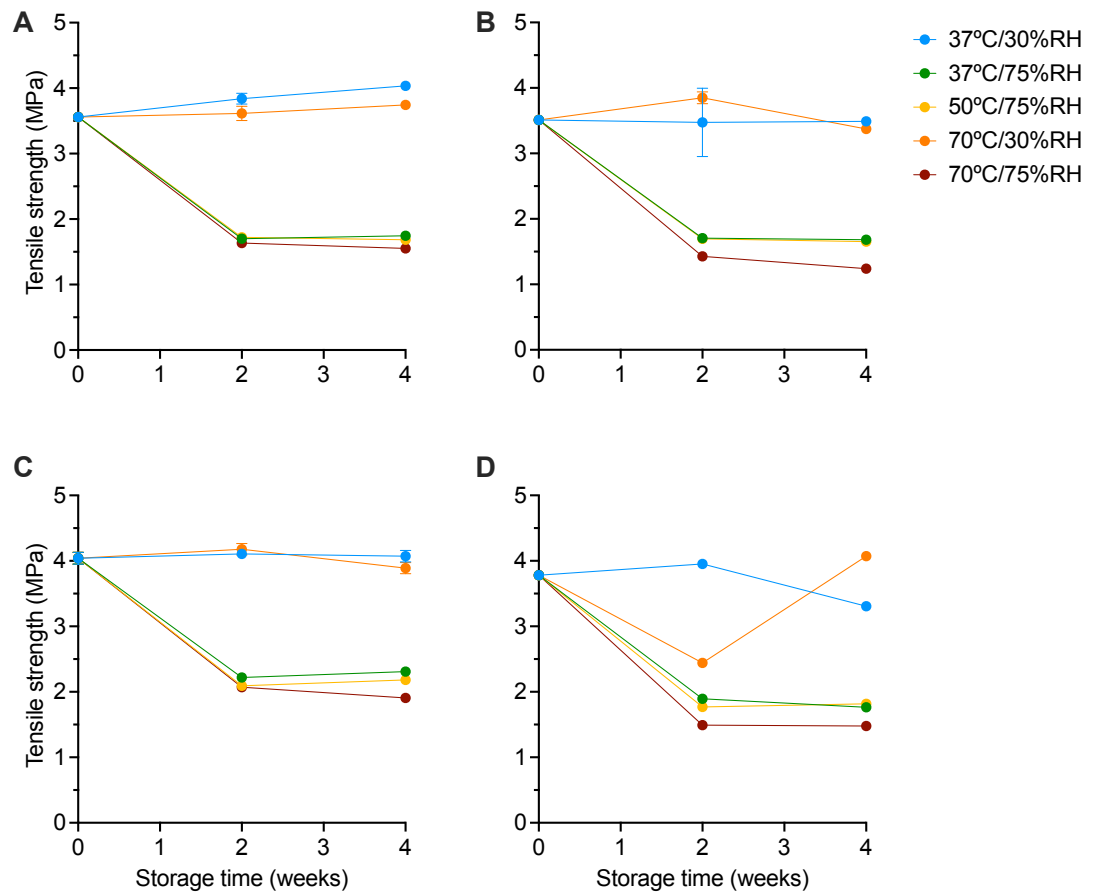


Figure E.1: The change in tensile strength for MCC/lactose-based tablets with (A) CCS, (B) XPVP, (C) L-HPC and (D) SSG after storage under accelerated storage conditions for 2 and 4 weeks. Mean \pm standard deviation, $n = 10$.

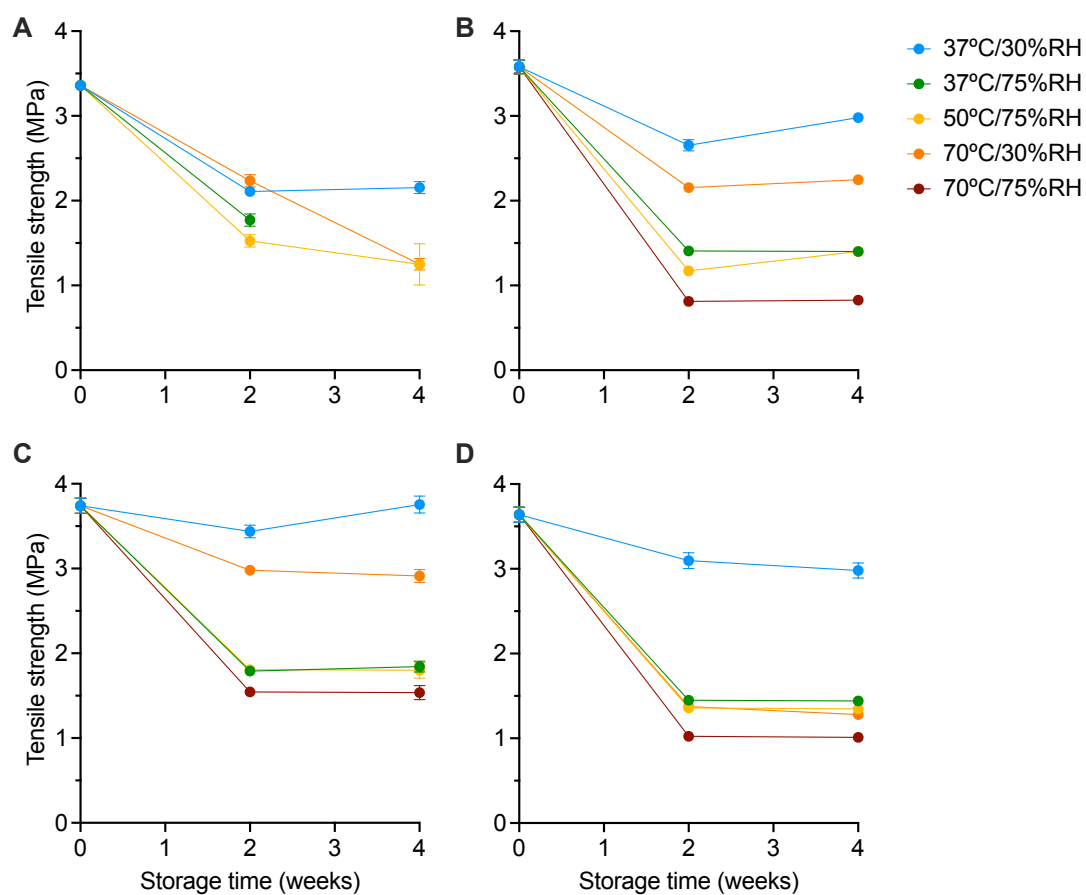


Figure E.2: The change in tensile strength for MCC/mannitol-based tablets with (A) CCS, (B) XPVP, (C) L-HPC and (D) SSG after storage under accelerated storage conditions for 2 and 4 weeks. Mean \pm standard deviation, $n = 10$.

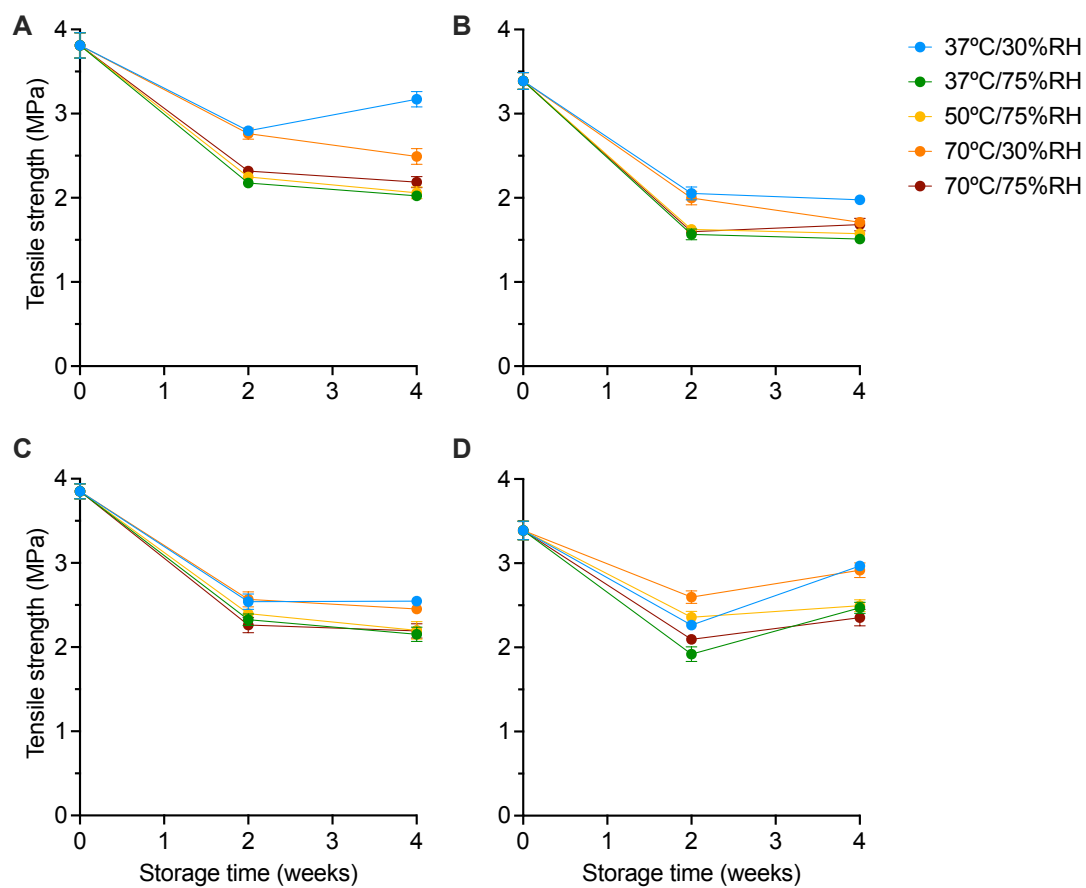


Figure E.3: The change in tensile strength for MCC/DCPA-based tablets with (A) CCS, (B) XPVP, (C) L-HPC and (D) SSG after storage under accelerated storage conditions for 2 and 4 weeks. Mean \pm standard deviation, $n = 10$.

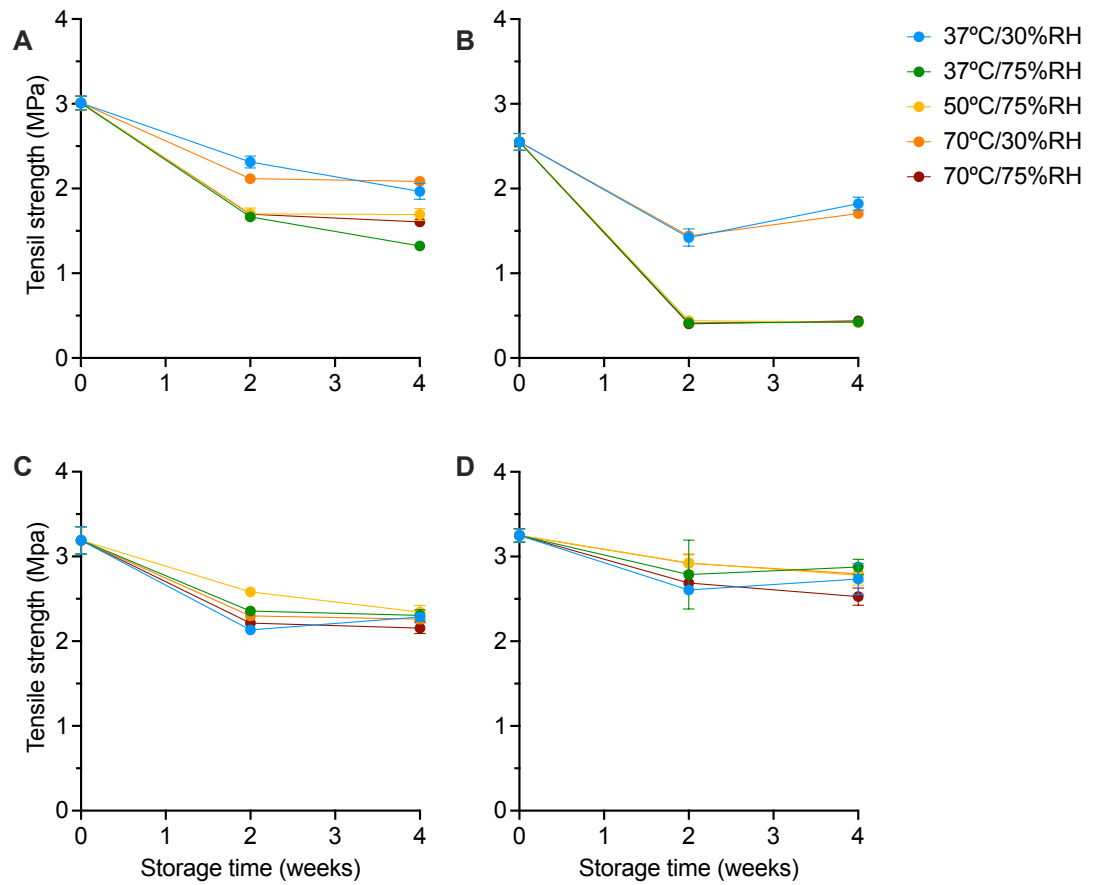


Figure E.4: The change in tensile strength for DCPA/lactose-based tablets with (A) CCS, (B) XPVP, (C) L-HPC and (D) SSG after storage under accelerated storage conditions for 2 and 4 weeks. Mean \pm standard deviation, $n = 10$.

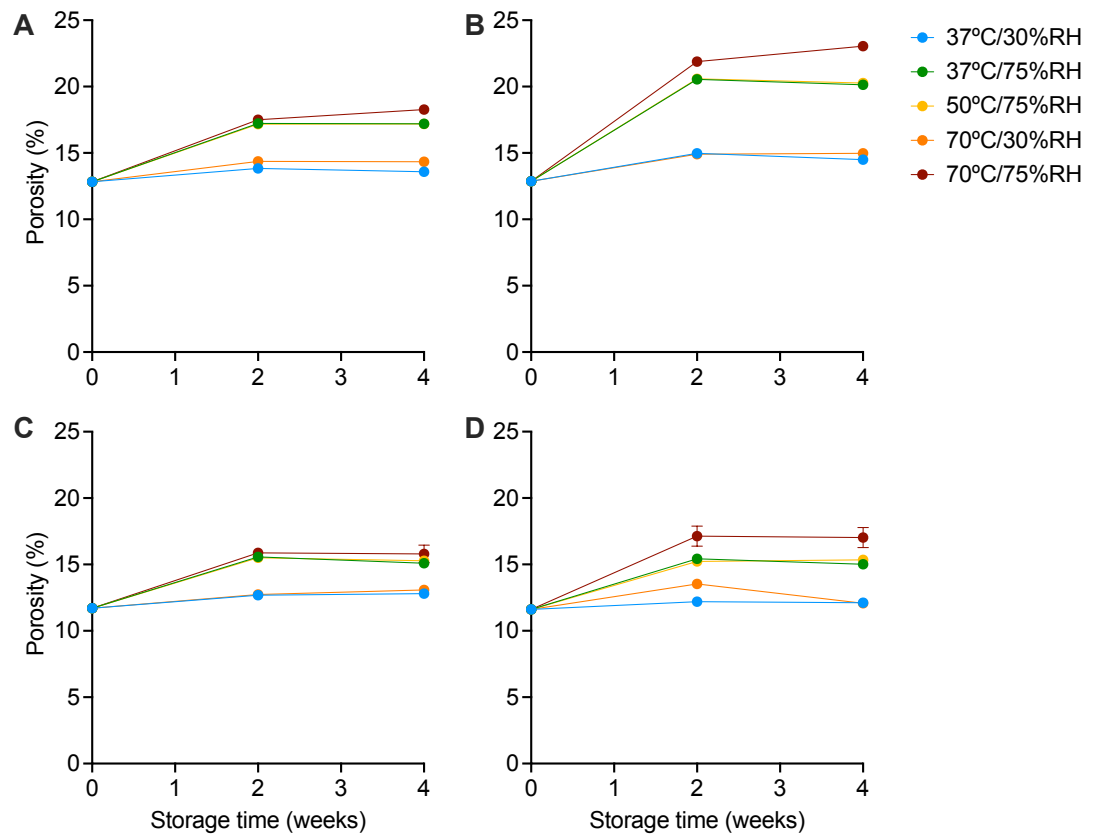


Figure E.5: The change in porosity for MCC/lactose-based tablets with (A) CCS, (B) XPVP, (C) L-HPC and (D) SSG after storage under accelerated storage conditions for 2 and 4 weeks. Mean \pm standard deviation, $n = 100$ (0 weeks) and $n = 10$ (2 and 4 weeks).

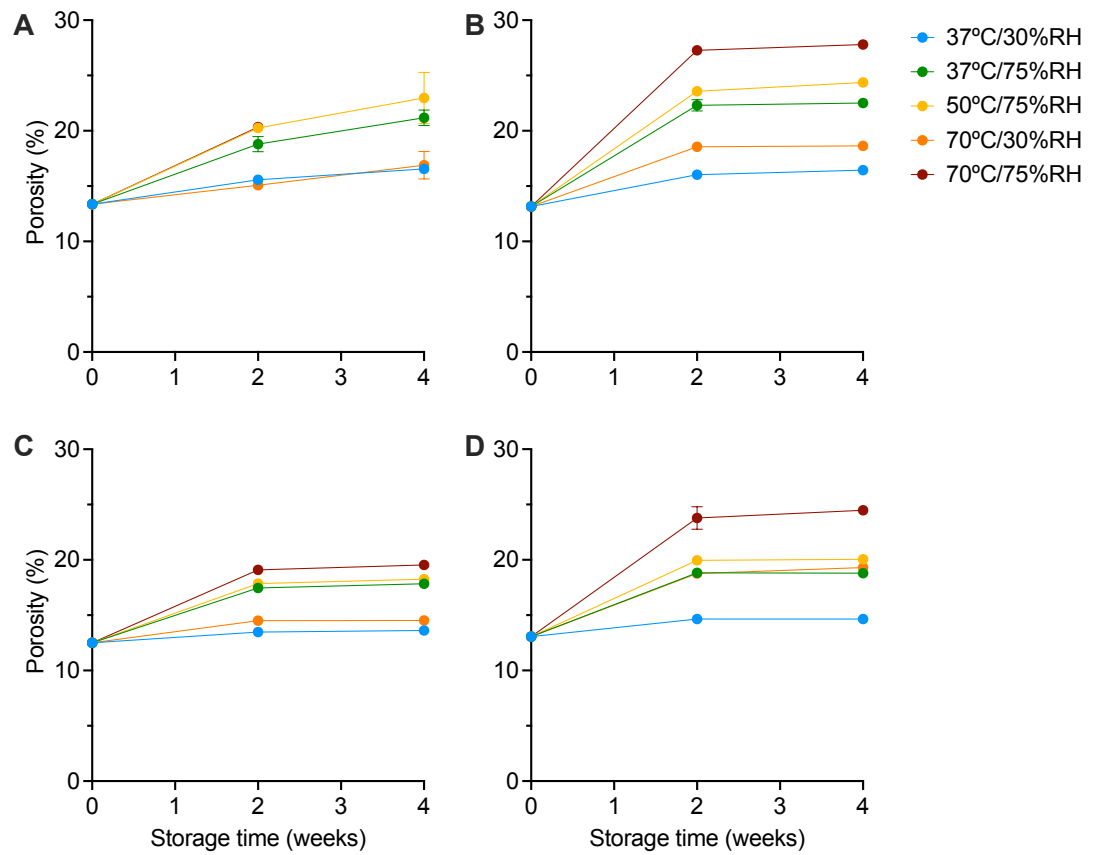


Figure E.6: The change in porosity for MCC/mannitol-based tablets with (A) CCS, (B) XPVP, (C) L-HPC and (D) SSG after storage under accelerated storage conditions for 2 and 4 weeks. Mean \pm standard deviation, $n = 100$ (0 weeks) and $n = 10$ (2 and 4 weeks).

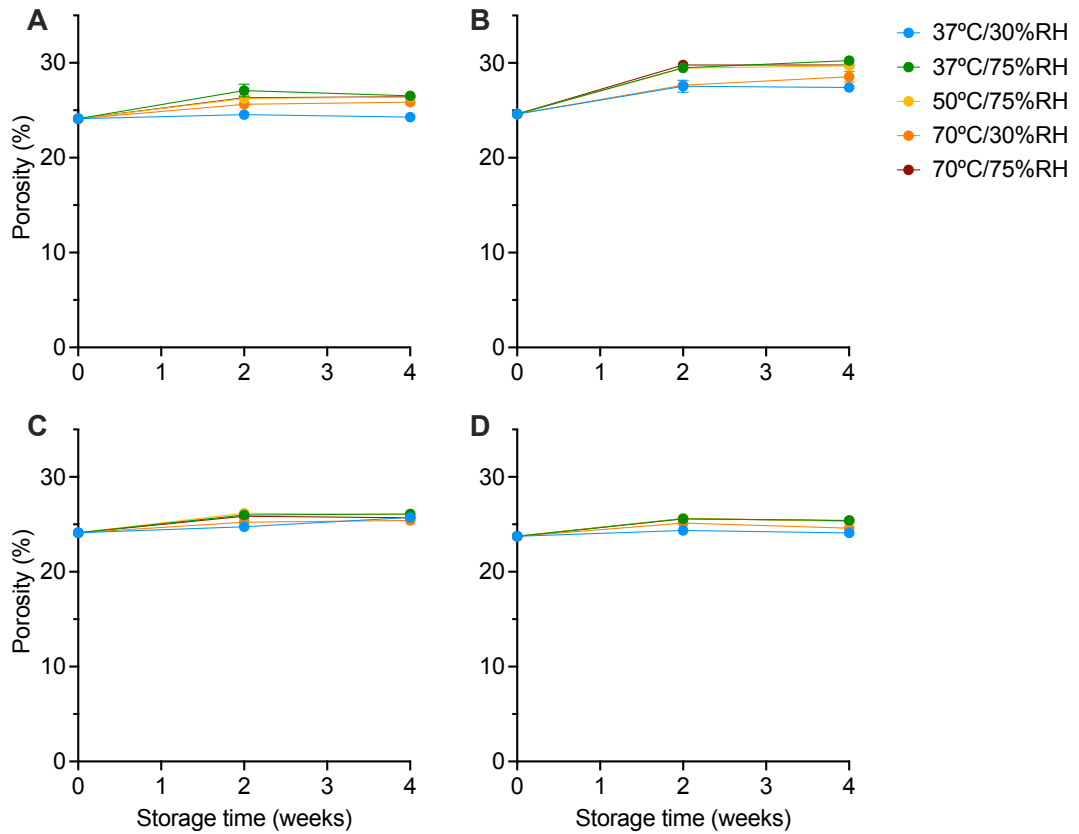


Figure E.7: The change in porosity for MCC/DCPA-based tablets with (A) CCS, (B) XPVP, (C) L-HPC and (D) SSG after storage under accelerated storage conditions for 2 and 4 weeks. Mean \pm standard deviation, $n = 100$ (0 weeks) and $n = 10$ (2 and 4 weeks).

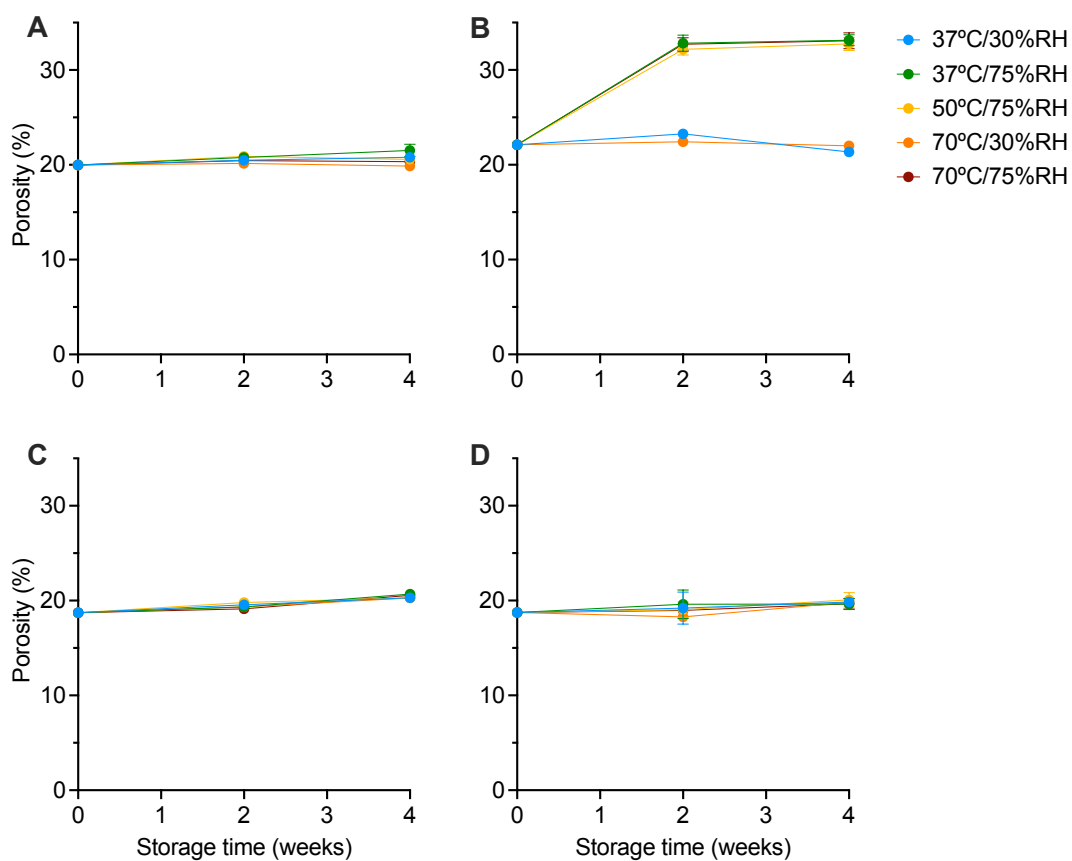


Figure E.8: The change in porosity for DCPA/lactose-based tablets with (A) CCS, (B) XPVP, (C) L-HPC and (D) SSG after storage under accelerated storage conditions for 2 and 4 weeks. Mean \pm standard deviation, $n = 100$ (0 weeks) and $n = 10$ (2 and 4 weeks).

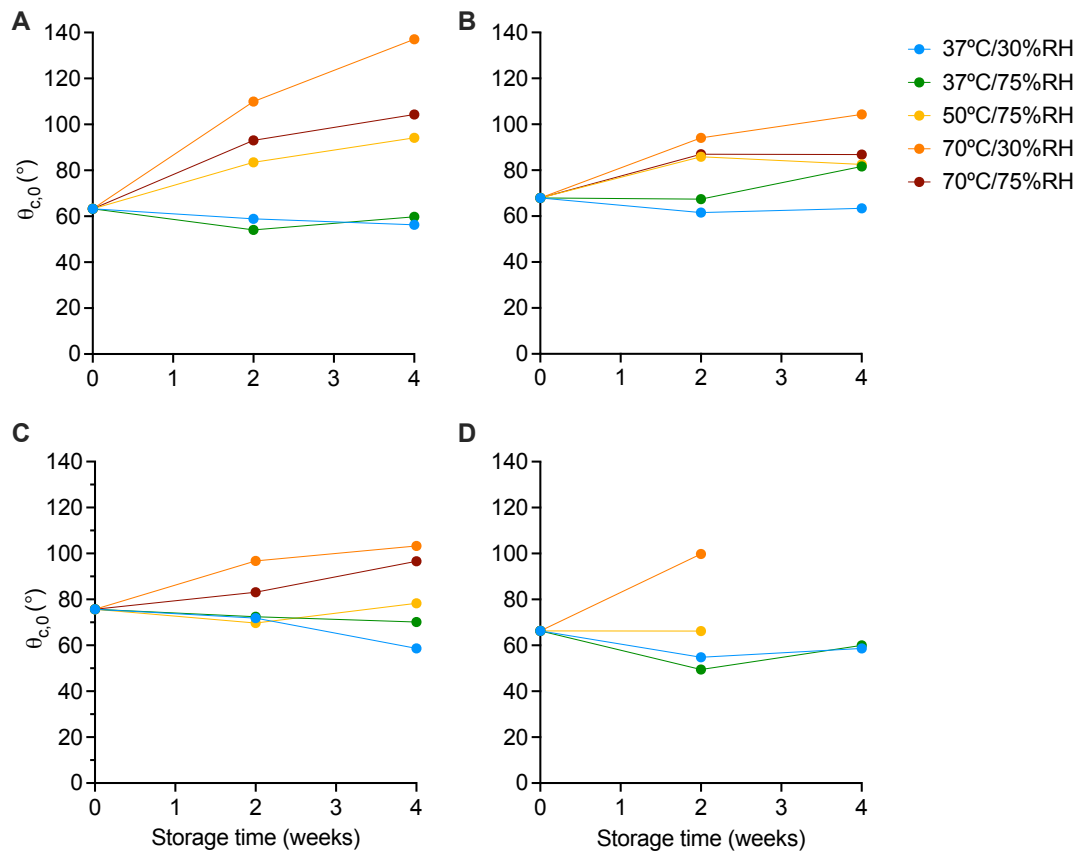


Figure E.9: The change in initial contact angle ($\theta_{c,0}$) for MCC/lactose-based tablets with (A) CCS, (B) XPVP, (C) L-HPC and (D) SSG after storage under accelerated storage conditions for 2 and 4 weeks. Mean, $n = 2$.

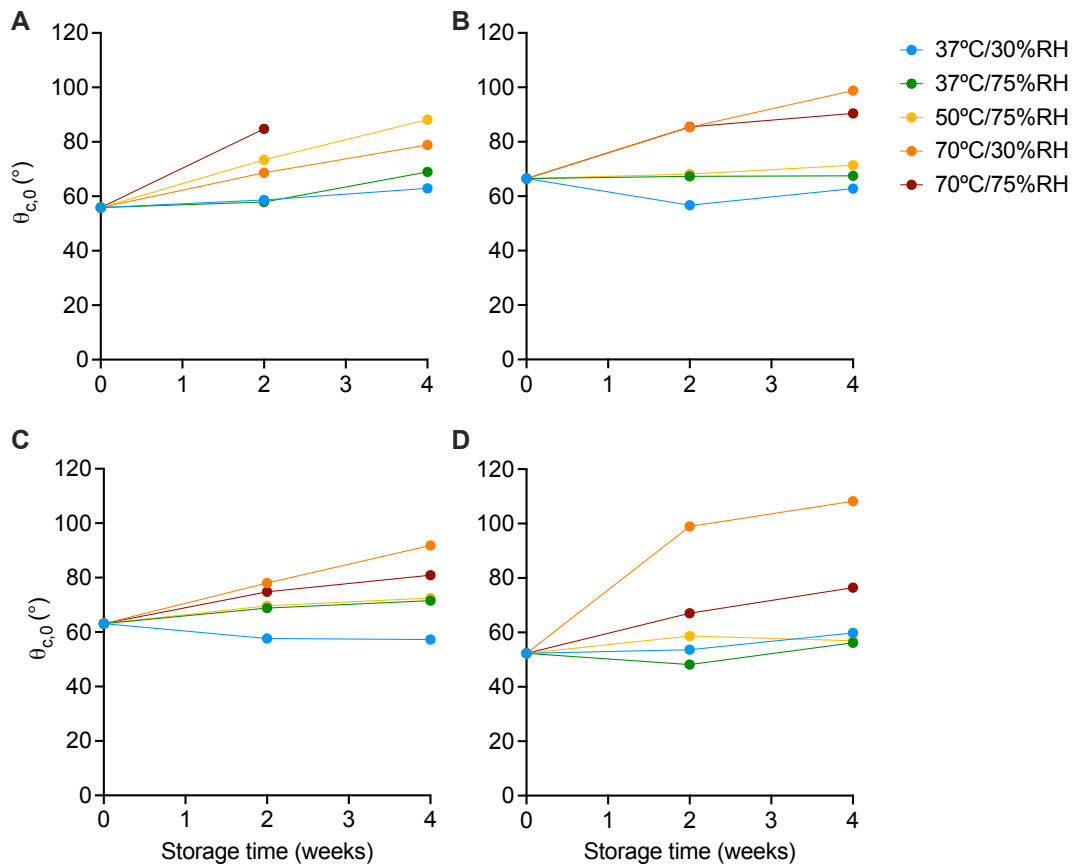


Figure E.10: The change in initial contact angle ($\theta_{c,0}$) for MCC/mannitol-based tablets with (A) CCS, (B) XPVP, (C) L-HPC and (D) SSG after storage under accelerated storage conditions for 2 and 4 weeks. Mean, $n = 2$.

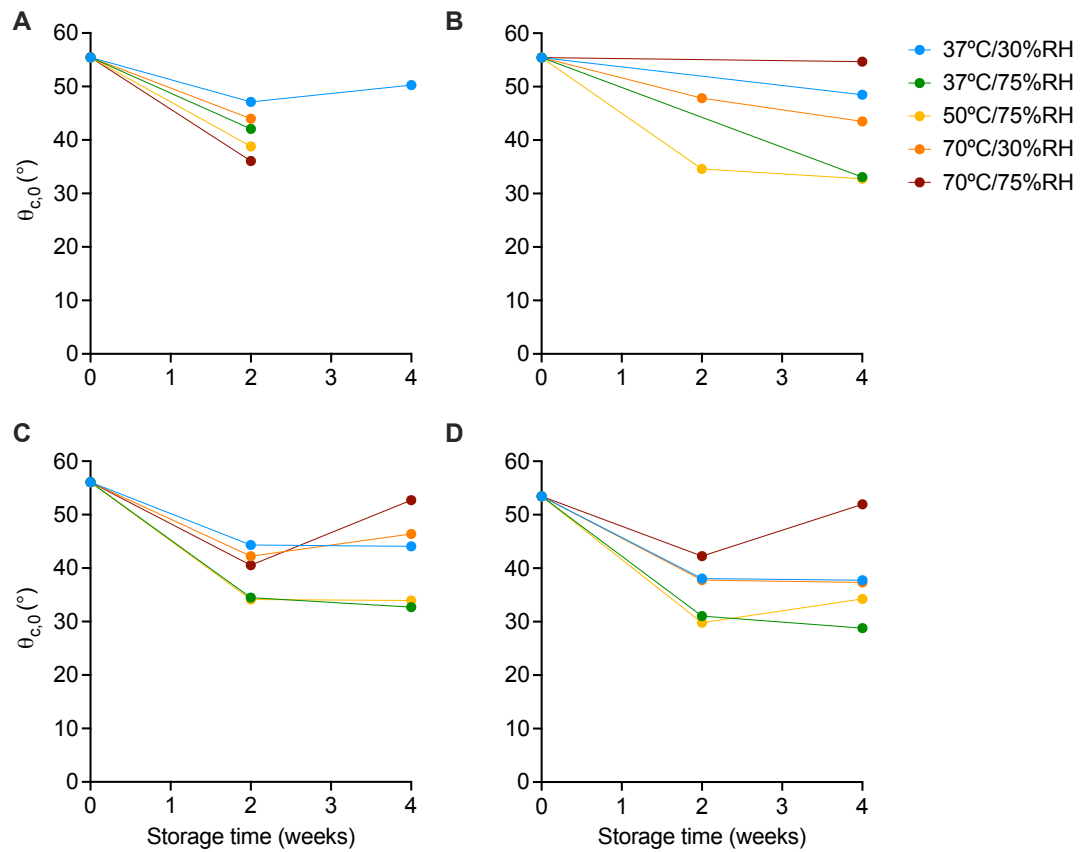


Figure E.11: The change in initial contact angle ($\theta_{c,0}$) for MCC/DCPA-based tablets with (A) CCS, (B) XPVP, (C) L-HPC and (D) SSG after storage under accelerated storage conditions for 2 and 4 weeks. Mean, $n = 2$.

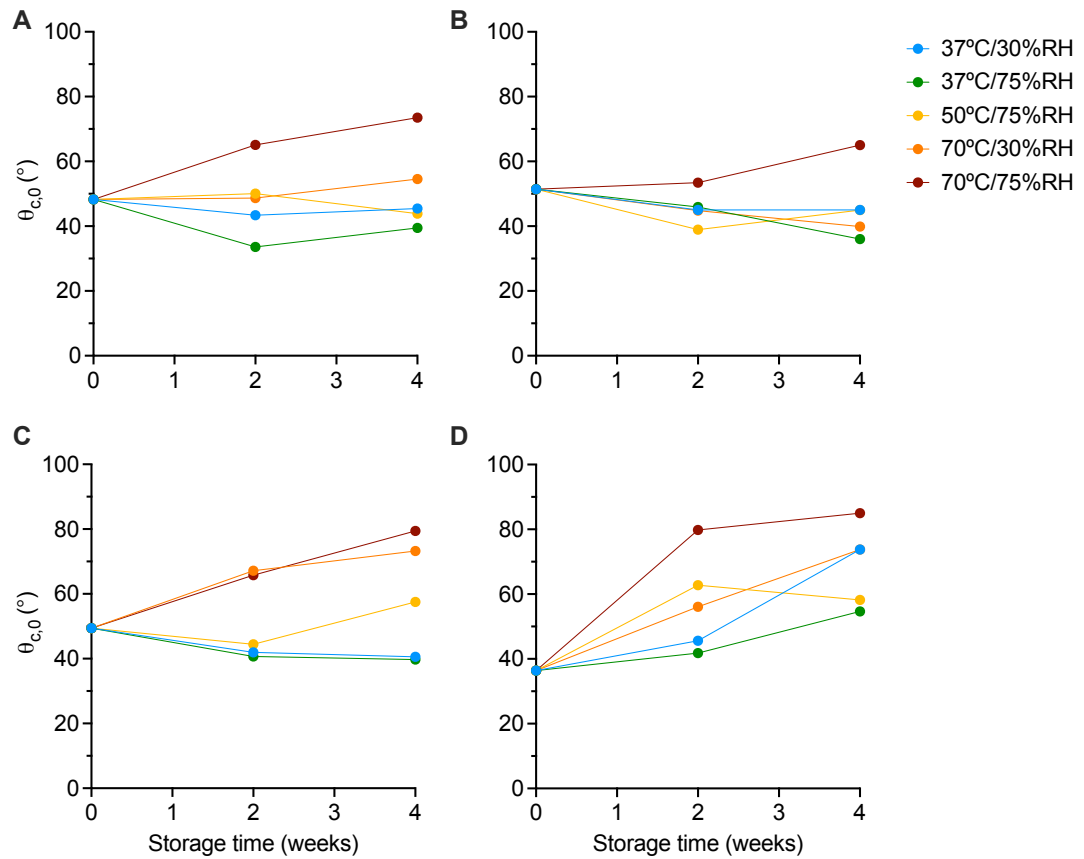


Figure E.12: The change in initial contact angle ($\theta_{c,0}$) for DCPA/lactose-based tablets with (A) CCS, (B) XPVP, (C) L-HPC and (D) SSG after storage under accelerated storage conditions for 2 and 4 weeks. Mean, $n = 2$.

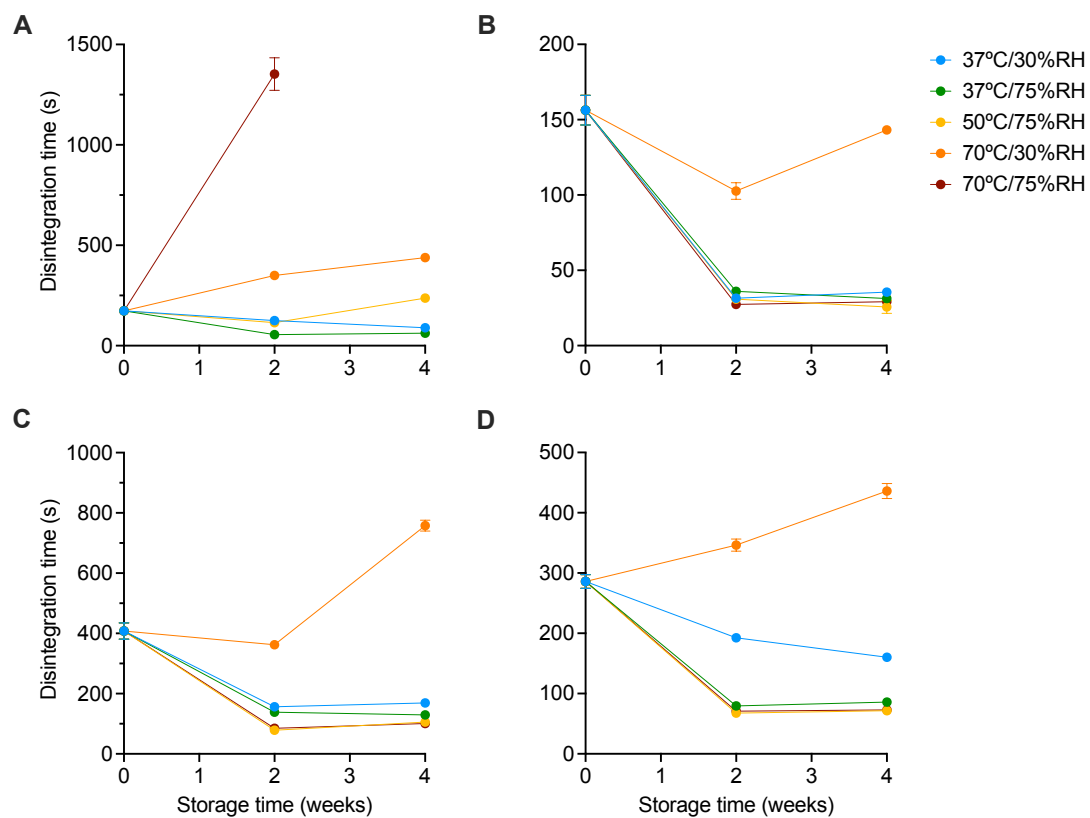


Figure E.13: The change in disintegration time for MCC/lactose-based tablets with (A) CCS, (B) XPVP, (C) L-HPC and (D) SSG after storage under accelerated storage conditions for 2 and 4 weeks. Mean \pm standard deviation, $n = 6$.

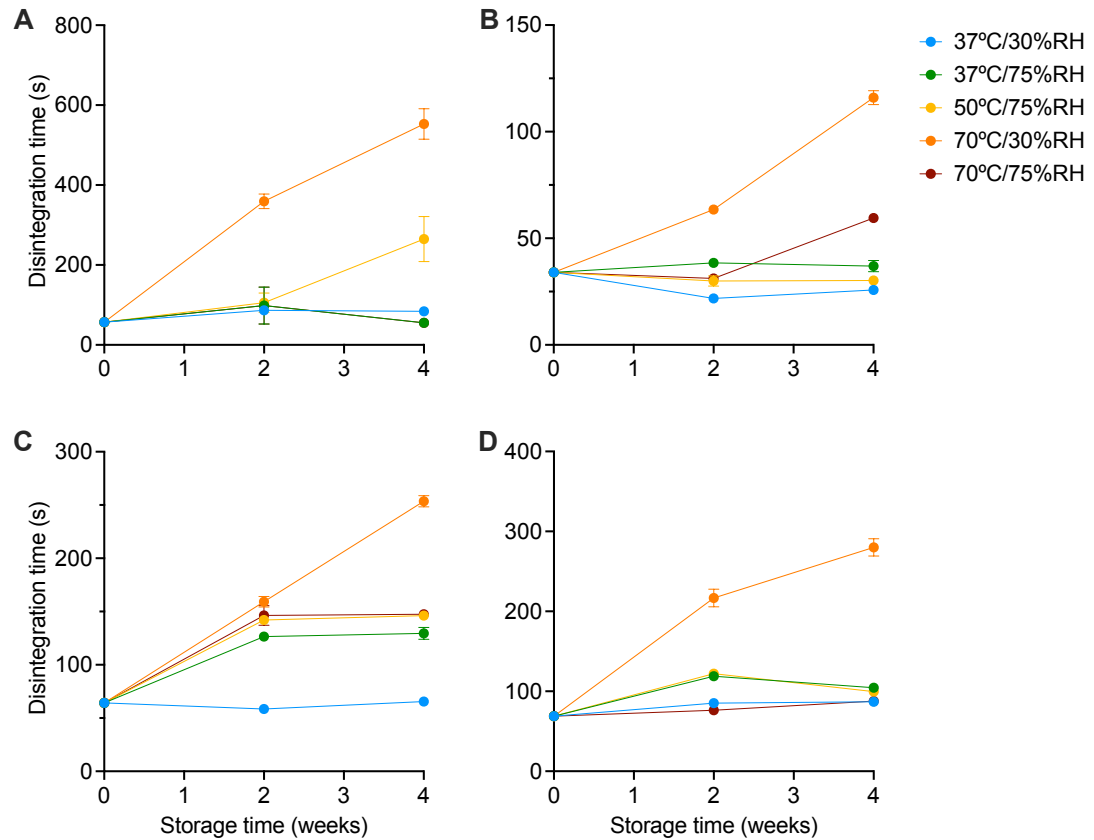


Figure E.14: The change in disintegration time for MCC/mannitol-based tablets with (A) CCS, (B) XPVP, (C) L-HPC and (D) SSG after storage under accelerated storage conditions for 2 and 4 weeks. Mean \pm standard deviation, $n = 6$.

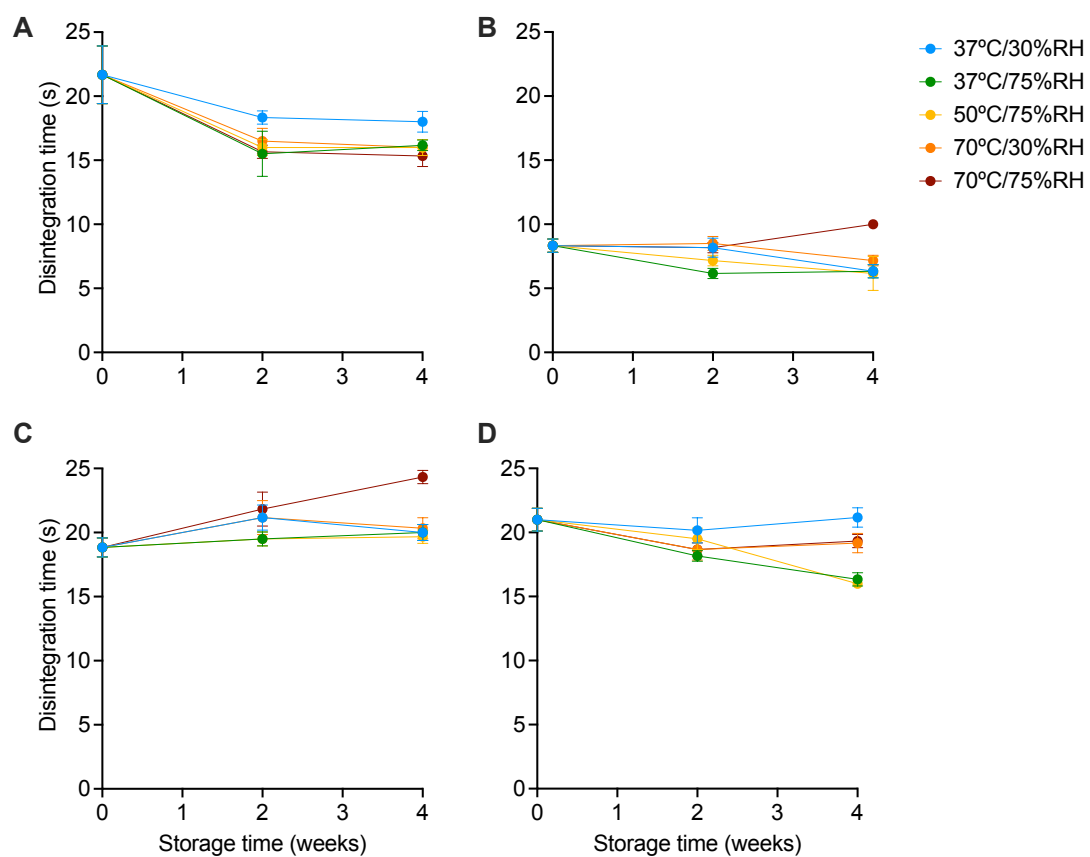


Figure E.15: The change in disintegration time for MCC/DCPA-based tablets with (A) CCS, (B) XPVP, (C) L-HPC and (D) SSG after storage under accelerated storage conditions for 2 and 4 weeks. Mean \pm standard deviation, $n = 6$.

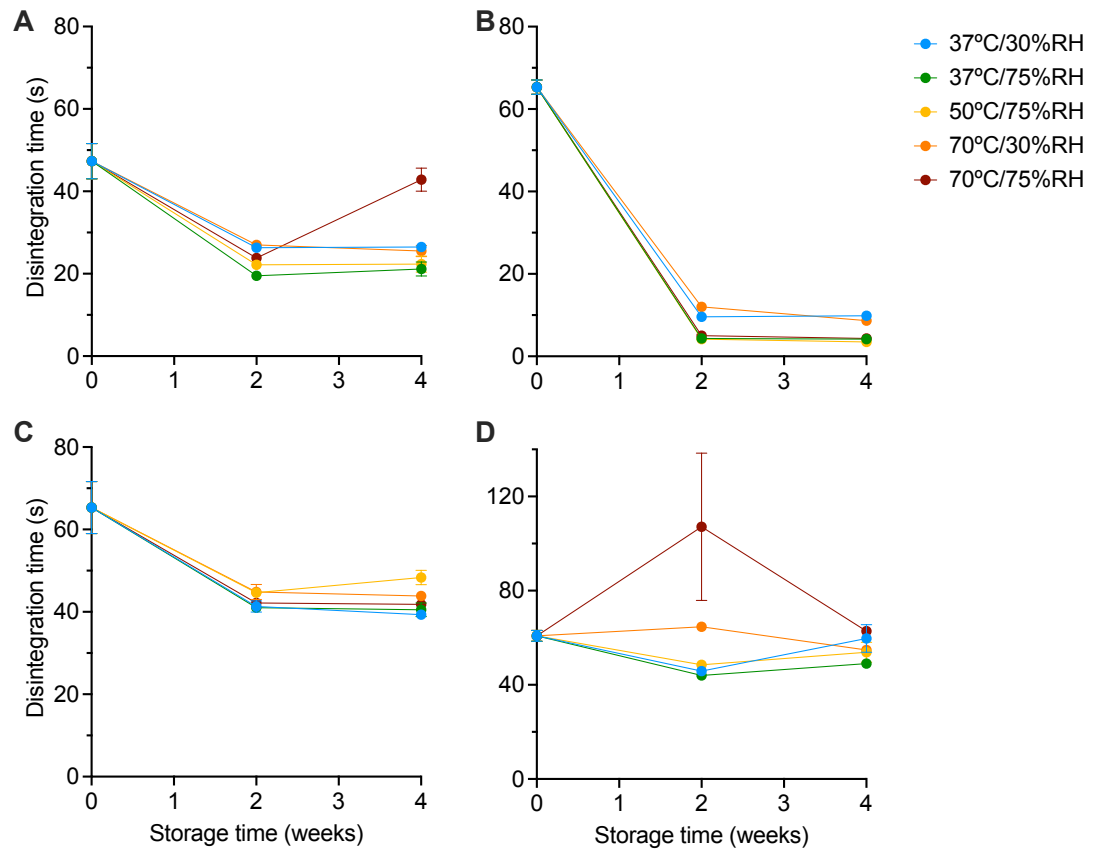


Figure E.16: The change in disintegration time for DCPA/lactose-based tablets with (A) CCS, (B) XPVP, (C) L-HPC and (D) SSG after storage under accelerated storage conditions for 2 and 4 weeks. Mean \pm standard deviation, $n = 6$.

Bibliography

2018a. *Accelerated Predictive Stability (APS)*. Academic Press.

Ahlneck, C., & Alderborn, G. 1989. Moisture adsorption and tableting. II. The effect on tensile strength and air permeability of the relative humidity during storage of tablets of 3 crystalline materials. *International Journal of Pharmaceutics*, **56**(2), 143–150.

Al-Sharabi, M., Markl, D., Mudley, T., Bawuah, P., Karttunen, A., Ridgway, C., Gane, P., Ketolainen, J., Peiponen, K., & Rades, T. 2020. Simultaneous investigation of the liquid transport and swelling performance during tablet disintegration. *International Journal of Pharmaceutics*, **584**(Jun), 119380.

Anwar, S., Fell, J. T., & Dickinson, P. A. 2005. An investigation of the disintegration of tablets in biorelevant media. *International Journal of Pharmaceutics*, **290**(1), 121–127.

Bajaj, S., Singla, D., & Sakhuja, N. 2012. Stability Testing of Pharmaceutical Products. *Journal of Applied Pharmaceutical Science*, **2**(3), 129–138.

Basaleh, S., Bisharat, L., Cespi, M., & Berardi, A. 2020. Temperature: An overlooked factor in tablet disintegration. *European Journal of Pharmaceutical Sciences*, **151**(Aug), 105388.

Bauhuber, S., Warnke, G., & Berardi, A. 2021. Disintegrant Selection in Hydrophobic Tablet Formulations. *Journal of Pharmaceutical Sciences*, **110**(5), 2028–2037.

Berardi, A., Bisharat, L., Blaibleh, A., Pavoni, L., & Cespi, M. 2018. A Simple and

- Inexpensive Image Analysis Technique to Study the Effect of Disintegrants Concentration and Diluents Type on Disintegration. *Journal of Pharmaceutical Sciences*, **107**(10), 2643–2652.
- Berardi, A., Bisharat, L., Quodbach, J., Abdel Rahim, S., Perinelli, D. R., & Cespi, M. 2021. Advancing the Understanding of the Tablet Disintegration Phenomenon - An Update on Recent Studies. *International Journal of Pharmaceutics*, Feb, 120390.
- Bisharat, L., AlKhatib, H. S., Muhaissen, S., Quodbach, J., Blaibleh, A., Cespi, M., & Berardi, A. 2019. The influence of ethanol on superdisintegrants and on tablets disintegration. *European Journal of Pharmaceutical Sciences*, **129**(Mar), 140–147.
- Caramella, C., Ferrari, F., Bonferoni, M. C., & Ronchi, M. 1990. Disintegrants in Solid Dosage Forms. *Drug Development and Industrial Pharmacy*, **16**(17), 2561–2577.
- Chang, C. K., Alvarez-Nunez, F. A., Rinella, J. V., Jr., Magnusson, L. E., & Sueda, K. 2008. Roller compaction, granulation and capsule product dissolution of drug formulations containing a lactose or mannitol filler, starch, and talc. *AAPS PharmSciTech*, **9**(2), 597–604.
- Chowhan, Z. T. 1980a. The Effect of Low- and High-Humidity Ageing on the Hardness, Disintegration Time and Dissolution Rate of Dibasic Calcium Phosphate-Based Tablets. *Journal of Pharmacy and Pharmacology*, **32**(1), 10–14.
- Chowhan, Z. T. 1980b. Role of binders in moisture-induced hardness increase in compressed tablets and its effect on in vitro disintegration and dissolution. *Journal of Pharmaceutical Sciences*, **69**(1), 1–4.
- Clancy, D., Patel-Jones, J., & Hutton, G. 2018. *Chapter 19 - Accelerated Stability Modeling: Investigation of disintegration time of a drug product with sodium bicarbonate*. Academic Press. Page 403–410.
- Colgan, Stephen T., Mazzeo, Tony, & Orr, Rachel. 2018. Chapter 2 - Regulatory Expectations and Industry Practice on Stability Testing. *Pages 15–32 of: Qiu, Fenghe, & Scrivens, Garry (eds), Accelerated Predictive Stability*. Boston: Academic Press.

- Collins, C. C., & Nair, R. R. 1998. Comparative Evaluation of Mixing Dynamics in USP Apparatus 2 using Standard USP Vessels and PEAK™ Vessels. *Dissolution Technologies*, **5**(2), 17–20.
- Desai, P. M., Liew, C. V., & Heng, P. W. S. 2012. Understanding Disintegrant Action by Visualization. *Journal of Pharmaceutical Sciences*, **101**(6), 2155–2164.
- Desai, P. M., Liew, C. V., & Heng, P. W. S. 2016. Review of Disintegrants and the Disintegration Phenomena. *Journal of Pharmaceutical Sciences*, **105**(9), 2545–2555.
- Dressman, J. J., & Kramer, J. (eds). 2005. *Pharmaceutical Dissolution Testing*. 1st edition edn. Boca Raton: CRC Press.
- Dvořák, J., Tomas, J., Lizoňová, D., Schöngut, M., Dammer, O., Pekárek, T., Beránek, J., & Štěpánek, F. 2020. Investigation of tablet disintegration pathways by the combined use of magnetic resonance imaging, texture analysis and static light scattering. *International Journal of Pharmaceutics*, **587**(Sep), 119719.
- Ekmekciyan, N., Tuglu, T., El-Saleh, F., Muehlenfeld, C., Stoyanov, E., & Quodbach, J. 2018. Competing for water: A new approach to understand disintegrant performance. *International Journal of Pharmaceutics*, **548**(1), 491–499.
- Fell, J. T., & Newton, J. M. 1970. Determination of Tablet Strength by the Diametral-Compression Test. *Journal of Pharmaceutical Sciences*, **59**(5), 688–691.
- Fuchs, Alexander, Leigh, Mathew, Kloefer, Bastian, & Dressman, Jennifer B. 2015. Advances in the design of fasted state simulating intestinal fluids: FaSSIF-V3. *European Journal of Pharmaceutics and Biopharmaceutics*, **94**, 229–240. Citation Key: FUCHS2015229.
- Galia, E., Nicolaidis, E., Hörter, D., Löbenberg, R., Reppas, C., & Dressman, J. B. 1998. Evaluation of Various Dissolution Media for Predicting In Vivo Performance of Class I and II Drugs. *Pharmaceutical Research*, **15**(5), 698–705.
- Gordon, M. S., & Chowhan, Z. T. 1990. The Effect of Aging on Disintegrant Efficiency

- in Direct Compression Tablets with Varied Solubility and Hygroscopicity, in Terms of Dissolution. *Drug Development and Industrial Pharmacy*, **16**(3), 437–447.
- Gordon, M. S., Chatterjee, B., & Chowhan, Z. T. 1990. Effect of the mode of croscarmellose sodium incorporation on tablet dissolution and friability. *Journal of Pharmaceutical Sciences*, **79**(1), 43–47.
- Gordon, M. S., Rudraraju, V. S., Dani, K., & Chowhan, Z. T. 1993. Effect of the Mode of Super Disintegrant Incorporation on Dissolution in Wet Granulated Tablets. *Journal of Pharmaceutical Sciences*, **82**(2), 220–226.
- Gordon, Marc S., & Chowhan, Zakaiddin T. 1987. Effect of Tablet Solubility and Hygroscopicity on Disintegrant Efficiency in Direct Compression Tablets In Terms of Dissolution. *Journal of Pharmaceutical Sciences*, **76**(12), 907–909.
- Hersen-Delesalle, C., Leclerc, B., Couarraze, G., Busignies, V., & Tchoreloff, P. 2007. The Effects of Relative Humidity and Super-Disintegrant Concentrations on the Mechanical Properties of Pharmaceutical Compacts. *Drug Development and Industrial Pharmacy*, **33**(12), 1297–1307.
- Hiew, T. N., Johan, N. A. B., Desai, P. M., Chua, S. M., Loh, Z. H., & Heng, P. W. S. 2016. Effect of Moisture Sorption on the Performance of Crospovidone. *International Journal of Pharmaceutics*, **514**(1), 322–331.
- Horhota, S. T., Burgio, J., Lonski, L., & Rhodes, C. T. 1976. Effect of Storage at Specified Temperature and Humidity on Properties of Three Directly Compressible Tablet Formulations. *Journal of Pharmaceutical Sciences*, **65**(12), 1746–1749.
- ICH. 2003. *Stability testing of new drug substances and products Q1A (R2)*. Current Step 4.
- Interest, Compound. 2016. *Understanding the Drug Discovery Process*.
- Jantratid, Ekarat, Janssen, Niels, Reppas, Christos, & Dressman, Jennifer B. 2008. Dissolution Media Simulating Conditions in the Proximal Human Gastrointestinal Tract: An Update. *Pharmaceutical Research*, **25**(7), 1663.

- Johnson, J. R., Wang, L., Gordon, M. S., & Chowhan, Z. T. 1991. Effect of Formulation Solubility and Hygroscopicity on Disintegrant Efficiency in Tablets Prepared by Wet Granulation, in Terms of Dissolution. *Journal of Pharmaceutical Sciences*, **80**(5), 469–471.
- Khattab, I., Menon, A., & Sakr, A. 1993. Effect of Mode of Incorporation of Disintegrants on the Characteristics of Fluid-bed Wet-granulated Tablets. *Journal of Pharmacy and Pharmacology*, **45**(8), 687–691. _eprint: <https://onlinelibrary.wiley.com/doi/pdf/10.1111/j.2042-7158.1993.tb07089.x>.
- Kossena, Greg A., Charman, William N., Boyd, Ben J., Dunstan, Dave E., & Porter, Christopher J.H. 2004. Probing drug solubilization patterns in the gastrointestinal tract after administration of lipid-based delivery systems: A phase diagram approach. *Journal of Pharmaceutical Sciences*, **93**(2), 332–348.
- Krishna, R., & Yu, L. (eds). 2008. *Biopharmaceutics Applications in Drug Development*. New York: Springer. OCLC: ocn166358030.
- Lausier, J. M., Chiang, Chia-Whei, Zompa, H. A., & Rhodes, C. T. 1977. Aging of Tablets made with Dibasic Calcium Phosphate Dihydrate as Matrix. *Journal of Pharmaceutical Sciences*, **66**, 1636–1637.
- Leane, M., Pitt, K., & Reynolds, G. 2015. A proposal for a drug product Manufacturing Classification System (MCS) for oral solid dosage forms. *Pharmaceutical Development and Technology*, **20**(1), 12–21.
- Li, H., Nadig, D., Kuzmission, A., & Riley, C. M. 2016. Prediction of the changes in drug dissolution from an immediate-release tablet containing two active pharmaceutical ingredients using an accelerated stability assessment program (ASAPprime®). *AAPS Open*, **2**(1), 7.
- Li, S., Wei, B., Fleres, S., Comfort, A., & Royce, A. 2004. Correlation and Prediction of Moisture-Mediated Dissolution Stability for Benazepril Hydrochloride Tablets. *Pharmaceutical Research*, **21**(4), 617–624.

- López-Solís, J., & Villafuerte-Robles, L. 2001. Effect of disintegrants with different hygroscopicity on dissolution of Norfloxacin/Pharmatose DCL 11 tablets. *International Journal of Pharmaceutics*, **216**(1), 127–135.
- Lu, Y., Tang, N., Lian, R., Qi, J., & Wu, W. 2014. Understanding the Relationship Between Wettability and Dissolution of Solid Dispersion. *International Journal of Pharmaceutics*, **465**(1), 25–31.
- Mann, J., Cohen, M., Abend, A., Coutant, C., Ashworth, L., Shaw, R., Reynolds, G., Nir, I., Shah, V., Shaw, S., Patel, A., Lu, X., Cicale, V., Mccallum, M., Patel, S., Topolski, J., Prufer, S., Tomaszewska, I., Kourentas, A., Mueller-Zsigmondy, M., Williams, J., Ainge, M., Berben, P., Bouquelle, A., Abrahamsson, B., Karlsson, A., Varghese, R., Li, F., Orce, A., Nickerson, B., & Shao, X. 2021. Stimuli to the Revision Process: The Case for Apex Vessels Stimuli articles do not necessarily reflect the policies of the USPC or the USP Council of Experts. *Dissolution Technologies*, **28**(4), 6–24. Publisher: Dissolution Technologies, Inc.
- Marais, A. F., Song, M., & De Villiers, M. M. 2003. Effect of compression force, humidity and disintegrant concentration on the disintegration and dissolution of directly compressed furosemide tablets using croscarmellose sodium as disintegrant. *Tropical Journal of Pharmaceutical Research*, **2**(1).
- Markl, D., & Zeitler, J. A. 2017. A Review of Disintegration Mechanisms and Measurement Techniques. *Pharmaceutical Research*, **34**(5), 890–917.
- Markl, D., Yassin, S., Wilson, D. I., Goodwin, D. J., Anderson, A., & Zeitler, J. A. 2017. Mathematical modelling of liquid transport in swelling pharmaceutical immediate release tablets. *International Journal of Pharmaceutics*, **526**(1), 1–10.
- Markl, D., Maclean, N., Mann, J., Williams, H., Abbott, A., Mead, H., & Khadra, I. 2021. Tablet Disintegration Performance: Effect of Compression Pressure and Storage Conditions on Surface Liquid Absorption and Swelling Kinetics. *International Journal of Pharmaceutics*, **601**(May), 120382.

- McMahon, M. E., Abbott, A., Babayan, Y., Carhart, J., Chen, C., Debie, E., Fu, M., Hoaglund-Hyzer, C., Lennard, A., Li, H., Mazzeo, T., McCaig, L., Pischel, S., Qiu, F., Stephens, E., Timpano, R., Webb, D., Wolfe, C., Woodlief, K., & Wu, Y. 2021. Considerations for Updates to ICH Q1 and Q5C Stability Guidelines: Embracing Current Technology and Risk Assessment Strategies. *The AAPS Journal*, **23**(6), 107.
- Mishra, S. M., & Sauer, A. 2022. Effect of Physical Properties and Chemical Substitution of Excipient on Compaction and Disintegration Behavior of Tablet: A Case Study of Low-Substituted Hydroxypropyl Cellulose (L-HPC). *Macromol*, **2**(1), 113–130. Number: 1 Publisher: Multidisciplinary Digital Publishing Institute.
- Molokhia, A. M., Moustafa, M. A., & Gouda, M. W. 1982. Effect of Storage Conditions on the Hardness, Disintegration and Drug Release from Some Tablet Bases. *Drug Development and Industrial Pharmacy*, **8**(2), 283–292.
- Nogami, H, Hasegawa, J, & Miyamoto, M. 1967. Studies on Powdered Preparations. XX. Disintegration of the Aspirin Tablets containing Starches as Disintegrating Agent. *Chemical and Pharmaceutical Bulletin*, **15**(3), 279–289.
- O’Mahoney, N., Keating, J. J., McSweeney, S., Hill, S., Lawrence, S., & Fitzpatrick, D. 2020. The sound of tablets during coating erosion, disintegration, deaggregation and dissolution. *International Journal of Pharmaceutics*, **580**(Apr), 119216.
- Patel, N. R., & Hopponen, R. E. 1966. Mechanism of Action of Starch as a Disintegrating Agent in Aspirin Tablets. *Journal of Pharmaceutical Sciences*, **55**(10), 1065–1068.
- PhRMA. 2015. *Biopharmaceutical Research & Development: The Process Behind New Medicines*. Tech. rept.
- Psachoulias, Dimitrios, Vertzoni, Maria, Butler, James, Busby, David, Symillides, Moira, Dressman, Jennifer, & Reppas, Christos. 2012. An In Vitro Methodology for Forecasting Luminal Concentrations and Precipitation of Highly Permeable Lipophilic Weak Bases in the Fasted Upper Small Intestine. *Pharmaceutical Research*, **29**(12), 3486–3498.

- Qiu, Fenghe. 2018b. *Chapter 1 - Accelerated Predictive Stability: An Introduction*. Academic Press. Page 3–14.
- Quodbach, J., & Kleinebudde, P. 2015. Performance of Tablet Disintegrants: Impact of Storage Conditions and Relative Tablet Density. *Pharmaceutical Development and Technology*, **20**(6), 762–768.
- Quodbach, J., & Kleinebudde, P. 2016. A critical review on tablet disintegration. *Pharmaceutical Development and Technology*, May, 1–12.
- Quodbach, J., Moussavi, A., Tammer, R., Frahm, J., & Kleinebudde, P. 2014a. Assessment of disintegrant efficacy with fractal dimensions from real-time MRI. *International Journal of Pharmaceutics*, **475**(1), 605–612.
- Quodbach, J., Moussavi, A., Tammer, R., Frahm, J., & Kleinebudde, P. 2014b. Tablet Disintegration Studied by High-Resolution Real-Time Magnetic Resonance Imaging. *Journal of Pharmaceutical Sciences*, **103**(1), 249–255.
- Rohrs, B. R., Thamann, T. J., Gao, P., Stelzer, D.J., Bergren, M. S., & Chao, R. S. 1999. Tablet Dissolution Affected by a Moisture Mediated Solid-State Interaction Between Drug and Disintegrant. *Pharmaceutical Research*, **16**(12), 1850–1856.
- Rowe, R. C., Sheskey, P. J., & Quinn, M. E. 2009. *Handbook of Pharmaceutical Excipients*. Sixth edition edn. Pharmaceutical Press.
- Rubinstein, M. H., & Birch, M. 1977. The Effect of Excipient Solubility on the in-vitro and in-vivo Properties of Bendrofluazide Tablets 5 MG. *Drug Development and Industrial Pharmacy*, **3**(5), 439–450.
- Sacchetti, M., Teerakapibal, R., Kim, K., & Elder, E. J. 2017. Role of Water Sorption in Tablet Crushing Strength, Disintegration, and Dissolution. *AAPS PharmSciTech*, **18**(6), 2214–2226.
- Scrivens, G. 2019. Prediction of the Long-Term Dissolution Performance of an Immediate-Release Tablet Using Accelerated Stability Studies. *Journal of Pharmaceutical Sciences*, **108**(1), 506–515.

- Shesky, P. J., Hancock, B. C., Moss, G. P., & Goldfarb, D. J. (eds). 2020. *Handbook of Pharmaceutical Excipients*. Ninth edn.
- Soundaranathan, M., Vivattanaseth, P., Walsh, E., Pitt, K., Johnston, B., & Markl, D. 2020. Quantification of swelling characteristics of pharmaceutical particles. *International Journal of Pharmaceutics*, **590**(Nov), 119903.
- Sun, C. C. 2017. Microstructure of Tablet—Pharmaceutical Significance, Assessment, and Engineering. *Pharmaceutical Research*, **34**(5), 918–928.
- Sun, W., Rantanen, J., & Sun, C. C. 2018. Ribbon density and milling parameters that determine fines fraction in a dry granulation. *Powder Technology*, **338**(Oct), 162–167.
- Sunada, H., & Bi, Y. 2002. Preparation, evaluation and optimization of rapidly disintegrating tablets. *Powder Technology*, **122**(2), 188–198.
- Suresh, P., Sreedhar, I., Vaidhiswaran, R., & Venugopal, A. 2017. A comprehensive review on process and engineering aspects of pharmaceutical wet granulation. *Chemical Engineering Journal*, **328**(Nov.), 785–815.
- Tomas, J., Schöngut, M., Dammer, O., Beránek, J., Zadražil, A., & Štěpánek, F. 2018. Probing the early stages of tablet disintegration by stress relaxation measurement. *European Journal of Pharmaceutical Sciences*, **124**(Nov), 145–152.
- Torjesen, I. 2015. Drug development: the journey of a medicine from lab to shelf. *The Pharmaceutical Journal (Online)*.
- Tsunematsu, H., Hifumi, H., Kitamura, R., Hirai, D., Takeuchi, M., Ohara, M., Itai, S., & Iwao, Y. 2020. Analysis of available surface area can predict the long-term dissolution profile of tablets using short-term stability studies. *International Journal of Pharmaceutics*, **586**(Aug), 119504.
- Uhumwangho, M. U., & Okor, R. S. 2005. Effect of humidity on the disintegrant property of α -cellulose. *Acta Poloniae Pharmaceutica - Drug Research*, **62**(1), 39–44.
- USP, (United States Pharmacopeia). 2020a. <701> *Disintegration*. Tech. rept.

- USP, (United States Pharmacopeia). 2020b. <711> *Dissolution*. Tech. rept.
- Waterman, K. C. 2011. The Application of the Accelerated Stability Assessment Program (ASAP) to Quality by Design (QbD) for Drug Product Stability. *AAPS Pharm-SciTech*, **12**(3), 932–937.
- Waterman, K. C., Carella, A. J., Gumkowski, M. J., Lukulay, P., MacDonald, B. C., Roy, M. C., & Shamblin, S. L. 2007. Improved Protocol and Data Analysis for Accelerated Shelf-Life Estimation of Solid Dosage Forms. *Pharmaceutical Research*, **24**, 780–790.
- Wenzel, R. N. 1936. Resistance of Solid Surfaces to Wetting by Water. *Industrial & Engineering Chemistry*, **28**(8), 988–994.
- Wewers, M., Czyz, S., Finke, J. H., John, E., Van Eerdenbrugh, B., Juhnke, M., Bunjes, H., & Kwade, A. 2020. Influence of Formulation Parameters on Redispersibility of Naproxen Nanoparticles from Granules Produced in a Fluidized Bed Process. *Pharmaceutics*, **12**(4).
- Williams, H., Stephens, D., McMahon, M., Debie, E., Qiu, F., Hoaglund, H., Sechler, L., Orr, R., Webb, D., Wu, Y., & Hahn, D. 2017. Risk-Based Predictive Stability – An Industry Perspective. *Pharmaceutical Technology*, **41**(3), 52–57.
- Williams, H. E., Bright, J., Roddy, E., Poulton, A., Cosgrove, S. D., Turner, F., Harrison, P., Brookes, A., MacDougall, E., Abbott, A., & Gordon, C. 2019. A comparison of drug substance predicted chemical stability with ICH compliant stability studies. *Drug Development and Industrial Pharmacy*, **45**(3), 379–386.
- Wouters, Olivier J., McKee, Martin, & Luyten, Jeroen. 2020. Estimated Research and Development Investment Needed to Bring a New Medicine to Market, 2009-2018. *JAMA*, **323**(9), 844–853.
- Yassin, S., Goodwin, D. J., Anderson, A., Sibik, J., Wilson, D. I., Gladden, L. F., & Zeitler, J. A. 2015. The Disintegration Process in Microcrystalline Cellulose Based

Tablets, Part 1: Influence of Temperature, Porosity and Superdisintegrants. *Journal of Pharmaceutical Sciences*, **104**(10), 3440–3450.

Zhao, N., & Augsburger, L. L. 2005a. Functionality comparison of 3 classes of superdisintegrants in promoting aspirin tablet disintegration and dissolution. *AAPS PharmSciTech*, **6**(4), E634–E640.

Zhao, N., & Augsburger, L. L. 2005b. The influence of swelling capacity of superdisintegrants in different pH media on the dissolution of hydrochlorothiazide from directly compressed tablets. *AAPS PharmSciTech*, **6**(1), 120–126.